IN VITRO MODELLING OF DERMAL ABSORPTION OF CHEMICALS FOLLOWING ENVIRONMENTAL OR ACCIDENTAL EXPOSURE

A thesis submitted in accordance with the conditions governing candidates
for the degree of

DOCTOR OF PHILOSOPHY

To Newcastle University

By

CRAIG ANDREW MOORE

BSc (Hons) Biomedical Sciences (Newcastle)

MRes Medical and Molecular Biosciences (Newcastle)

2010

Toxicology Unit
Institute of Cellular Medicine
Institute of Research on Environment and Sustainability
Newcastle University
Devonshire Building
Devonshire Terrace
Newcastle upon Tyne
NE1 7RU

Abstract

Due to the difficulties involved in assessing dermal exposure of bioactive agents, it is necessary to identify less toxic, surrogate compounds *in vitro*, which can be used to predict dermal absorption of bioactive agents *in vivo*. It is also important to understand factors influencing dermal absorption of chemicals for the purposes of risk assessment for exposure to civilians, as many studies tend to focus on occupational or military exposure. These studies were aimed at identifying potential surrogate compounds for dermal absorption of bioactive agents *in vitro* using flow through and static cell diffusion systems, and also to generate novel data on the effects of application vehicle on chemical absorption following low level exposure. For protection and risk assessment purposes, the influence of 'everyday' clothing, and skin surface decontamination on dermal chemical absorption was also assessed.

The model compounds (caffeine and benzoic acid), and the surrogate compounds (chlorpyrifos, dichlorvos and phorate) were generally found to be poor marker chemicals for comparison with HD absorption through human and pig skin *in vitro*. However, benzoic acid absorption from a finite dose in IPA more closely matched the absorption profile of HD applied as a finite dose in IPA. Dichlorvos absorption was greatest from all vehicles compared with chlorpyrifos and HD absorption *in vitro*. Dermal absorption of chlorpyrifos was enhanced when applied in PG compared with absorption from IPA or IPM. No differences were observed between absorption of neat HD and HD in IPA in terms of percentage of applied dose absorbed at 24 hours. Absorption of HD through full thickness pig skin more closely matched absorption through full thickness human skin, split thickness pig skin overestimated absorption of HD *in vitro* in comparison.

'Everyday' clothing (cotton shirt) significantly reduced absorption of dichlorvos, chlorpyrifos and HD through human skin. Chemicals were applied to clothed skin in IPA to mimic finite exposure, and left in contact for 30 minutes (dichlorvos), 4 hours (chlorpyrifos), and 1 hour (HD). For all chemicals, removal of clothing followed by immediate skin surface decontamination with 0.5% (v/v) soap solution further reduced absorption compared with removal of clothing alone. Despite these differences not being significant, in terms or civilian exposure, it would be recommended to remove clothing and decontaminate as early as possible post-exposure to minimise the potential for dermal absorption and localised toxicity within the skin.

In conclusion, the organophosphate compounds used in these studies (chlorpyrifos and dichlorvos) could potentially be useful surrogates for organophosphate agents such as VX or sarin, however, further work is needed to make these comparisons. The vehicle in which a chemical is applied to the skin can have a profound effect on dermal absorption, and this knowledge is important for risk assessment for exposure to a range of chemicals. Cotton shirt material significantly reduced dermal absorption of all chemicals used compared with 24 hour exposure. Despite this clothing not being designed for protective purposes, this may have a significant impact for reducing dermal absorption and toxicity *in vivo* as a result of chemical exposure. Further investigation is needed to assess absorption of a wider range of chemicals and application vehicles for risk assessment purposes, and to identify chemicals that more closely mimic dermal absorption of bioactive agents *in vitro* for extrapolation to *in vivo* exposure scenarios

Table of Contents

Acknowledgements

First and foremost, I would like to thank Professor Faith Williams for her help and guidance throughout the course of this project.

I also thank Dr Simon Wilkinson for providing me with help and expertise whenever necessary.

I also wish to thank Dr Gillian Aust, for her help and support throughout this project, and to Dr Michael Dunn for his help and expertise in using the GC-MS for analysis of many of my samples.

I thank Dr John Jenner, Oliver Payne and Stuart Graham for helping me to conduct my studies at Dstl and for giving up so much of their time during my 6 week placement to make sure I got all of the studies completed on time. I also wish to thank Dr Robert Read for analysing my samples on the LC-MS-MS.

I would like to thank the remaining members of the toxicology group in the Devonshire building and the Wolfson Unit who have helped me throughout the project. I would particularly like to thank my fellow PhD student, Seth Remington, for his help and support throughout the project and for making the PhD years so enjoyable. It has been absolutely brilliant to share the experience!

I have made many friends throughout my time studying at Newcastle and through supervising students during my PhD, and so I wish to thank all of them for making my 8 years in Newcastle the most enjoyable and memorable years of my life so far.

Finally, I would like to thank my family for all of their encouragement and support (both emotional and financial!) throughout my time at university and in everything I have ever done. I couldn't have achieved any of this without their support and for this I am eternally grateful.

List of Figures

List of Tables

List of Abbreviations

ANOVA -	Analysis of Variance
BSA –	Bovine Serum Albumin
CYP450 –	Cytochromes P450
DPM –	Disintegrations per Minute
FT –	Full Thickness
GC-MS –	Gas Chromatography Mass Spectrometry
HD –	Sulphur Mustard
IPA -	Isopropanol
IPM –	Isopropyl Myristate
Kp -	Permeability Coefficient
Log P –	Octanol Water Partition Coefficient
MEM –	Minimum Essential Media
NPE -	Nonylphenolethoxylate
PG –	Propylene Glycol
PPE –	Personal Protective Equipment
QSAR –	Quantitative Structure-Activity Relationship
RSDL –	Reactive Skin Decontamination Lotion
SEM –	Standard Error of the Mean
ST –	Split Thickness
TEWL –	Trans-Epidermal Water Loss

List of Abstracts and Presentations

1. **'How do vehicle properties impact on the dermal absorption and distribution of chlorpyrifos?'** – Abstract, Poster and Oral presentation, Perspectives in Percutaneous Penetration Conference, La Grande Motte, France 2007.

2. **'Investigating the effectiveness of everyday clothing for reducing dermal absorption of chlorpyrifos in vitro'** – Abstract and Poster presentation, British Toxicology Society Conference, Durham University, 2009.

3. **'The influence of everyday clothing on percutaneous absorption and distribution of model penetrants in vitro'** – Abstract and Feature Oral Presentation, Occupational and Environmental Exposure of Skin to Chemicals (OEESC) Conference, Edinburgh University, 2009. Prize: OEESC Young Scientist of the Year 2009.

Chapter 1

Introduction

1. Introduction

1.1: Structure of Skin

The average adult male has a skin surface area of approximately 1.8-2.2m^2, although these figures are variable depending on a number of factors, such as an individual's height and weight. The skin has many different functions, primarily as a barrier to prevent loss of water, nutrients and essential compounds from the body. However, the skin also operates in a protective capacity to limit absorption. As a result of this, the skin plays a pivotal role as a barrier to the potential absorption of hazardous compounds into the body (Grandjean, 1990). One of the main factors in enabling the skin to limit absorption is its relatively small surface area. In comparison, organs which have evolved to efficiently facilitate absorption, such as the lungs (approximately 150m^2) and the gastrointestinal tract (approximately 200m^2) have much larger surface areas (Chilcott and Price, 2008). However, the role of skin as a protective barrier is not exclusive to chemicals. It also provides physical, immunological and pathogen protection, as well as limiting absorption of UV radiation (Menon, 2002).

The skin also plays a significant role in thermoregulation and maintaining the core temperature of the body. The skin has also been shown to contain some metabolising enzymes (Merk *et al*. 1996, Jewell *et al*. 2007, and Traynor *et al*. 2008). However, the levels of metabolising enzymes in the skin are generally regarded to be low in comparison to the liver, the main site of metabolism (Williams, 2008).

Structurally, the skin can be divided into three main layers. These are the epidermis, the dermis and the hypodermis (figure 1.1). The outermost skin layer, the epidermis, can be further subdivided on the basis of cellular differentiation. This, along with the dermis provides the structural components. The hypodermis comprises mainly of adipose and connective tissue.

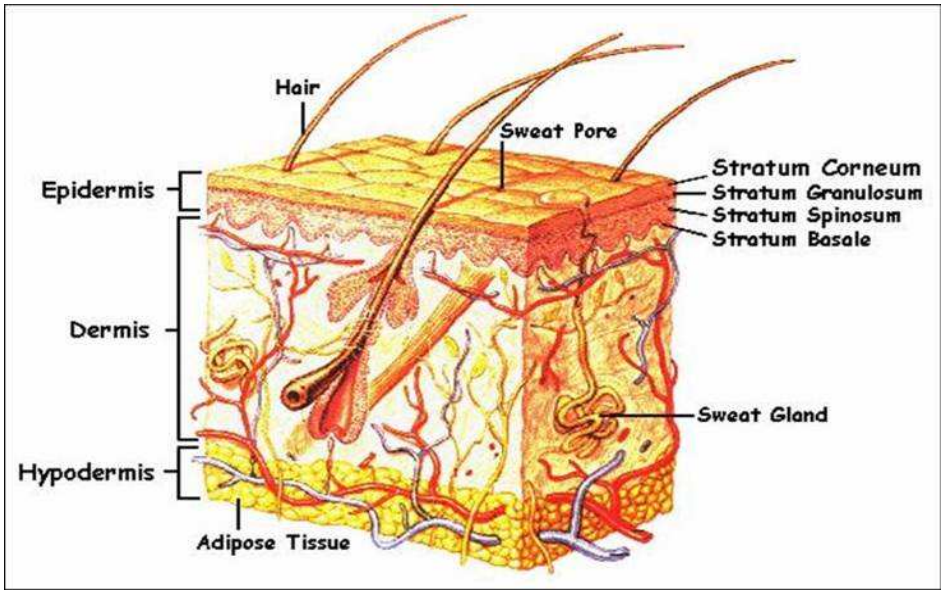

Fig.1.1 structure of a typical skin section (adapted from 'human physiology: fifth edition' (Fox, 1996)

1.1.1: Epidermis

The epidermis is the outermost layer of the skin, and is made up of multiple layers of stratified squamous epithelial cells. These layers of epithelium can be further subdivided into four distinctive layers (from outermost to innermost); the stratum corneum, stratum granulosum, stratum spinosum and the stratum basale, which can be distinguished by the differentiation of the cells present in the epidermis. Approximately 80-95% of cells in the

epidermis are keratinocytes, with the remainder of cells in this layer of skin being made up of melanocytes (involved in pigment formation), Langerhans cells (involved in immunological function), and Merkel cells (involved in sensory perception) (Monteiro-Riviere, 1996; Menon, 2002).

The innermost layer of the epidermis is the stratum basale. This is a single layer of epidermal stem cells occupying the basement membrane of the skin and is anatomically attached to the stratum by hemidesmosomes (rivet-like structures in the stratum basale). The cells of the stratum basale differentiate into epithelial cells which are linked to adjacent cells by desmosomes (specialised protein structures involved primarily in cell to cell adhesion). Cells constantly undergo apical migration from the stratum basale to produce the remaining layers of the epidermis.

The stratum spinosum is characterised by a spiny appearance microscopically due to the abundance of desmosomal connections within this layer. The stratum spinosum has a profusion of lamellar bodies, which are a major component in the synthesis of epidermal lamellar lipids including ceramides, fatty acids and cholesterol (Wertz and Downing, 1989). This helps to provide the skin with its ‘water-proof’ feature. There is also a greater amount of keratin filaments in the stratum spinosum compared with the basal layer of the skin.

The stratum granulosum is so called due to its grainy appearance. Here, the epidermal cells take on a flatter appearance compared with the more basal

layers, and also contains keratohyalin granules, which gives rise to the grainy appearance of this skin layer. Keratohyalin granules contain filaggrin (stored as profilaggrin, a 400kDa phosphorylated protein consisting of 10-12 repeats of filaggrin). This facilitates bundling of keratin later on during cell differentiation. Filaggrin is essential in the formation, structural integrity and barrier function of the upper layer of the epidermis, the stratum corneum. Filaggrin is synthesised in the cytoplasm and is stored in keratohyalin granules. During terminal cell differentiation, profilaggrin is proteolytically cleaved into multiple copies of the 37kDa filaggrin protein (Dale *et al*. 1985, Gan *et al*. 1990). Filaggrin binds to keratin fibres causing it to bundle into highly insoluble macrofibrils. It is this aggregation of protein fibres that causes the collapse of the cytoskeleton, which results in the compaction of keratinocytes to form corneocytes found in the stratum corneum (Chilcott and Price, 2008). An increase in lamellar bodies is also seen in the stratum granulosum, with lipids derived from these lamellar bodies being secreted into extracellular spaces as the cells differentiate into corneocytes.

The stratum corneum is the outermost layer of the epidermis, and is made up of approximately 15-20 layers (this varies depending on anatomical location) of flattened, keratinised, dead cells known as corneocytes. These cells are surrounded by lipids that occupy the intercellular spaces. The structure of the stratum corneum is often referred to as resembling a ‘brick and mortar’ arrangement ((figure 1.2), Williams and Elias 1993), and is credited with being the body’s main barrier against percutaneous absorption of xenobiotic compounds, as well as helping to keep the body hydrated by

preventing water loss from the skin surface. The epidermis contains no blood vessels and so it relies on diffusion of nutrients from the dermis in order to be maintained. Cells in the epidermis migrate upwards from the stratum basale and undergo considerable differentiation. During this process, considerable amounts of protein and lipid (especially ceramides, a class of polar lipids) are synthesised in the stratum spinosum and stratum granulosum. The polar lipids are extruded into the extracellular spaces in the upper layer of the stratum granulosum. The final stage of differentiation is formation of the corneocytes, non-viable cells, devoid of nucleus and organelles, filled with highly cross linked keratin bundles, and surrounded by a thickened cell membrane, known as the cornified cell envelope. The corneocytes are eventually lost from the upper layers of the stratum corneum, a process termed desquamation, in which the corneocytes are continuously being 'sloughed off' and replaced with cells from the underlying skin layers. This maintains the stratum corneum at a constant thickness. In the cells of the upper stratum corneum, filaggrin is proteolysed into a complex mixture of hygroscopic chemicals, including amino acids and derivatives. This chemical mixture is termed the 'skin natural moisturising factor' (NMF). This plays a role in determining the level of stratum corneum hydration.

1.1.2: Dermis

The dermis is the largest layer within the skin structure and is situated directly below the epidermis. This layer is made up of dense connective tissue situated within an extracellular matrix, consisting of collagen, elastin

and proteoglycans. The dermis is highly vascular, containing networks of blood vessels, capillaries, lymphatic systems and nerve fibres. These systems are necessary in order to support the various glandular structures found within the dermis, including sweat glands, sebaceous glands and hair follicles. These structures are referred to as appendages, and penetrate through the dermis and into the stratum corneum to form pores on the skin surface. The uppermost layer of the dermis is named the papillary layer. It is this section of the skin that contains blood vessels and nerve fibres that provide nutrients to the avascular epidermis. The lower layer, although indiscernible from the upper layer, is termed the reticular layer. This contains an abundance of thick, densely packed collagen fibres and connective tissue (Montiero-Riviere, 2004).

1.1.3: Appendages

The term ‘appendages’ refers to the glandular structures, such as hair follicles, sweat glands and sebaceous glands that are present within the dermis. These pass from the dermis, through the epidermis and the stratum corneum to form pores on the skin surface. The appendageal route can provide an alternative route of absorption through the skin to those demonstrated in figure 1.2. This is particularly important for chemicals which may be to large in structure to penetrate the stratum corneum under normal circumstances (Montiero-Riviere, 2004).

1.1.4: Dermal absorption and penetration

It is important to study the dermal absorption and penetration of chemicals for a number of reasons. Humans come into contact with a wide variety of chemicals on a daily basis, whether it is through topically applied drugs, cosmetics, household products or through occupational, environmental or accidental exposure to chemicals. It is therefore vitally important to understand the permeation of chemicals through the skin. Chemicals that come into contact with human skin have the potential to be dermally absorbed, and so they also have the potential to cause local or systemic toxicity effects. Therefore, by investigating the dermal absorption of a series of chemicals with differing physicochemical properties, the absorption of these chemicals through skin will be better understood and this data can then be used for developing risk assessment strategies that may help to minimise the effects of exposure to hazardous compounds.

1.1.5: The function of skin as a barrier to absorption

As mentioned previously, the stratum corneum provides the main barrier to dermal absorption of chemicals which come into contact with the skin. Although the skin is a barrier to penetration of xenobiotic compounds, it is by no means infallible in this role, due to the fact that most chemicals are able to penetrate into the skin to some degree. The stratum corneum is not impermeable, but it does function to limit the penetration and absorption or the vast majority of compounds.

The two predominant components of the stratum corneum are the corneocytes and the intercellular lamellar lipids. It is thought that the intercellular lamellar lipids give then skin its permeability by creating a porous route between the corneocytes through which compounds can be absorbed (Elias and Friend, 1975, Wertz, 2004).

1.2: Routes of dermal absorption

Percutaneous absorption is largely considered to be a passive diffusion process, with the stratum corneum involved in limiting the rate of absorption of xenobiotic compounds. However, most compounds can penetrate the stratum corneum to some extent (depending on their physicochemical properties). There are several routes by which molecules can pass through the stratum corneum and into the viable epidermis (and hence potentially reach the systemic circulation); these are termed the intercellular, transcellular and the appendageal routes (figure 1.2).

The intercellular route, which involves passage of compounds through the lipid matrix between corneocytes in the stratum corneum, is widely considered to be the principal route of percutaneous absorption of most xenobiotic compounds (Bodde *et al*. 1991, Kitson and Thewalt, 2000).

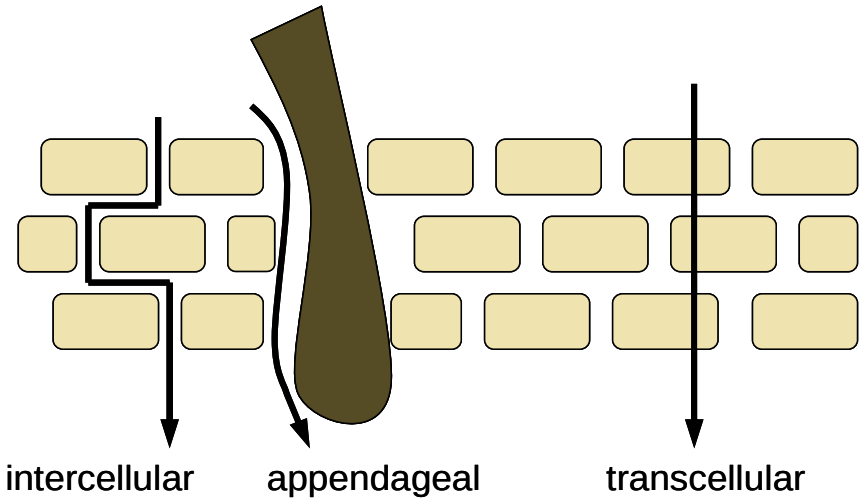

Fig 1.2. Routes of transcellular, appendageal and intercellular penetration.

Transcellular absorption occurs when a compound passes through both the corneocytes and the lipid matrix within the stratum corneum. The significance of this route of absorption is unclear because passage of chemicals through multiple layers of corneocytes and intercellular lipids is a thermodynamically and kinetically unfavourable process (Flynn, 1990). Appendageal absorption involves passage through the appendages, such as hair follicles and sweat glands; therefore bypassing absorption through the stratum corneum (Maibach *et al*. 1971). However, this route of absorption is considered to be of less significance for the absorption of chemicals with a lower molecular weight, partially due to the fact that appendages are relatively sparse, and cover approximately 11cm^2 (Monteiro-Riviere, 1996) of human skin. Chemicals with a low molecular weight are more likely to be absorbed through the skin via the other alternative absorption routes.

Little is known regarding the exact route of absorption specific to individual chemicals, although experiments have been undertaken to attempt isolation

of the appendageal route (Grams and Bouwstra, 2002, Barry, 2002). The approach employed by Barry, 2002, was a novel 'sandwich' technique to isolate the appendageal route. Here, two stratum corneum layers were 'sandwiched' together, leading to a blockage of the appendages through both stratum corneum layers. Therefore, it could be assumed that if absorption of a compound was restricted through the stratum corneum 'sandwich', then the appendageal route could be deemed of importance in terms of dermal absorption of a particular compound.

1.3: Kinetics of dermal absorption

Diffusion can be defined as the process by which molecules move from an area of high concentration to an area of low concentration due to random molecular movement. Diffusion kinetics can be applied to dermal absorption using Fick's law of diffusion for absorption across a membrane at steady state.

$$J = k_p \, dC$$

This equation is used to determine the rate of absorption at a steady state (J) of a compound passing through the skin, per unit area, per hour (e.g. $\mu g/cm^2/h$). Where K_p corresponds to the permeation coefficient of a given chemical across the skin and dC refers to the concentration difference across the skin membrane (Grandjean, 1990). A maximum absorption rate is achieved when the system reaches a steady state of absorption. The term 'steady state absorption rate' (or steady state flux), refers to a situation where the concentration of a chemical on the skin surface and beneath the

skin surface are in a state of equilibrium, and also when the rate of absorption remains constant over time. In order for steady state absorption to be truly achieved, the chemical penetrant must be applied to the skin surface at an infinite concentration, so that the concentration on the skin surface does not become depleted sufficiently over time and therefore reduce the rate of absorption.

The permeability coefficient (K_p) (expressed as cm/hour) is characterised by the ratio of the 'flux' or maximum absorption rate and the concentration of the test compound (K_p=flux/C). It provides a quantitative estimate of the rate of absorption across the skin. This is a useful indicator for the rate of absorption, particularly when comparing different concentrations of the chemical of interest. This means that the permeability coefficient is independent of the concentration of chemical applied to the skin surface. This can only be calculated accurately when the chemical applied to the skin surface at an infinite dose and when the system is at steady state (USEPA, 1992).

Lag time is defined as the time it takes in hours for a chemical to reach a steady state of absorption. The lag time for a particular chemical can be determined by extrapolating a line of best fit through the linear section of a cumulative absorption graph to the x-axis. The point where the line of best fit intercepts the x-axis is the lag time (fig. 1.3). This is a theoretical value derived from *in vitro* dermal absorption studies and therefore does not truly reflect the time it takes for a compound to be absorbed through the skin.

However, identifying lag time is a useful indicator for comparing dermal absorption of different compounds with differing properties.

The maximum rate of absorption (flux) can be also be determined from a cumulative absorption profile; with the gradient of the line of best fit of the linear phase (steady state) being relative to the maximum rate of absorption. The linear phase corresponds to the steady state of absorption, when the concentration of a chemical on the skin surface and below the skin surface is in equilibrium.

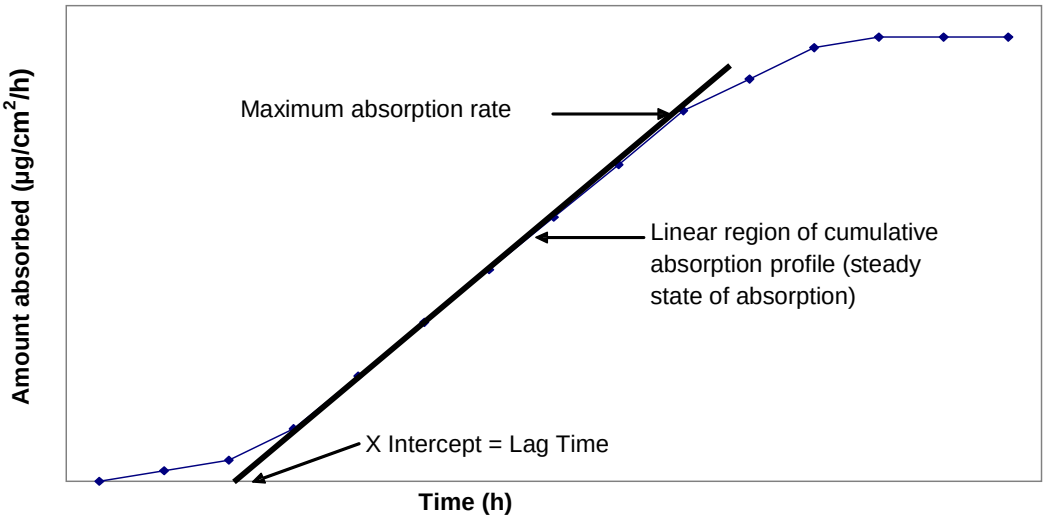

Fig.1.3. Diagrammatical representation of steady state absorption, maximum absorption rate and lag time

It is important to understand that diffusion of compounds across the stratum corneum is driven by a thermodynamic gradient and is not determined solely by a concentration gradient. Diffusion through the skin does have a degree of reliance on the concentration of which a substance is applied to the skin surface, as the more molecules of a substance there is on the skin surface,

the greater the probability that molecules will diffuse from an area of high to low concentration over time. However, it is also important to take into consideration interactions between molecules (when diffusing between the application vehicle and the stratum corneum). The term ‘fugacity’ can be used to describe the outcome of these molecular interactions. Fugacity can be defined as the tendency of a molecule to move from one environment to another. This is important to consider with respect to dermal absorption, for instance, because a lipophilic molecule dissolved in a hydrophilic vehicle will exhibit a greater fugacity for the lipids of the stratum corneum than a hydrophilic molecule would if dissolved in the same vehicle. In some instances, the thermodynamic gradient can be the opposite of the concentration gradient, an example of this is hexachlorobenzene in octanol: water (Chilcott and price, 2008). The maximum thermodynamic activity of a molecule occurs when it is dissolved to saturation in a particular application vehicle. Theoretically, the thermodynamic activity of a particular molecule should be the same, regardless of application vehicle provided it is in a saturated solution. However, the thermodynamic activity of a molecule at the same concentration in two vehicles (but not saturated), will be different. Thermodynamic activity and concentration are only ever approximately equal when using very dilute concentrations.

The theoretical principles of diffusion mentioned above have been used to create mathematical models for the purpose of predicting dermal absorption of chemicals based on their physicochemical properties (Flynn, 1990a, Potts and Guy, 1992**,** van der Merwe, 2006). These mathematical models are

known as quantitative structure-activity relationships (QSARS). QSARs are usually formed upon the correlation of the physicochemical properties of the chemical of interest (such as molecular weight, permeability coefficients and solubility), and the vehicle in which the compound is applied to the skin surface. The Flynn dataset compiled in 1990 (Flynn 1990a), gave information on 97 permeability coefficients for 94 different compounds through *in vitro* human skin, however, the data were compiled from 15 different laboratories. This meant that the data contained a high degree of experimental error due to inter-laboratory variation in experimental procedure. Flynn used simple algorithms for low and high molecular compounds, assuming that hydrophilic compounds had low skin permeability, and that lipophilic compounds had high skin permeability. It was also stated that octanol: water partition coefficient dependent QSARs could be used to predict skin absorption of high and low molecular weight compounds. The dataset presented by Flynn has led to vast amounts of research being conducted into generating models for prediction of dermal absorption, most of which has been extensively reviewed in the literature (Moss et al. 2002, Vecchia and Bunge, 2002, Godin and Touitou, 2007)

1.4: Factors influencing dermal absorption

There are a number of factors that can affect skin absorption of chemicals. These may relate to the skin membrane through which a chemical may be absorbed (biological factors) or to the penetrating chemical or its vehicle for application to the skin surface (physicochemical factors).

1.4.1: Biological factors affecting dermal absorption

Biological factors relate to the variability seen in the structure of the skin. Differences in the influence of biological factors can be seen intra or inter-individually, as well as between different species. The main biological factors that influence dermal absorption include the anatomical location of the skin, gender, age, skin damage/disease and also species.

1.4.1.1: Anatomical location of the skin

It is important to consider anatomical location when investigating dermal absorption because different areas of the body have different permeabilities (Maibach *et al*. 1971). Areas of the body where the stratum corneum is thickest, such as the palms of the hands (400μm) and soles of the feet (600μm) will be far less permeable to xenobiotic compounds than an area of the body where the stratum corneum is much thinner, such as the scrotum (5μm) (Scheuplein and Blank, 1971). Exposure of scrotal skin to organic solvents has shown a fifty-fold increase in permeability when compared to areas with thicker skin (Boman and Maibach, 2000). An investigation into absorption of sunscreen lotion has also identified that absorption is approximately four times greater when applied to the face compared with absorption when applied to the back (Benson *et al*. 2005). For the purposes of *in vitro* skin diffusion studies, excised human breast or abdomen skin are most commonly used due to the reduced variability in permeation when using skin samples from these sites (Southwell *et al*. 1984).

Not only does skin thickness vary from one anatomical location to another, but there is also variation in the composition and amount of lipids present in the stratum corneum, which may also contribute to variations in permeability between anatomical locations (Lampe *et al*. 1983). Stratum corneum lipid composition has also been shown to differ, not only intra-individually, but also inter-individually. High ceramide to cholesterol ratios were observed in the wrists area, which coincided with a high level of trans-epidermal water loss. However, no correlation between ceramide levels and barrier function were found (Norlen *et al*. 1999).

1.4.1.2: Gender differences

It has also been seen that differences in the gender can affect dermal absorption. A study carried out by Jacobi et al. 2005, investigating the differences in the physiology of the stratum corneum through tape stripping showed that variations in structure, permeability and protein composition of the stratum corneum exist between genders.

1.4.1.3: Skin damage

Percutaneous absorption of compounds can also be greatly affected by damage to the skin. This can be as a result of physical trauma (e.g. open wounds), chemical insult (in which the arrangement of stratum corneum lipids is perturbed), irritation, or as a result of skin diseases. Skin diseases can either increase or decrease dermal absorption depending on how a particular disease affects the structure of the skin. It has been suggested that slight skin damage (caused by pre-exposure with sodium lauryl

sulphate), can significantly affect the absorption rate, lag time, and total penetration of a variety of chemicals, particularly with more hydrophilic compounds (Nielsen, 2005).

1.4.1.4: Species differences

The thickness of the stratum corneum differs greatly between commonly studied mammalian species. For instance, the dorsal stratum corneum is 3 times thicker in humans than it is in rats (Monteiro-Riviere *et al*. 1990), meaning that absorption of compounds will be greater through rat skin than through human skin. This is one of the reasons why investigating dermal absorption through rat skin *in vitro* as a model for human exposure to particular compounds can lead to an overestimation of absorption. Absorption of demeton-s-methyl has also been shown to be two fold greater through pig ear skin compared with human skin in vitro (Vallet *et al*. 2007). However, when VX (*0*-ethyl-*S*-[2(di-isopropylamino) ethyl] methyl phosphonothioate) was applied to human, pig and guinea pig skin *in vitro*, no statistically significant differences in absorption were found between human and pig skin. However, absorption through guinea pig skin was seen to be seven fold higher than through human skin (Dalton *et al*. 2006). Despite various differences in absorption between species, pig skin is generally regarded to be the most suitable animal model for human skin absorption (Simon and Maibach, 2000).

Another factor causing variation in absorption between different species is hair follicle density. For example, dorsal skin of the rat and mouse has 289

and 658 follicles/cm^2 respectively. However, human back skin has only 11 follicles per cm^2 (Bronaugh *et al*. 1982). In this study, hairless 'nude' mice with an approximate hair follicle density of 75 per cm^2 were shown to have a reduced rate of absorption compared to normal mice. The appendageal route of absorption through the skin is likely to contribute much more significantly to the penetration of a compound through rodent skin than it will through human skin, due to the fact that rodents have far more hair follicles than humans. Again, this could lead to an overestimate of penetration if using rat skin samples to model for how a compound will penetrate through human skin. Differences in hair follicle density may also contribute to differences in permeability between anatomical sites, but this is controversial because areas of skin with high follicle density, such as the human forehead and mandible, also have reduced stratum corneum thickness.

1.4.2: Physicochemical factors affecting dermal absorption

There are also a number of physicochemical factors that can influence percutaneous absorption in addition to factors of biological skin structure. The main physicochemical factors that can affect the degree to which a compound is dermally absorbed include the lipophilicity of the compound of interest, molecular weight, the vehicle of application to the skin and also the type of dose applied.

1.4.2.1: Lipophilicity of a penetrant

Lipophilicity is a major factor determining the dermal penetration of a particular compound. The lipophilicity of a compound is expressed as Log P

(the logarithm to base ten of the partition coefficient between octanol and water). The higher the log P value, the more lipophilic the chemical is. The majority of compounds lie within the log P range of -4 to 7. For example, the log P of water is -1.38, caffeine is 0.07, benzoic acid is 1.83 and testosterone is 3.32. Compounds with a Log P above 3 are considered lipophilic. Lipophilicity affects dermal absorption because a more lipophilic substance will readily partition into the stratum corneum, but cannot pass easily through the skin into systemic circulation due to the aqueous nature of the viable epidermis. The more lipophilic a compound is, the less likely it is to have the ability to partition into the epidermis. In contrast to this, absorption of hydrophilic compounds is limited by the lipophilicity of the stratum corneum; however, once a hydrophilic compound has penetrated through this, it will partition readily into the epidermis and into systemic circulation (Bronaugh, 2004).

1.4.2.2: Molecular weight of a penetrant

The molecular weight of a compound will also impact upon its ability to penetrate through the skin. Smaller molecules will pass through the skin much more rapidly than compounds that have a higher molecular weight. Routes of absorption also have different levels of importance depending on molecular weight; for instance, the appendageal route is more important for the absorption of larger molecules than for smaller molecules (Scheuplein, 1965). It is generally considered that chemicals with a molecular weight of greater than 500Da do not penetrate the skin under ‘normal’ circumstances (Bos and Meinardi, 2000). Despite this, there is some evidence that larger

molecules, such as cyclosporin A (1203Da), which is traditionally a poorly penetrating compound, can have its absorption significantly enhanced by introducing polar side chains in the form of a prodrug. This despite the fact that by adding polar side chains, the molecular weight of cyclosporin is increased (Billich et al. 2005).

1.4.2.3: Solvent vehicle for application of a penetrant

Percutaneous absorption of a compound can be influenced by the solvent vehicle in which it is applied to the skin surface. The absorption of a compound into the skin may be impeded if it is more soluble in the vehicle it is applied in than the stratum corneum (Jacobi *et al*. 2006). Contrary to this, if a compound is less soluble in its application vehicle than the stratum corneum, then the compound is more likely to penetrate into the stratum corneum.

As percutaneous absorption is a passive process, the rate of absorption will have some dependence on the concentration gradient across the stratum corneum, though the absolute concentration in the donor solution is less important than the thermodynamic activity. This depends on the solubility of the penetrant in the application vehicle. The rate of percutaneous absorption is maximal when the penetrant in the donor chamber is saturated in its application vehicle (because thermodynamic activity is maximal). Hence, a lipophilic chemical dissolved in an aqueous vehicle will be absorbed more rapidly than at the same concentration from a more lipophilic solvent. Furthermore, some solvent vehicles are able to act as penetration enhancers

(Bach and Lippold, 1998, Williams and Barry, 2004, Duracher *et al*. 2009), either by perturbing the arrangement of stratum corneum lipids, or by entering the stratum corneum and creating a reservoir for dissolution of the penetrant. Therefore, it is important to take into consideration the effect a solvent vehicle will have on the dermal absorption compounds.

1.4.2.4: Dose of a penetrant

Finally, the dose applied to the skin can have a significant influence on dermal absorption. Compounds can either be applied to the skin as a finite or infinite dose. An infinite dose involves applying the penetrant as a saturated solution, in a large volume to the skin surface (usually 1ml/cm^2) so that the maximum rate of absorption of the compound at steady state can be reached, and the chemical continues to penetrate at the same rate throughout the duration of skin contact. Theoretically, the rate of absorption does not decrease following application of an infinite dose because the surface dose does not get depleted significantly with time. Determination of the maximum absorption rate and permeability coefficient of compounds is considered to be important when considering risk assessment for exposure (Howes *et al*. 1996, OECD, 2004). Infinite dosing to obtain maximum absorption rates and permeability coefficients of a variety of compounds is also important for the purpose of modelling exposure, for instance, when looking at QSAR predictions for dermal exposure.

A finite dose is a lower concentration or volume applied to the skin (we use 10µl/cm^2). Following application of a finite dose, absorption may not reach a steady state because the application dose is usually significantly depleted

over time (Franz, 1978). Finite doses mimic occupational or accidental exposure to chemicals, and so they are most relevant when investigating how chemicals will be dermally absorbed in a typical exposure scenario. However, when assessing the suitability of a topically applied pharmaceutical product, an infinite dose may be more suitable to identify the maximum absorption rate of a compound (OECD, 2004).

1.5: Use of skin *in vitro* to predict dermal absorption

Assessing dermal absorption *in vitro* is often the only feasible method for ethically obtain important dermal absorption data relevant to human exposure (Bronaugh, 2004). This is of particular importance when considering the dermal absorption of highly toxic compounds, which cannot be administered to human volunteers *in vivo*. Excised sections of skin obtained from surgical procedures, such as mammoplasty and abdominoplasty, are commonly used for the purposes of in vitro dermal absorption (Harrison *et al*. 1984, Bronaugh *et al*. 1986, Howes *et al*. 1996, Wester *et al*. 2000, Wilkinson and Williams, 2002, Schreiber *et al*. 2005, Miller and Kasting, 2010). The use of excised human skin is seen as the 'gold standard' for comparing *in vitro* absorption data with human *in vivo* data (Howes *et al* .1996).

Absorption studies in vitro have been shown to predict the in vivo absorption of a variety of compounds. However, penetration of a compound may be altered by blood flow, or inflammatory responses to the compound applied to the skin surface *in vivo*, however, these systems do not exist when using

excised skin *in vitro*, meaning that the absorption of some chemicals may not be accurately predicted (OECD, 2004, Williams, 2006).

1.5.1: Diffusion Cells

Studies using skin mounted in diffusion cells are the most common method for *in vitro* determination of percutaneous penetration. This system is used in order to mimic the *in vivo* absorption and penetration of chemicals through the skin as closely as possible. The main principle is that a section of *ex vivo* skin can be mounted, stratum corneum facing up, above a receptor chamber containing a receptor fluid. Test compounds can then be applied to the skin surface. The compound can penetrate through the skin, and be recovered in the receptor fluid beneath the skin and the rate of penetration can then be determined.

Two main types of diffusion cell are used to measure in vitro percutaneous absorption; the static diffusion cell and the flow through diffusion cell. The original diffusion cells were static cells (Franz, 1975). These were so called because the cell consists of a receptor chamber, containing a fixed volume of receptor fluid, which remains in contact with the underside of the skin. In static cells, the receptor fluid is sampled by the removal of aliquots of the receptor fluid within the chamber at given time points to assess penetration, and replaced with the same quantity of fresh receptor fluid. Commonly used receptor fluids include aqueous saline or a mixture of ethanol and water.

The flow through diffusion cell (Bronaugh and Stewart, 1985) is an alternative system for measuring percutaneous absorption. The principle behind the flow through system is that the receptor fluid is constantly being removed from the receptor fluid chamber and replenished with fresh receptor fluid by an automatic peristaltic pump at a constant rate. When this system is used in conjunction with an automatic fraction collector, aliquots of receptor fluid can be collected at regular intervals, therefore eliminating the need for manual sampling of receptor fluids.

One advantage of the constant replenishment of receptor fluid beneath the skin surface in the flow through diffusion system is that the skin is continually being provided with fresh nutrient. This helps to maintain the viability of the skin for the duration of the experiment. Another advantage of the flow through system can be seen when using compounds that are known to penetrate rapidly are applied to the skin. If a fast penetrating compound is applied to the skin surface in a static cell, the chemical may penetrate through the skin so rapidly that a sufficiently large amount of the chemical may accumulate in the receptor chamber and reduce the concentration gradient across the epidermis. This effectively reduces further partitioning of the test substance into the skin and results in an underestimation of penetration (Bronaugh, 2004). However, the static diffusion cell system is still a very useful method for measuring absorption, particularly with chemicals that penetrate the skin poorly. This is because the receptor fluids can be collected at longer intervals in order to concentrate up the amount of

chemical within the receptor fluids so that it can be more easily detected. This is especially useful if ‘cold’ analysis methods are being implemented.

The receptor fluids most commonly used in the flow through diffusion system are saline, buffer, or a culture medium containing nutrients. This receptor fluid is typically aqueous, and so partitioning of more lipophilic compounds can be limited depending on their solubility in the receptor fluid phase. To overcome the issue of the solubility of lipophilic chemicals limiting percutaneous dermal absorption, receptor fluids can be supplemented with 2% (w/v) bovine serum albumin (BSA) (Surber *et al*. 1991, Dick *et al*. 1996). This helps to facilitate absorption of more lipophilic compounds through the skin and gives rates of penetration that more closely match those seen *in vivo* (Bronaugh, 2004). The use of 50% ethanol in water has also been used to facilitate absorption of more lipophilic compounds into the receptor fluid (Scott *et al*. 1987). However, ethanol: water has been shown to increase the permeability of skin to the penetration of water, and so it has been suggested that more physiological solutions, such as culture medium or saline are more favourable for diffusion studies (Wilkinson and Williams, 2002).

There are many variations on the flow through diffusion cell introduced by Bronaugh and Stewart, however, the fundamental design remains the same. One particular variation (used in the flow through studies of this thesis), is the Scott-Dick flow through diffusion cell (figure 1.4). In this system, it is

possible to run 15 diffusion cells in parallel, compared with only 7 cells in the Bronaugh and Stewart system.

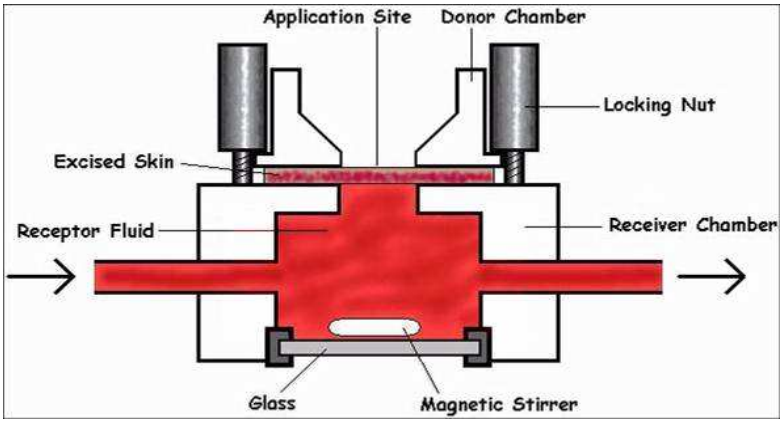

Fig.1.4. Schematic diagram of a Scott-Dick flow through diffusion cell (Wakefield, 2006)

The Flow through diffusion cell shown in figure 1.4 is designed so that the donor chamber can be un-occluded and exposed to ambient conditions similar to those that would be expected in vivo, or, the skin can be occluded after application of a test compound, for instance, in order to mimic the effects that clothing may have on dermal absorption. A collection chamber containing a carbon filter can be used to collect material which may evaporate from the skin surface over time. This is of particular importance when a volatile substance is being tested (Jewell *et al*. 2000). The flow through diffusion cells used for the purposes of investigations in this thesis were made from polytetralfluoroethylene (PTFE - Teflon), which is resistant to binding of compounds applied to the skin surface, which could affect dermal absorption (Bronaugh *et al*. 2001).

Upon termination of an *in vitro* dermal absorption study, the stratum corneum can be removed from the skin so that the amount of chemical within the stratum corneum can be determined separately to the viable epidermis. Chemicals remaning within the stratum corneum have been considered to be systemically unavailable due to the constant turnover of cells from basal skin layers upwards helping to remove chemicals from the skin by 'sloughing-off' of skin cells (Bronaugh, 2004). However, OECD guidelines on dermal absorption state that any test chemical remaning within the skin, including both the stratum corneum and the viable epidermis, should be considered systemically available until experimentally proven otherwise (OECD, 2004).

1.5.2: Skin Preparation

In vitro skin studies have been carried out using various skin preparations, including full thickness skin, split thickness skin (dermatomed skin) or epidermal membranes. The use of different skin thicknesses may produce differing absorption, depending on the test compound. For example, *in vitro* studies using full thickness skin sections have the ability to underestimate the absorption of a particular chemical into receptor fluid, particularly for more lipophilic chemicals, as these may become retained in the dermis (Bronaugh, 2000, Bronaugh, 2004). When a chemical penetrates the epidermis *in vivo*, it is systemically available due to the dense vasculature within the dermis. However, when full thickness skin is being used *in vitro*, the compound has to pass through both the epidermis and the dermis in order to reach the receptor fluid. Essentially, this means that a compound

has to penetrate further *in vitro* than it does *in vivo* to be considered systemically available.

The alternative method to using full thickness skin is to use dermatomed skin preparations or epidermal membranes. The process of dermatoming involves shaving a layer of skin (we use a depth of approximately 330μm), which separates the stratum corneum and the viable epidermis from the majority of the dermis. This enables the *in vitro* system for measuring dermal absorption to more closely model the situation *in vivo* (Hawkins and Reifenrath, 1986, USEPA, 1992, Bronaugh, 2004, OECD, 2004). Investigations have shown that there are no significant differences in dermal absorption between full thickness and dermatomed skin when using highly water soluble compounds (Dick and Scott, 1992, Moser *et al*. 2001). Further to this, no significant differences have been identified between full thickness and dermatomed skin with regard to the dermal penetration of caffeine (hydrophilic), whereas penetration of testosterone (lipophilic) was found to be 10 fold higher through dermatomed skin compared with full thickness skin (Wilkinson *et al.* 2006). Studies using other non-lipophilic chemicals, such as glycol ethers, ethoxyethanol and butoxyethanol have also demonstrated increased penetration through dermatomed skin compared with full thickness skin (Wilkinson and Williams, 2002, Wilkinson *et al*. 2006). This suggests that the lipophilicity is a highly important aspect to consider when assessing dermal penetration of chemicals.

1.5.3: Measurement of dermal barrier integrity

Prior to the start of a dermal penetration study, stratum corneum integrity should be checked once the skin has been prepared and placed in a diffusion cell to ensure that the skin hasn't sustained any damage during preparation. This is important to consider, because any damage to the skin could lead to increased penetration of a chemical through the skin. This is in coordination with OECD guidelines (OECD, 2004).

The method of membrane integrity measurement used for the purpose of the studies conducted in this project was electrical resistance across the stratum corneum. However, there are other methods that can be implemented, including trans-epidermal water loss (TEWL) measurements, and penetration of tritiated water (^{3}H).

Measurement of electrical resistance (kΩ) to an alternating (AC) current across the skin can be measured by attaching an AC impedance meter to electrodes that protrude from the outer walls of the donor and receiver chambers of the flow through diffusion cell. Prior to measurement of electrical resistance, physiological saline solution is applied to the skin surface, with the same saline solution in the receptor chamber. Following equilibration for 30-60 minutes, the electrical resistance between the donor and receptor chambers is determined. The general consensus is that skin is considered to be undamaged when the resistance is greater than 20kΩ (Diembeck *et al*. 1999, OECD, 2004).

TEWL involves measuring water loss from the stratum corneum (Oestmann et al. 1993). The theory behind this method is that damaged skin will give rise to increased TEWL due to reduced barrier integrity compared with skin that is healthy and intact (Nangia *et al*. 1998). TEWL is measured by placing two vapour pressure sensitive electrodes parallel to the skin surface. The vapour pressure gradient above the skin is then converted to water loss from across the stratum corneum ($g/m^2/h$) (Levin and Maibach, 2005). A rate between 4 and $10g/m^2/h$ is considered to be a normal rate of trans-epidermal water loss; however, this can potentially increase by up to 30 times if the stratum corneum is badly damaged (Charbonnier *et al*. 2004). The use of TEWL as a barrier integrity measurement has been questioned, as no correlation was identified between basal transepidermal water loss rates and the permeability of human epidermal membranes to tritiated water or sulphur mustard (Chilcott *et al*. 2002a). However, in contrast to the findings by Chilcott *et al,* TEWL has been shown to linearly correlate with tritiated water flux through full thickness pig skin *in vitro* (Elmahjoubi *et al*. 2009). Other recent studies have also suggested that TEWL is a useful indicator of skin barrier *in vitro* and *in vivo* (Tsai et al. 2003, Fluhr *et al*. 2006, Elkeeb *et al*. 2010).

Another method for assessing dermal membrane integrity is to determine the penetration of tritiated water through the skin (Heylings *et al*. 2001). The penetration of tritiated water can be determined prior to the application of the test chemical to the skin surface. However, one negative aspect of using this method is that skin sections in vitro decrease in viability over time, and so

the skin may deteriorate as a result of testing the penetration of the reference chemical (tritiated water) before being able to measure absorption of a test chemical. Due to this, it is possible that using a reference penetrant such as tritiated water may lead to an overestimate of penetration of a test chemical (Nangia *et al*. 1998, OECD, 2004). To overcome this problem, it is possible to apply tritiated water to the skin concurrently with, for example, a ^{14}C-labelled test chemical. Therefore, barrier function and penetration of the test compound can theoretically be measured simultaneously. However, this can only be implemented if the concentration of tritiated water is low enough to have no effect on the thermodynamic activity of the test compound (OECD, 2004).

1.5.4: *In vitro* stratum corneum tape-stripping

Tape stripping of the stratum corneum is a technique that can be carried out upon termination of a diffusion cell study. This method allows quantitation of the amount of the test compound remaining within the stratum corneum at the end of the exposure period, independently of the viable epidermis, dermis and basal skin layers.

Tape stripping involves applying a section of adhesive tape to the skin surface with gentle pressure, and subsequently removing it. Sequential tape strips are taken to remove successive layers of the stratum corneum. This can be a useful technique, because individual tape strips can be analysed to identify the amount of the test compound present in each layer of the stratum

corneum. The human stratum corneum is 10-20μm thick and requires approximately 15 tape strips to remove *in vitro*.

Despite the useful aspects of this method, its main limitation is the variability in the amount of corneocytes removed with each tape strip. Therefore, the number of cells removed may not be proportional to the amount of tape strips taken, and so the amount of corneocytes removed with each tape strip is likely to vary between skin samples.

Other factors which may also affect the amount of corneocytes being removed with sequential tape strips include the level of skin hydration, anatomical site and inter-individual variations in skin composition (Marttin *et al*.1996). The composition of the stratum corneum itself can also inhibit the accuracy of tape stripping. The stratum corneum has ‘furrows’ running across the surface, meaning that tape strips may not take cells from the same layer, because the cells from the base of these furrows will not be taken at the same time as those that are on the ‘peaks’ of the furrow (van der Molen *et al*. 1997).

1.6: Test Compounds

This project has focused on investigating the dermal absorption of compounds that can potentially be used to model absorption of a wider range of chemicals in real life scenarios. The compounds used for these *in vitro* studies were, benzoic acid, caffeine, testosterone, methyl paraben, chlorpyrifos and dichlorvos. Dermal absorption of sulphur mustard (HD) and

phorate were also investigated in order to compare absorption profiles of model compounds with more toxic substances.

1.6.1: Model compounds for dermal absorption

It is extremely useful when undertaking dermal absorption studies to identify the absorption profile of chemicals whose dermal absorption profiles are already well established. One of the major factors affecting dermal absorption is the physicochemical properties of the chemical being tested, and so assessing the penetration of chemicals with differing physicochemical properties; which also have well defined absorption profiles based on a wide range of studies will generate confidence in the data generated from absorption studies testing chemicals where knowledge of penetration is lacking. This is especially important if the data is being obtained using new equipment or different methods to ones used to generate the pre-existing data to which you are trying to compare. OECD guidelines also stipulate that in order to demonstrate the reliability of a test system for predicting dermal absorption, results for known test compounds should be in accordance with published literature (OECD, 2004).

Some compounds have become traditionally recognised as markers for assessing dermal penetration. These compounds include caffeine, testosterone, benzoic acid and methyl paraben, which have been used predominantly due to their differing physicochemical properties (van de Sandt *et al*. 2004, Wilkinson *et al*. 2006).

1.6.2: Caffeine

Caffeine (1, 3, 7 trimethylxanthine) is a xanthine alkaloid that is commonly found in everyday beverages such as tea and coffee. It is found in the beans, leaves and fruits of a variety of plants and is well known as a central nervous system stimulant in humans. Caffeine exerts its effect as a stimulant as it is a non selective antagonist of adenosine. Caffeine is similar in structure to adenosine, and so it blocks adenosine receptors and prevents adenosine from binding and eliciting its effects. Adenosine is important in energy transfer processes (as adenosine triphosphate (ATP) and adenosine diphosphate (ADP) and, under normal circumstances, decreases firing of cholinergic, dopaminergic, glutaminergic, and noradrenergic receptors. However, by binding to adenosine receptors, caffeine causes increased firing of these neurones, which leads to excessive stimulation as a result of caffeine intake (Daly and Fredholm, 1998).

Caffeine is a hydrophilic (Log *p* = -0.07) compound that has a moderate molecular weight (194.19). It has been used in a range of dermal absorption studies due to its physicochemical properties, where it has been compared with a variety of compounds with differing properties (Bronaugh and Franz, 1986, Greaves *et al*. 2002, van de Sandt *et al*. 2004, Wilkinson *et al*. 2006, Akomeah *et al*, 2007). Caffeine does not readily partition into the stratum corneum when in contact with the skin, predominantly due to the hydrophilic nature of caffeine, and the lipophilic nature of the stratum corneum. Despite this, once caffeine has penetrated the stratum corneum, it will readily partition into the more hydrophilic layers of the skin; the viable epidermis and

dermis. From here, caffeine can become systemically available. The stratum corneum is the main barrier to caffeine absorption and is therefore the rate limiting step for penetration (Kitson and Thewalt, 2000).

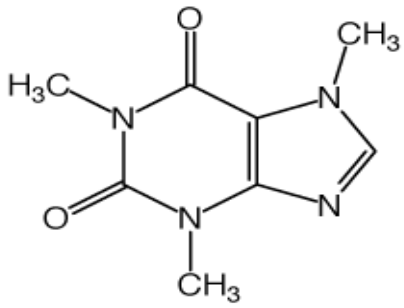

Fig.1.5. the structure of caffeine

A range of *in vitro* studies have been undertaken to assess the penetration of caffeine through excised sections of skin taken from a number of different species, including rat, pig, mouse and human ((breast and abdomen), Reifenrath *et al*. 1984, Bronaugh and Franz, 1986, Monti *et al*. 2001, Akomeah *et al*. 2004, Wilkinson *et al.* 2006, Duracher *et al*. 2009)). A multi-centre experiment involving 9 independent European laboratories was undertaken to assess inter and intra-laboratory variations in dermal absorption of model penetrants, including caffeine, through human skin *in vitro*. The total amount of caffeine found to be absorbed through human skin after 24 hour exposure (averaged over 9 laboratories) was 24.5 ± 11.6% of the applied dose (van de Sandt *et al*. 2004).

1.6.3: Benzoic acid

Benzoic acid has also been used as a model penetrant in a number of dermal absorption studies, utilising excised skin from a variety of different

species including human and rat skin (Reifenrath *et al*. 1991, Yoshida *et al*. 2000, van de Sandt *et al*. 2004, JB Nielsen *et al*. 2009).

It is the simplest carboxylic acid containing a carboxyl group bonded directly to a benzene ring (figure1.6). It is a weak acid, commercially produced by partial oxidation of toluene with oxygen and its salts are commonly used as a food preservative. Benzoic acid differs from caffeine as it has a relatively low molecular weight (122.12) and is also a more lipophilic chemical (log p = 1.87).

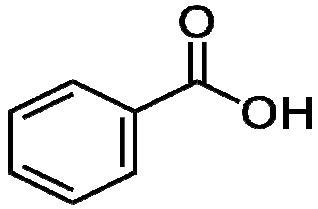

Fig.1.6. the structure of benzoic acid

Due to benzoic acid being a moderately lipophilic compound, it is more likely that it will partition more readily from the skin surface into the stratum corneum. However, once it has penetrated into the stratum corneum, it will be unable to partition as readily into the viable epidermis and dermis where it would become systemically available. The ability of benzoic acid to penetrate the skin faster than more hydrophilic compounds such as caffeine was demonstrated by Nielsen *et al*. 2009. Caffeine was found to have a lag time of approximately 7 hours when applied to human skin as a 4mg/ml dose, however, the same concentration of benzoic acid produced a lag time of only 1.5 hours. This study also demonstrated that almost double the amount of benzoic acid was found to be recovered from within the skin after 24 hour

exposure compared with caffeine. However, nearly 5 times as much benzoic acid was recovered in the receptor fluid after 24 hour exposure.

1.7: Chemicals of Interest – Surrogate compounds

Dichlorvos and chlorpyrifos were chosen due to their differing physicochemical properties, allowing a range of exposure scenarios to be investigated. These chemicals were chosen as a surrogate for nerve agent exposure because they are both organophosphates and have a similar mechanism of action to highly toxic nerve agents such as VX and sarin.

1.7.1: Chlorpyrifos

Chlorpyrifos (O, O-diethyl-O-(3, 5, 6-trichloro-2-pyridyl) phosphothioate) is a non systemic toxic organophosphate insecticide which is commonly used in for agricultural purposes in a number of countries, including the USA. It is a lipophilic compound (log P = 4.96), and also has a relatively high molecular weight (MW =350.59). Chlorpyrifos is in a P=S form (inactive as an anticholinesterase). This means that it has to undergo oxidative desulphuration via cytochrome P450 (CYP450) enzymes; predominantly through CYPs 2B6, 3A4, 2D6, and 3A5 in the liver to convert into its oxon (P=O) form in order to elicit its more potent toxic effects as an anticholinesterase (Mutch *et al*. 2006).

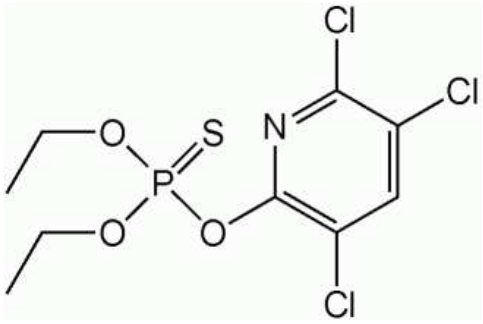

Fig.1.7. the structure of chlorpyrifos

Due to its physicochemical properties, it has been suggested that chlorpyrifos can partition into the stratum corneum *in vitro*, and create a 'reservoir' of penetrated chlorpyrifos that can be released over a long period of time. It has also been shown that the solvent vehicle in which chlorpyrifos is delivered can have a significant impact on its rate of dermal penetration (Griffin *et al*. 2000).

Like many other organophosphate compounds and nerve agents, the acute toxic effects of chlorpyrifos exposure are primarily due to inhibition of the enzyme acetylcholinesterase. This enzyme is responsible for breaking down the neurotransmitter acetylcholine, into inactive metabolites, choline and acetate at the synaptic cleft of the neuromuscular junction. Therefore, inhibition of acetylcholinesterase results in an excessive accumulation of active acetylcholine in the synapse and at the neuromuscular junction. This leads to over stimulation and potential paralysis of muscarinic and nicotinic receptors. Severe intoxication can potentially lead to death, usually as a result of respiratory failure.

1.7.2: Dichlorvos

Dichlorvos (2, 2-dichlorovinyl dimethyl phosphate), like chlorpyrifos, is an organophosphate compound that is widely used in agriculture as a pesticide. This compound was selected because, unlike chlorpyrifos, it is in a P=O form, meaning it does not require metabolism to elicit its toxic effects. Dichlorvos also has a mechanism of action similar to that of nerve agents.

Dichlorvos has different physicochemical properties to chlorpyrifos, and so are both interesting compounds to compare and contrast for the purposes of identifying different exposure profiles for *in vitro* absorption studies. Dichlorvos differs from chlorpyrifos in a number of ways. As already mentioned, dichlorvos is an oxon (P=O), and therefore does not require metabolism by cytochrome P450 enzymes to exert toxicity.

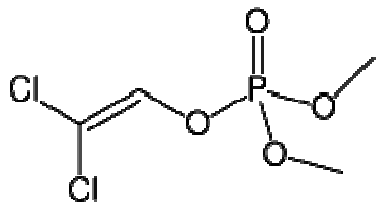

Fig. 1.8. the structure of Dichlorvos

Dichlorvos is also less lipophilic than chlorpyrifos (log P = 1.47), and also has a lower molecular weight (MW = 220.98). Therefore, it is likely that dichlorvos will not partition into the stratum corneum as readily as chlorpyrifos, however, it is more likely to enter into systemic circulation once it has penetrated through the epidermis where it will have a greater affinity for the more hydrophilic sections of the skin.

To my knowledge, there are few published studies regarding the dermal penetration and distribution of dichlorvos *in vivo* or *in vitro*. However, the toxicity of dichlorvos applied to rat skin *in vivo* has been previously investigated (Luty *et al*. 1998). In this study, histopathological changes were found in lungs, lymph glands, thymus, liver, heart and kidneys of rats exposed to dichlorvos for 4 hours a day for 4 weeks at concentrations of 37.5mg/kg (1/2 LD50), or 7.5mg/kg (1/10 LD50). This shows that dichlorvos can penetrate the skin barrier, however, no information was provided on the fate of dichlorvos within the skin itself. The fact that dichlorvos has been found to be dermally absorbed suggests that it is a highly important compound to study in terms of dermal exposure. The data generated for this thesis will provide useful, novel information on the dermal absorption and distribution of dichlorvos through human skin *in vitro*.

1.7.3: Phorate

Phorate (O, O-diethyl S-ethylthiomethyl phosphorodithioate), is a highly toxic organophosphate insecticide. It is a lipophilic chemical (Log p = 3.56) with a moderately high molecular weight (260.38) and a very low vapour pressure (0.000638 mmHg at 25˚C).

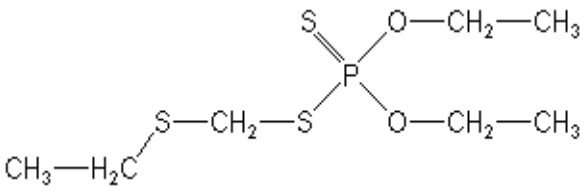

Fig.1.9. Structure of Phorate

It would be reasonable to assume that phorate would readily partition into the stratum corneum due to its lipophilicity. Despite this potential for rapid

penetration into the upper skin layers, it is likely that penetration into the viable epidermis and dermis would be slow, as phorate will have a greater fugacity for the lipophilic sections of the skin than for the more hydrophilic basal skin layers. Therefore, the viable epidermis and dermis are likely to be the rate limiting barrier for systemic absorption.

At present, and to my knowledge, no studies have been undertaken to investigate the dermal absorption and distribution of phorate *in vitro* or *in vivo*. Due to the fact that little is known about dermal absorption of phorate, and that it is a lipophilic liquid (similar to HD), this was chosen as a chemical to investigate to compare with dermal absorption of HD, as well as absorption of lipophilic solids such as chlorpyrifos.

1.8: Bioactive agent

1.8.1: Sulphur Mustard (HD)

Sulphur mustard (2, 2'-dichloroethyl sulphide) is a potent vesicating agent that causes blistering of the skin and mucous membranes. It was first used as a chemical warfare agent by Germany in the First World War against French troops at the Ypres, Belgium in 1917. Subsequently, HD has been reportedly used in more than 10 conflicts, including the Iran-Iraq conflicts of the 1980's (Saladi *et al*. 2005). HD may be absorbed through respiration, dermal contact, or through the outer membrane of the eye. It can also be absorbed through the GI tract if ingested. HD is a lipophilic chemical (Log p = 2.4) with a molecular weight of 159.08. HD also has a low vapour pressure

(0.1059), meaning it is a poorly volatile compound which remains in contact with the skin for a long time after deposition

.

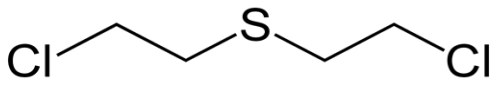

Fig.1.10. the structure of sulphur mustard (HD)

Due to HD being a lipophilic compound, it preferentially enters the lipophilic stratum corneum but is slow to penetrate further into the more hydrophilic epidermis and dermis. It has been shown that HD forms a 'reservoir' within epidermal membranes following dermal exposure in human (in vivo and in vitro, and pig skin (Smith *et al*. 1919, Hattersley *et al*. 2008). Smith *et al*. 1919 showed that, despite rapid absorption of HD into the skin, it was possible to extract HD from within the skin by washing with a low-volatility solvent followed by washing with soap and water up to 10-15 minutes after exposure. This suggested that a large proportion of the dose remained on or near the skin surface. The study by Hattersley *et al*. 2008 confirmed the presence of a skin reservoir up to 24 hours after HD exposure to dermatomed human and pig skin (0.5mm thickness). The effectiveness of solvents to extract the available dose from on, or near the skin surface was also demonstrated (using acetonitrile).

The primary toxic effects of HD are localised as a result of its physicochemical properties. It has been estimated that 4.5μg/cm^2 of HD vapour and 20μg/cm^2 is sufficient to cause severe blistering of the skin surface (Chilcott *et al*. 2001). This suggests that the mechanism by which

HD acts as an incapacitating agent is far more important to understand than the ability of HD to cause death. This was further demonstrated by the fact that only 2% of soldiers exposed during World War I were killed as a result of direct exposure to HD (Maynard *et al*. 1991).

Previous studies have investigated absorption of HD through human skin *in vivo* and *in vitro* (Smith *et al*. 1919, Chilcott *et al*. 2001, Hattersley *et al.* 2008), decontamination of HD from pig ear skin and human skin (Chilcott *et al*. 2001), and also the effect of barrier creams on absorption of HD through human skin *in vitro*, and through pig skin *in vitro* and *in vivo* (Chilcott *et al*. 2007).

Decontamination of HD from heat separated human skin was found to be most effective using fuller's earth when compared to ambergard or BDH granules. However, decontamination of pig ear skin was marginally more effective using ambergard when compared with fuller's earth. Chilcott *et al.* 2001 suggested that pig skin may not be a suitable model for decontamination of human skin exposed to HD.

Barrier creams have been shown to be effective at preventing, or reducing the localised effects of HD on the skin, both in human (*in vitro*), and in pig (*in vitro* and *in vivo*). Novel perfluorinated barrier creams in particular, gave up to an 18 fold reduction in absorption rate through human skin *in vitro*, and reduced the amount of HD penetrating the skin by 95% (Chilcott *et al*. 2002). Similar results using perfluorinated barrier creams were obtained using pig skin *in vivo* and *in vitro* (Chilcott *et al*. 2007).

These studies have generally been undertaken from a military perspective in terms of the potential of HD as a chemical warfare agent and how to prevent or reduce the effects of HD in contact with military personnel. From a modelling perspective, methyl salicylate has similar physicochemical properties to HD, in terms of molecular weight, vapour pressure and water solubility. This has been shown to be a good model for HD absorption *in vitro* through the isolated perfused porcine skin flap, with HD having approximately a 1.5 to 2 fold higher absorption rate than methyl salicylate (log p – 2.55, molecular weight – 152.15) (Riviere *et al*. 2001).

1.9: Current knowledge of dermal chemical absorption from civilian perspectives

Few studies have been conducted specifically investigating the dermal absorption of chlorpyrifos and the effects of different application vehicles on absorption rates *in vitro*; however, one particular study (Griffin *et al.* 2000) has investigated the effect that donor vehicles (ethanol and commercial concentrate) have on the dermal absorption of chlorpyrifos. This study indicated that the solvent vehicle used can affect percutaneous absorption of pesticides, with absorption from ethanol being slower than from a commercial concentrate. Some *in vivo* studies have also been carried out using human volunteers in order to investigate dermal absorption by identifying urinary metabolites produced as a result of chlorpyrifos absorption (Mueling *et al*. 2005, Griffin *et al*. 1999). The main urinary metabolite produced from the metabolism of chlorpyrifos is 3, 5, 6 trichloropyridinol (TCP). This is mainly

carried out by CYP3A4, CYP2D6 and CYP2C19. Studies using lymphoblastoma cells expressing human cytochrome p450 isoforms (CYP450) have identified CYP1A2, 2B6, 2C9*1, 2C19 and 3A4 as being the main isoforms that are involved in metabolism of chlorpyrifos (Tang *et al*. 2001). The metabolism of chlorpyrifos has also been investigated using human hepatocytes (Choi *et al*. 2006). This study has suggested that the liver could play an important role in detoxifying chlorpyrifos, as no chlorpyrifos-oxon was found in the hepatocytes treated with chlorpyrifos and chlorpyrifos-oxon.

In contrast to modelling civilian scenarios of chemical exposure, some studies have been conducted at the defence science and technology laboratories (DSTL) using similar approaches to those being implemented in this project in order to investigate the dermal absorption of chemicals such as VX (Dalton *et al*. 2006) and HD (Chilcott *et al*. 2001). The latter of the two studies investigated HD absorption, and decontamination procedures for HD exposure in both human and pig skin. This showed that pig skin is a good model for dermal absorption in humans, but is a relatively poor model for testing decontamination systems. The dermal route of absorption is of particular importance for sulphur mustard exposure as this induces local skin lesions when in contact with the skin.

At present, little or no information exists regarding the dermal absorption of chemicals that is specific to environmental exposure of members of the public. The majority of studies relate to occupational exposure or to military personnel. Much of the available data on dermal absorption of chemical

compounds focuses on military exposure to nerve agents and occupational exposure to pesticides. The public may be exposed to an accidental release of a chemical in the form of a spray or vapour, which may have the potential to deposit on the skin surface. This type of exposure scenario can be mimicked using a finite dose applied to skin in diffusion cell studies. Therefore, it is important to investigate dermal penetration of chemicals from a civilian perspective, because it is known that organophosphate compounds can penetrate the skin and enter systemic circulation, and so it is important to be able to model how significant this route is when compared to other routes of exposure, such as inhalation.

Both *in vivo* and *in vitro* studies using rodent, pig and human volunteers have been carried to investigate the percutaneous penetration of a range of different pesticides; however, few studies put their results into a civilian context. Absorption of carbamate pesticides, such carbofuran, carbosulfan and furathiocarb have been studied with rat skin using static diffusion cell systems (Liu *et al.* 2003) in order to assess the usefulness of in vitro rat skin studies for predicting dermal absorption of pesticides. This study showed that the amount of pesticide penetrating the skin increased with dose and water solubility, although rat skin is not a particularly good model for human exposure.

Studies investigating the effect of donor vehicle on in vitro percutaneous penetration have been carried out using methyl parathion (Sartorelli *et al.* 1997), and lindane, an organochlorine insecticide, both in both *in vivo* and *in*

vitro (Dick *et al*. 1997a, Dick *et al*. 1997b). In the study by Sartorelli et al., it was found that significantly higher dermal penetration of methyl parathion occurred from a commercial concentrate than from an equivalent dose in acetone. The lowest percentage of absorption of lindane through skin was also found to be from an acetone vehicle. This may be due to the fact that acetone is a highly volatile chemical (vapour pressure 232 mm Hg @ 25˚C), and so the dose vehicle may evaporate before the compound of interest has the opportunity to penetrate the skin surface.

The effects of donor vehicle on the in vitro dermal absorption of epoxiconazole, fenpropimorph and metsulfuron-methyl (all fungicides) through human skin have also been investigated (Aust *et al*. 2007). This study showed that absorption profiles from different vehicles (ethanol: water and commercial concentrate) were quite similar, with absorption of fenpropimorph being greatest, and absorption from metsulfuron-methyl being lowest from both donor vehicles.

Some *in vivo* and *in vitro* studies investigating dermal absorption of Malathion, (another phosphorothioate insecticide) have been carried out which are of relevance to civilian scenarios. Firstly, the rate of Malathion absorption through skin in vivo has been determined (Boutsiouki *et al*. 2001). In this study, microdialysis was used to assess the dermal penetration of Malathion, whilst the effect of local blood flow on systemic uptake of Malathion was also investigated. The results from this study showed that Malathion can be dermally absorbed, and also that increasing local blood

flow can increase systemic uptake. Therefore, cooling of the skin locally to where contact is made with the chemical can reduce systemic uptake. Another study has investigated *in vitro* dermal absorption of Malathion from cotton fabrics (Wester *et al*. 1996). This study showed that dermal absorption from wetted cotton (to simulate sweating) increased in comparison to absorption from dry cotton. The effect of clothing on the absorption of chemicals through the skin is an important consideration when investigating the effects of chemical exposure in the civilian sector.

1.10: Aims of the study

The overall aim of this project was to investigate the dermal absorption of a range of chemicals (caffeine, benzoic acid, dichlorvos and chlorpyrifos) with different physicochemical properties in a variety of vehicles (IPA, IPM and PG) in order to assess factors affecting dermal absorption *in vitro*. The absorption profiles of these chemicals can then be ranked against the absorption profile of a 'bioactive agent' (HD) to identify whether the chemicals used in these studies could potentially be used to predict the outcomes of exposure to highly toxic chemicals *in vivo*. Low dose concentrations were used to mimic low level exposure of civilians who may be exposed to chemicals on the periphery of an accidental or deliberate chemical release. To continue the assessment of risk for chemical exposure to civilians, the influence of 'everyday' clothing (cotton shirt material) was also investigated for the purpose of reducing dermal absorption of chemicals in contact with the skin, as the majority of published data are concerned with

assessing the protective nature of personal protective equipment and clothing designed specifically to protect the skin from chemical exposure.

Chapter 2

General Methods

2: General methods

2.1: The flow-through diffusion cell system

In this system, female human breast skin from mammoplasty was placed on the receptor chamber of a PTFE (Teflon) flow through diffusion cell (adapted from a Scott-Dick flow through diffusion cell) with the stratum corneum facing up so that a test chemical could be applied to the skin surface. The skin samples are secured in place by attaching the donor chamber to the receptor chamber using threaded nuts. The application area for these cells is 0.64 cm^2. Prior to the skin being secured in place, each skin sample was dermatomed to produce a skin section approximately 320μm in depth, containing the stratum corneum, the entire viable epidermis, and the upper dermis. Once the skin samples were clamped to the diffusion cell, a receptor media (Minimum Essential Medium Eagle (MEM) (supplemented with 2% (w/v) bovine serum albumin (BSA) for lipophilic chemicals only) was pumped continuously beneath the skin through an electric peristaltic pump (at a flow rate of approximately 1.5ml/hour) with continuous stirring using magnetic followers placed in the receptor fluid chambers, and collected in individual collection tubes with an autosampler every hour for 24 hours.

Prior to the application of the test compound to the skin surface, the integrity of the skin was assessed by measuring the electrical resistance to an alternating current across the skin sample. A solution of 0.9% (w/v) saline was applied to the skin surface and left to equilibrate for 30 minutes before measurement. As a general rule, the skin was considered to be undamaged if the resistance measured was greater than 40kΩ. Cells in

which resistance was found to be below 40kΩ were still included in the actual experiment, but not used for the purposes of analysis. The saline solution was then removed so the dose could be applied to the surface of the skin.

For in vitro dermal diffusion studies, it is possible to use one of two dosing regimes; these are infinite dose or finite dose. Infinite dosing involves application of a large volume of a chemical at a high concentration so that the dose concentration on the skin surface does not deplete significantly over time, whereas finite dosing involves application of a small volume of chemical to the skin surface to more closely mimic exposure *in vivo* (specific details on dosing for each study is stated in each results chapter).

For some studies where volatile vehicles were used, attachments were placed above the donor chamber containing a carbon filter, in order to trap any evaporated dose. This ensured maximal recovery of the applied dose material for a more accurate mass balance study.

For flow-through diffusion studies undertaken to assess the ability of 'everyday' clothing (cotton shirt) to reduce absorption of organophosphates, the clothing was held in place above the skin surface by using the donor chamber attachment more commonly used to contain carbon filters to trap volatile chemicals. By screwing the donor chamber attachment over the cotton shirt material ($1cm^2$), a 1mm air gap (approximate) was created between the skin surface and the clothing. This was done deliberately to

mimic how clothing fits in ‘real life’, as usually clothing is not completely skin-tight. Once the clothing had been screwed into place, the dose (10µl/cm^2) was applied to the clothing, which resulted in the clothing ‘sticking’ to the skin surface briefly while the dose spread out over the clothing. Upon removal of the clothing, the donor chamber attachment was removed, and the clothing was placed in a large scintillation vial containing 10ml of scintillation fluid. This was left for at least 36 hours to allow the chemical to be desorbed.

At the end of the experiment, the collection tubes containing receptor fluid samples taken hourly were capped and frozen. Tissue swabs using aqueous teepol (3% v/v) were used to wash both the skin surface/donor chamber (to measure the amount of test compound remaining unabsorbed) and the receptor fluid chamber in triplicate. Tape strips were also taken in order to separate the stratum corneum from the rest of the skin sample to identify how much of the applied compound remained in the stratum corneum, which could potentially act as a reservoir for further systemic penetration over longer periods of time. Usually no more than 15 tape strips were taken before the stratum corneum completely separated from the rest of the epidermis. Once the tape strips had been taken, the remaining skin sample was added to 2ml of 1.5mol/L potassium hydroxide in ethanol: water (4:1 v/v) in a scintillation vial and left overnight to digest (providing the compound was radiolabelled).

If the compound applied to the skin was radiolabelled, samples from the receptor fluids, tissue swabs, carbon filters, skin digests and tape strips were added to 10ml scintillation fluid (Optiphase HiSafe 3, Perkin Elmer) and radioactivity measured on a liquid scintillation counter (Packard Tri-Carb 2100TR liquid scintillation analyser). If the compound was not radiolabelled (dichlorvos and phorate), then the samples collected were analysed using gas chromatography-mass spectrometry (GC-MS).

2.1.2: Scintillation counting and data interpretation

Samples obtained from studies using ^{14}C labelled chemicals were analysed using a scintillation counter. The liquid scintillation counter measures ionising radiation emitted from samples placed within the counter. The samples produced in each study were added to a liquid scintillation 'cocktail' containing benzene and scintillant additives. Beta particles emitted from each sample transfer their energy to solvent particles within the scintillation fluid, which in turn transfer energy to the scintillant molecules. It is these molecules which become 'excited' and disperse the energy created by fluorescing.

The data produced by the liquid scintillation counter is interpreted as disintegrations per minute (DPM). The DPM corresponds to the number of atoms that have decayed in one minute. The DPM measured in the sample can be converted into an absolute amount of the test compound of interest with respect to the specific activity and the applied dose, since the specific

activity relates to the number of decays per second, per amount of substance.

The average DPM of 5 dose solutions was taken to be the amount of test compound applied to each skin surface, with the total amount recovered being relative to this average dose for each individual diffusion cell. Each receptor fluid sample was measured in whole and added to 10ml scintillation fluid to avoid the potential for quenching (loss of fluorescence). This can occur if too much radiolabelled sample is added to a volume of scintillation fluid leading to reduced efficiency of the scintillation fluid (dilution quenching). The DPM obtained from each receptor fluid sample was converted into a percentage of the total dose applied and then plotted as a cumulative absorption curve against time. From this cumulative absorption profile, it was possible to calculate the maximum absorption rate (from the linear portion of the curve) and also the lag time. The DPM remaining on the skin surface, within tape strips, in the skin membranes and absorbed in the receptor fluid over 24hrs were measured as a percentage of the applied dose to determine the dose distribution in all compartments.

2.1.3: Chemicals used in flow through diffusion studies

Isopropanol (propan-2-ol) 99.8% (purchased from Fisher Scientific).

Isopropyl myristate Purum,>98% (Sigma-Aldrich)

Propylene glycol, Puriss >99.5% (Sigma-Aldrich)

4-^{14}C Testosterone in ethanol (specific activity 1.98MBq/mmol), (NEN, Boston, MA)

1-methyl-^{14}C Caffeine, specific activity 1.9GBq/mmol (Perkin Elmer Life Sciences, Boston, MA)

^{14}C Benzoic acid (>95% purity) purchased from Sigma Aldrich

^{14}C Chlorpyrifos (pyridine-2 6-^{14}C), specific activity 370-740MBq/mmol, was purchased from American Radiolabelled Chemicals Inc.

Dichlorvos (1g), purchased from Greyhound Chromatography and Allied Chemicals, Birkenhead.

Deuterated dichlorvos (dimethyl - D^6), was purchased from Chem Service Inc, West Chester, PA, USA.

Receptor fluid was made up of MEM (Sigma-Aldrich) at a concentration of 9.6g/l in sterilised water. Sodium hydrogen carbonate ($NaHCO_3$) (Sigma-Aldrich) was also added to a final concentration of 2.2g/l, along with Gentamycin (Sigma Aldrich), at a concentration of 200µg/l. When using particularly lipophilic compounds such as chlorpyrifos, BSA was added to the receptor fluid at 2% w/v. The pH of the media was adjusted to 7.4 using 1M hydrochloric acid (Fisher Scientific).

Potassium hydroxide (Sigma-Aldrich) added to 4:1 ethanol: water (v/v) at a concentration of 1.5M was used to solubilise skin samples prior to addition of scintillation fluid ready for scintillation counting. Teepol (purchased from VWR International) was used at a concentration of 0.5% in warm water to remove excess dose from the skin surface and also for the receptor chamber swabs. The scintillation fluid used was Optiphase ‘HiSafe III’ (purchased from Fisher Scientific).

2.2: Static cell diffusion experiments

Static diffusion cell studies were carried out at dstl, and accounted for all of the studies conducted using sulphur mustard and phorate. Static cells are widely used to predict *in vivo* outcomes for dermal absorption of a variety of different chemical compounds.

Static diffusion cell experiments were conducted in order to identify the dermal absorption profile of sulphur mustard (HD) through full thickness human skin compared with absorption through full and split thickness pig abdomen skin. Also, an investigation was undertaken to identify the 24-hour dermal absorption profile of phorate through split thickness pig abdomen skin.

2.2.1: Chemicals used in static diffusion studies

Sulphur Mustard (synthesised by Dstl).

Phorate 0.1g (purchased from QMX laboratories).

Deuterated phorate D^{10} (O, O-diethyl –d10) (QMX Laboratories)

Ethanol, 99.5% absolute (Sigma-Aldrich)

HPLC grade Methanol (Sigma-Aldrich)

Isopropanol (propan-2-ol) (Fisher Scientific)

Soluene 350 (Perkin Elmer)

'Ultima gold' Scintillation fluid (Perkin Elmer)

The receptor fluid used in these studies was made by mixing ethanol with water (50:50 v/v). Each receptor fluid chamber was filled with 5ml of pre-warmed receptor fluid. Each time an aliquot (20µl) was taken from the

receptor fluid during the course of the experiment, it was replaced with the equivalent amount of fresh receptor fluid.

Skin samples were digested in 20ml of soluene (an organic based solubilisation fluid formulated with toluene) for at least 72 hours, or until the skin was completely dissolved. Aliquots from the skin digests were taken (20µl) and added to scintillation fluid (5ml) ready for analysis. Cotton wool swabs of the skin surface were soaked in 20ml of isopropanol (IPA) for at least 72 hours, 20µl aliquots of these were also added to 5ml scintillation fluid for analysis.

2.2.2: Human breast skin preparation

Human breast skin samples were obtained from four skin donors (Biopredic International) and used in experiments conducted at Dstl – Porton Down. Prior to studies being commenced, all human skin samples were prepared by removing any excess subcutaneous fat and blood from the skin before being cut into sections using scalpel blades and frozen at -80°C in aluminium foil ready for immediate use in each experiment. All human breast tissue was used as full thickness for the purpose of static diffusion experiments.

2.2.3: Pig skin sample preparation

Five domestic female pigs (5 week old, weanling pigs, supplied by Dstl) were sacrificed and the abdomen skin removed from each in order to be used in the remaining three static diffusion studies to be conducted at Dstl. The skin from each pig abdomen was cut into sections and prepared as full or split thickness. The split thickness skin was dermatomed using a hand-held, gas

powered dermatome to approximately 500 microns in thickness. This thickness was used in order to prevent leakage of receptor fluid through to the stratum corneum due to the hair follicle depth in pig skin. The skin was then wrapped in aluminium foil and stored at -80°C separately until needed for each experiment. The remaining skin was prepared by removing excess fat and muscle tissue from the subcutaneous section of the skin. The skin was also shaved using electric hair clippers in order to reduce the amount of hair to which the applied compound could stick to and prevent skin contact. The skin was then wrapped in aluminium foil and frozen under the same conditions as the dermatomed skin.

2.2.4: Experimental procedure

Prior to the start of each experiment, skin samples were removed from the freezer and allowed to defrost naturally at room temperature. Static diffusion cells made from glass (5ml receptor chamber, 2.54cm^2 receptor chamber surface area) were used in each experiment. Skin samples were carefully placed stratum corneum side up, directly above the receptor chamber, and then clamped firmly in place with the donor chamber compartment. Once the skin was held in place, the receptor chamber was filled with 50:50 v/v ethanol: water using a syringe and the volume of each receptor fluid chamber was recorded separately to account for any differences between individual cells. The diffusion cells were set up on heated plates set to 32 ± 1°C within a fume cupboard. Each heated plate (4 in total, incorporating 6 static cells each) was mounted on a magnetic stirring plate. Magnetic stirrers were placed in each receptor fluid chamber and the skin samples were then left overnight in the

static cells to equilibrate. On the morning of the experiment, the receptor fluid in each receptor fluid was replaced with fresh ethanol: water that had been pre-warmed in the water bath at 37°C.

The test compound of interest was applied to the skin surface and left in contact for the necessary amount of time required for the experiment (24 hours or 1 hour). At the initial time of application of the test compound to the skin, a 20µl sub-sample of the receptor fluid was taken, placed into individual 10ml scintillation fluid vials, and replaced with 20µl of fresh media. This process was repeated at 30 minutes after application of the test compound, and then hourly for the first 6 hours of the experiment. Following on from this, sub-samples of media were then taken at 20, 22 and 24 hours after the test compound was administered to the skin surface.

For the purposes of the clothing studies, the cotton shirt material was cut into squares to fit the application area (2.54cm^2). Prior to the clothing being placed over the skin, a 1mm x 1mm stainless steel washer was placed on the skin surface to provide a 1mm air gap between the clothing and the skin surface. The clothing was placed on top of the washer before the dose (20µl) was applied to the clothing. Once the dose had been administered, a stainless steel weight was placed over the top of the clothing in order to keep it in place above the skin surface. Upon removal of the clothing after 1 hour exposure, the stainless steel weight was removed and swabbed with 5% soap solution to remove any dose that may have made contact with the weight. The clothing

was placed in a glass wheaton vial containing 20ml of HPLC grade methanol, and left to be desorbed for at least 24 hours.

After the final aliquot of receptor fluid was taken at 24 hours after application, the experimental procedure was terminated. This involved swabbing the skin surface with cotton wool soaked in 5% soap solution, and then repeating this step with dry cotton wool to remove any remaining dose from the skin surface. The two swabs taken for each skin sample were then put into 20ml glass wheaton vials and 20ml of HPLC grade methanol was added to each vial to allow the dose recovered on the swabs to be desorbed. The remaining skin from each static cell was also put into individual 20ml glass wheaton vials, with 20ml of soluene added to each. The cotton wool swabs and skin samples were then left for at least 72 hours until the skin had dissolved. Following this period, 20µl samples from each glass wheaton vial were added to labelled scintillation fluid vials filled with 10ml of 'ultima gold' scintillation fluid (Perkin Elmer).

2.3: Gas chromatography-mass spectrometry (GC-MS)

GC-MS is a method that can be implemented to identify and quantitate substances within a test sample. The gas chromatograph implements a capillary column, which separates molecules within a sample as they travel along the column following injection through a high temperature sample injector. The separated molecules take different amounts of time to be eluted from the GC column; this is called the retention time. As a result of these molecules having different retention times due to their different molecular

properties, the mass spectrometer (MS) can capture, ionise and detect each molecule separately.

The ionisation method used to analyse samples of dichlorvos obtained from dermal penetration studies was electron impact ionisation (EI). In this method, sample molecules collide with high energy electrons at high speed. These collisions cause the sample molecules to become fragmented and ionised. These fragments are then detected based on their mass to charge ratio. Results obtained were analysed by selected ion monitoring (SIM). This method of analysis involves selecting the most abundant fragments from a compound of interest to monitor. This is advantageous over a full scan of all fragments, because SIM reduces the detection limit by only looking for selected ions. This also allows more scans per second to take place and reduce the analysis time. To make sure that the fragments being detected were the correct ones, samples of dichlorvos were spiked with a known concentration of deuterated (D^{-6}) dichlorvos as an internal standard. By identifying the ion fragments from the deuterated dichlorvos, it was possible to compare the ion ratios from the dichlorvos in each sample against a known reference standard.

The GC-MS conditions used to analyse samples of dichlorvos was as follows:

Column: 30m x 0.25mm x 0.25ìm Rtx-5
GC Conditions:
Injector Temp: 220˚C
Oven Temp Programme:
50˚C hold 1 min: 30˚C/min to 250˚C hold 1min
Mass Spec Conditions:
Mass Spec: DSQ II Single Quadrupole

Operating Mode: Electron Impact Ionisation - EI, Selected Ion Monitoring
SIM Ions:
Dichlorvos: 220, 185, 109
Dichlorvos D^{-6}: 226, 191, 115

2.3.1: Sample preparation

1ml aliquots of each receptor fluid sample were taken, to which 10µl of internal standard (deuterated dichlorvos (d_6) was added at a concentration of 20ng/ml. Ethyl acetate (1ml) was then added to each individual sample and shaken vigorously for 10 seconds. Each sample was then thoroughly vortexed for 30 seconds and centrifuged at 1500rpm for 5 minutes. The supernatant was then removed from each sample and added to a glass vial ready for injection on the GC-MS. For the skin samples, each section of skin was cut into small pieces and homogenised in 1ml of ethyl acetate. Skin surface swabs were soaked in 2ml of water for 24 hours and vortexed thoroughly for 30 seconds. Tissues were then squeezed to remove any excess fluid. The excess fluid was then added to 1ml of ethyl acetate and the same procedure as mentioned above for the receptor fluid samples was carried out. Standards were produced to run on the GC-MS prior to analysis of the samples, ranging in concentration from 200ng/ml to 1ng/ml. All samples collected were diluted accordingly to fit within this range for analysis. An example of a dichlorvos calibration standard curve is shown in figure 2.1.

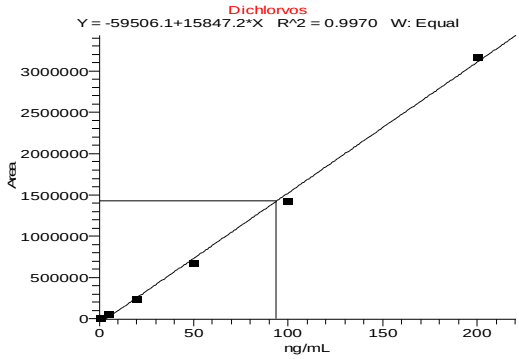

Fig 2.1. Dichlorvos calibration standard curve obtained from GC-MS analysis

The sample standards generated were analysed on the GC-MS prior to experimental samples analysis. Once the experimental samples had been analysed, it was then possible to extrapolate the results to the standard curve of known concentrations of dichlorvos (shown in figure 2.1). This made it possible to ascertain the concentration of dichlorvos in each experimental sample. In some cases, samples required dilution to fit to into the standard curve range, and in these cases, the result from the GC-MS were multiplied up to give the total concentration present in the whole sample recovered.

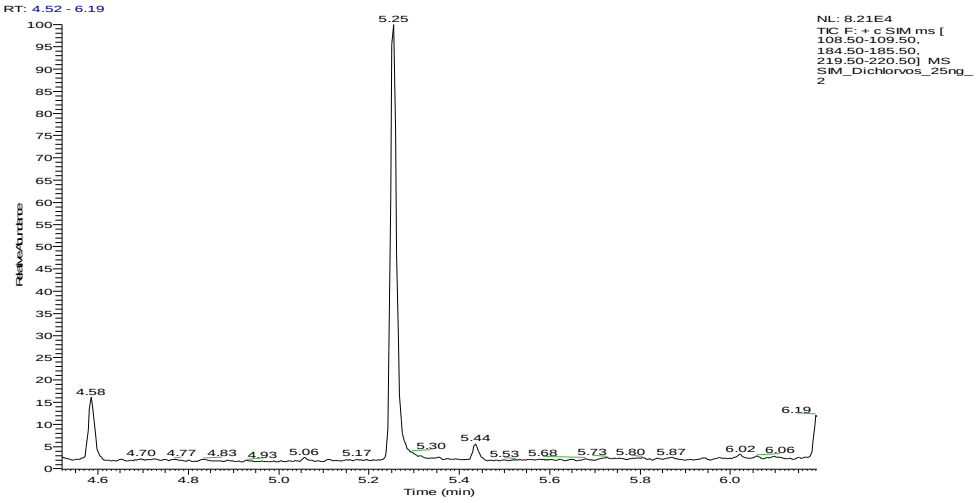

Figure 2.2. Dichlorvos SIM peak following GC-MS analysis

2.4: Liquid Chromatography- tandem mass Spectrometry (LC-MS-MS)

LC-MS-MS was used to analyse receptor fluid samples containing phorate obtained at Dstl. LC-MS-MS was implemented due to the complex nature of the samples being processed in order to identify ion fragments from the sample.

Liquid chromatography – tandem mass spectrometry was carried out on a ThermoFinnigan TSQ Quantum triple quadrupole instrument fitted with a Surveyor LC pump and autosampler. The mass spectrometer was operated in selected reaction monitoring (srm) mode with electrospray ionisation.
Chromatography was performed on an ACE 3 C8, 50 x 2.1 mm, 3µm, column with a mobile phase consisting of 0.02 M ammonium formate in water / methanol 25:75 at a flow rate of 0.2 ml/min. The column was maintained at ambient temperature.

Electrospray ionisation conditions were as follows: spray voltage 3 kV, capillary temperature 300 ℃, sheath gas (nitrogen) 50 (arbitrary units), auxiliary gas (nitrogen) 15 (arbitrary units). The mass spectrometer was set up to monitor the srm transitions m/z 261.1 → 75.2 for phorate and m/z 271.1 → 75.2 for d_{10}-phorate, 0.2 sec each. Scan width was 0.5Da, collision energy 18 eV and collision gas (argon) pressure 1.0 mTorr. Instrument tuning was optimised on m/z 261 from phorate.

2.4.1: Receptor fluid samples (Phorate)

Receptor fluid samples consisted of 20µl of receptor fluid (ethanol / water 50:50 v/v) collected in glass autosampler vials. To the receptor fluid sample, 20µl of d_{10}-phorate internal standard solution (0.5ng/µl in ethanol / water 50:50 v/v) was added and made up to 0.5ml by addition of 460µl of ethanol / water 50:50 (v/v). Samples were analysed by LC-MS-MS with electrospray ionisation, with each sample being injected in triplicate. Quantitation of ions was performed against calibration curves constructed from analysis of standard solutions of phorate prepared as for samples. Calibrations were linear over the ranges 0.02 to 1ng/µl (R^2 0.997) and 0.1 to 25ng/µl (R^2 0.999). The higher mass range calibration was used for quantitation of samples with concentrations exceeding 1ng/µl determined from the lower range calibration.

2.4.2: Skin surface decontamination samples in IPA

Skin surface decontamination swabs (cotton wool desorbed in IPA) were diluted with ethanol / water 50:50 (v/v) to bring the concentration within the calibration range. Final dilutions contained d_{10}-phorate internal standard at a concentration of 10ng/ml. Samples were analysed by LC-MS-MS with electrospray ionisation, each sample being injected in duplicate. Quantitation was performed against standard solutions of phorate, containing 10ng/ml of internal standard, over the range 0.5 to 100ng/ml (R^2 0.999).

2.4.3: Skin samples in soluene

100µl of each skin digest sample was transferred to a 10ml Pyrex screw-capped tube and 1.9ml of ethanol / water 50:50 (v/v) was added. The tube was centrifuged at 5000xg for 10 min and 100µl of supernatant transferred to a glass autosampler vial. 100 µl of d_{10}-phorate solution (1µg/ml) and 800µl of ethanol / water 50:50 (v/v) were added. Samples were analysed by LC-MS-MS with electrospray ionisation.

2.5: Statistical Analysis

Data obtained for dermal absorption and distribution of chemicals were expressed as mean ± sem. Mass balance data were expressed as the percentage of the total applied chlorpyrifos dose found at each test site (receptor fluid, skin digest (penetrated dose), tape strip (stratum corneum), unabsorbed (skin surface) and carbon filter). Comparison of means was performed using one-way ANOVA followed by Tukey's posthoc test for multiple comparisons using SPSS (SPSS Ltd). Significance was defined as $p<0.05$.

Chapter 3

Dermal absorption of model compounds in vitro

3: Dermal absorption of model compounds *in vitro*

3.1: Introduction

Due to the high toxicity of many organophosphate compounds and chemical warfare agents that individuals may become exposed to as a result of accidental or deliberate release into the atmosphere, it is important to investigate the dermal absorption of less harmful compounds which may potentially be useful as surrogate or marker compounds for exposure to more harmful compounds based on their varying physicochemical properties. The approach was to investigate dermal absorption of model chemicals and to then relate these to surrogate chemicals of interest, and to then finally relate both model and surrogate chemicals to absorption of bioactive agents.

The compounds chosen in these initial studies to investigate the dermal absorption from infinite and finite saturated doses were caffeine and benzoic acid. As mentioned in sections 1.5.2 and 1.5.3 of chapter 1 respectively. Caffeine and benzoic acid have been used in the laboratories at Newcastle University (van der Sandt *et al*. 2004, Wilkinson *et al*. 2006) as marker compounds for investigating intra and inter-laboratory differences, as well as intra, and inter-individual differences when using *in vitro* absorption techniques. As a result of this, the absorption profiles of these compounds are already well established, and so these were ideal model compounds to use in these studies, and also to ensure that the *in vitro* diffusion methods being implemented throughout this project were capable of producing reliable data. Generating data on dermal absorption of model compounds also makes it easier to rank the chemicals of interest (surrogates and bioactive agents).

Caffeine and benzoic acid have different physicochemical properties. Caffeine is a hydrophilic (Log p = -0.07) compound with a moderate molecular weight (194.19). Benzoic acid however, is a lipophilic compound (Log p = 1.87), with a relatively low molecular weight (122.12). As molecular weight and lipophilicity are major factors that can affect dermal penetration, studying these two compounds could highlight any potential differences in absorption that could be caused by differences in chemical properties.

In parallel to investigating the influence of chemical property on dermal absorption, the effect of different application vehicles was also investigated. The application vehicles chosen were isopropanol (IPA), and propylene glycol (PG). IPA is an amphipathic solvent (Log p = 0.05) with a high vapour pressure (45.4mmHg at 25˚C) and will volatilise rapidly from the skin surface. This makes it a useful solvent to use in dermal penetration studies, as it can potentially more closely mimic 'real life' exposure to droplets of chemicals released into the atmosphere as a spray or a vapour. In contrast, PG is a hydrophilic solvent (Log p = -0.92) and has a low vapour pressure (0.129mmHg at 25˚C). Due to its low volatility, PG is likely to remain in contact with the skin for longer than IPA when applied to the skin surface. Also, PG has been reported to be a penetration enhancer (Williams and Barry, 2004**,** Duracher *et al.* 2009). The mechanism for penetration enhancement by PG is thought to be that PG enters the stratum corneum and modifies lipid and protein structures within the skin, resulting in reduced barrier integrity of the

stratum corneum. This is known as the 'lipid protein partitioning theory'. **(**Barry, 1988, Bach and Lippold, 1998, Barry, 2001).

3.2: Aims

The purpose of these studies was to identify the finite and infinite dose dermal absorption profiles of caffeine and benzoic acid through dermatomed human breast skin. This was carried out with the aim of producing data to allow ranking of surrogate and bioactive agents to be tested after generating dermal absorption data of model compounds.

3.3: Results

3.3.1: 24 hour exposure of dermatomed human breast skin to an infinite dose of ^{14}C caffeine, using IPA and PG as vehicles

Methods

For the purpose of this study, 11 flow-through diffusion cells were used containing dermatomed human breast skin samples from two skin donors. Caffeine was applied to the skin in 2 different vehicles, with 5 cells exposed to caffeine as a saturated solution in IPA (10mg/ml), and 6 cells exposed to caffeine as saturated solution in PG (12mg/ml). The dose applied was infinite, with 1ml/cm^2 of the dose applied to the skin surface. The exposed area of skin measured 0.64cm^2 in the flow-through diffusion cell, so 640µl of caffeine in IPA or PG was applied to the skin surface. Doses were left in contact with the skin for 24 hours before termination of the study. Receptor fluid samples and the remaining dose on the skin surface was analysed by scintillation counting.

Results

The cumulative absorption profile of caffeine from an infinite dose applied to dermatomed human breast skin for both IPA and PG vehicles is shown in figure 3.1. It can be seen that the absorption profiles from IPA and PG differ, with the profile of caffeine absorbed from the PG vehicle remaining linear throughout the 24 hour exposure period. Caffeine applied in IPA was slower to penetrate through the skin initially when compared with absorption from PG. Despite this, and because absorption of caffeine from PG was greater up until 21 hours after exposure, the total amount of caffeine absorbed from the IPA vehicle was greater after 24 hour exposure (523 ± 225.5µg/cm^2) compared with absorption from PG (446 ± 38.6µg/cm^2). However, there was no statistically significant difference in total absorption between the two vehicles due to wide interindividual variability (following 1-way ANOVA analysis).

As caffeine was applied as an infinite, saturated dose in both vehicles, it was possible to calculate the maximum absorption (flux) rate of caffeine from IPA and PG. The maximum flux was highest when caffeine was applied in IPA (49.7 ± 20.5µg/cm^2/h, 19-24 hours), compared with 18.8 ± 3.4µg/cm^2/h from PG (1-24 hours). Despite absorption being greatest from the IPA vehicle, the lag time was shorter for caffeine absorption from the PG vehicle (1.7 ± 1.1 hours) compared with absorption from the IPA vehicle (12 ± 2.6 hours) (shown in table 1).

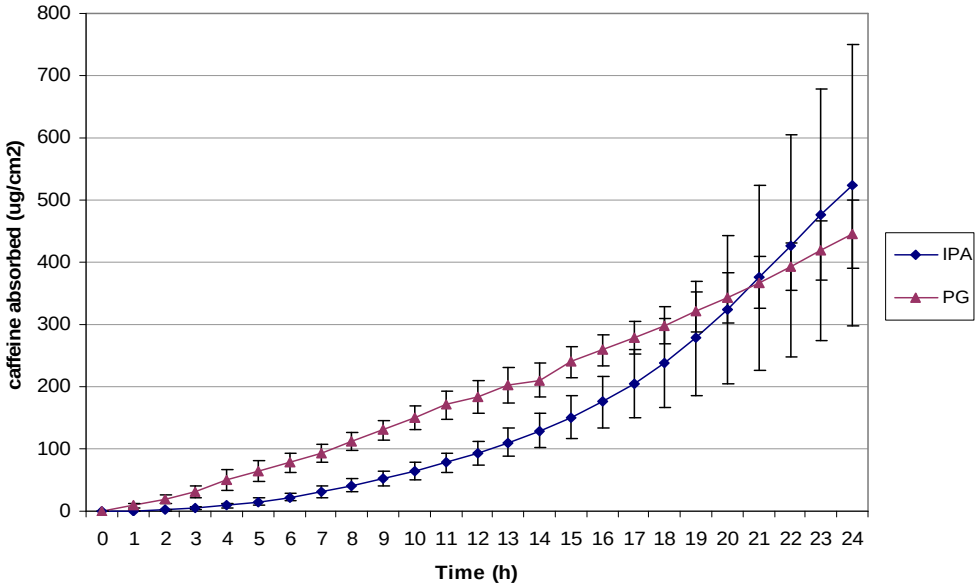

Fig.3.1. 24 hour cumulative absorption profile of an infinite dose of ^{14}C caffeine. Values for caffeine applied in IPA are mean ± SEM of 5 cells (2 donors). Values for caffeine applied in PG are mean ± SEM of 6 cells (2 donors). Skin sections were mounted in flow through cells with an exposed area of 0.64cm^2. Caffeine in IPA was applied to the skin surface as a saturated dose (1ml/cm^2) at a concentration of 10mg/ml. Caffeine in PG was also applied as an infinite dose, at a concentration of 12mg/ml. Each 640µl (1ml/cm^2) dose in both IPA and PG contained approximately 1x10^5 dpm.

Dose	Flux (µg/cm^2/h)	K_p x 10^{-3} (cm/h)	Lag Time (h)	Linear range
Caffeine in IPA (infinite dose)	49.7 ± 20.5*	42.7 ± 19.1	12.1 ± 2.6*	19-24
Caffeine in PG (infinite dose)	18.8 ± 3.4	16.8 ± 8.3	1.7 ± 1.1	1-24

Table 1. Steady state absorption rates, partition coefficients and lag times of caffeine applied to the skin surface as infinite doses in IPA and PG. values are means ± SEM**.** A single asterisk denotes a significant difference between vehicles ($p<0.05$ with one way ANOVA).

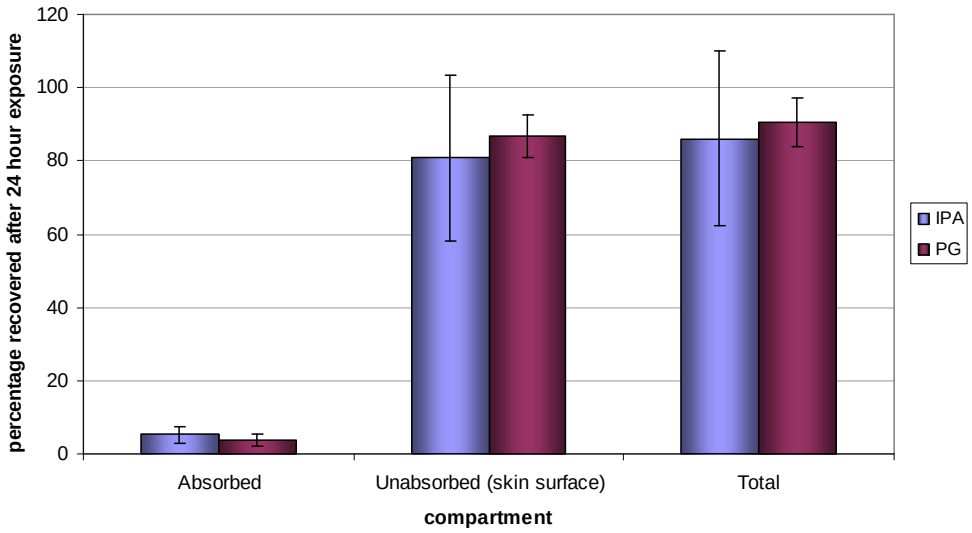

Fig.3.2. Dose distribution of ^{14}C caffeine applied as an infinite dose to dermatomed human breast skin. Values are mean ± SEM of 5 cells (2 donors) for IPA, and values for PG are mean ± SEM of 6 cells (2 donors). The absorbed dose accounts for the total amount recovered in the receptor fluid after 24hr exposure. The unabsorbed dose was recovered by swabbing the skin surface with alternate wet (0.5% soap solution) and dry tissue pieces (3 wet and 3 dry swabs). The total is the sum of the absorbed and unabsorbed recoveries.

The distribution profile of caffeine applied as a saturated, infinite dose in IPA or PG (figure.3.2), shows that the amount of caffeine absorbed from either vehicle accounted for only a small proportion of the dose applied to the skin surface. From the IPA vehicle, 5.2 ± 2.1% of the dose of caffeine was absorbed, whereas 2.5 ± 0.6% of the dose from PG was absorbed. The majority of the applied dose remained on the skin surface after 24 hour exposure (81.8 ± 22.5% from IPA and 86.8 ± 3.2% from PG respectively).

3.3.2: 24 hour exposure of dermatomed human breast skin to a finite dose of ^{14}C caffeine using IPA and PG as vehicles

Methods

For this study, 12 flow-through diffusion cells were used, with 6 cells dosed with caffeine saturated in IPA (10mg/ml), and 6 cells dosed with caffeine saturated in PG (12mg/ml). A dose volume of 10µl/cm^2 was used to give a finite exposure. The dose was kept in contact with the skin surface for 24 hours, before terminal procedures were carried out for dose distribution analysis by scintillation counting.

Results

The absorption profile of caffeine applied in IPA and PG vehicles as a saturated finite dose can be seen in figure 3.3. The absorption profiles differ more greatly between vehicles than for the infinite dose study. The absorption rate from IPA was initially very fast, but decreased after 3-4 hours, whereas absorption from PG was initially slower, and continued to increase up to 24 hours after exposure despite finite dosing. The difference in absorption was reflected in the maximum flux rates, with 3.3 ± 0.9µg/cm^2/h absorbed from IPA and 0.3 ± 0.1µg/cm^2/h from PG respectively (table 2). Despite the absorption profiles of caffeine differing between vehicles, the total amount absorbed from both vehicles after 24 hour exposure were similar, with 16.3 ± 2.7µg/cm^2 being absorbed from IPA and 16.1 ± 4.3µg/cm^2 from the PG vehicle respectively.

From the distribution profile shown in figure 3.4, it can be seen that the distribution of caffeine applied in both IPA and PG is comparable following 24 hour exposure. Similarly to the distribution from the infinite dose study in shown in figure 3.2, the majority of the applied dose from both vehicles was remaining on the skin surface after 24 hour exposure (69.8 ± 3.6% from IPA and 70.6 ± 6.7% from PG respectively). Slightly more of the applied dose was found within the skin from the PG dose (4.9 ± 1.8%) compared with IPA (3.4 ± 0.7), although this was not statistically significant following 1-way ANOVA. A small proportion (2 ± 0.3%) of the applied dose was also found remaining in the stratum corneum (tape strips) from both vehicles.

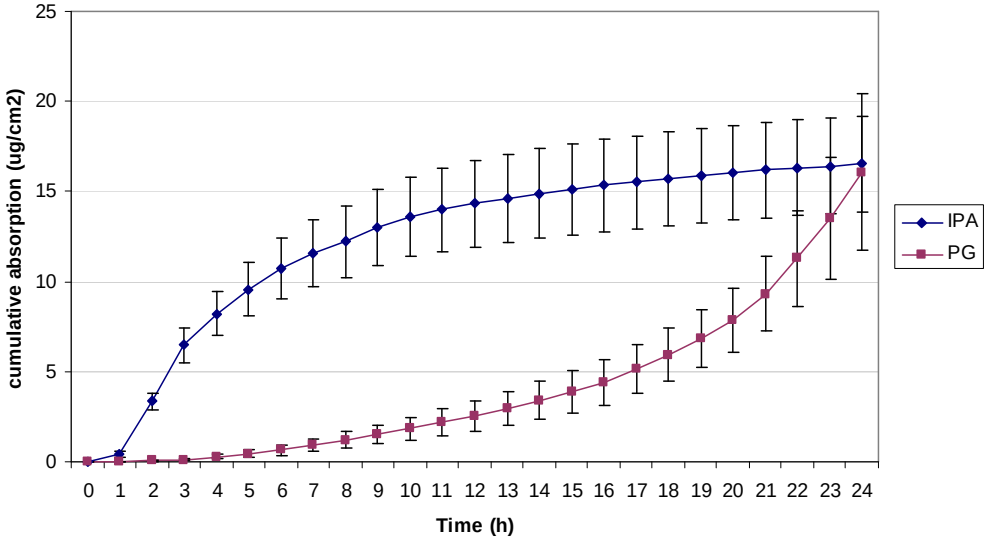

Figure.3.3. 24 hour cumulative absorption profile of a finite dose of ^{14}C caffeine. Values for caffeine applied as a finite dose in IPA are mean ±SEM for 6 cells (2 donors), and 6 cells (2 donors) for caffeine applied as a finite dose in PG. ^{14}C caffeine (containing approximately 1x10^5 DPM) was applied to the skin surface in a finite dose (10µl/cm^2) at a concentration of 10mg/ml in IPA and 12mg/ml in PG.

Dose	Flux (µg/cm^2/h)	K_p x 10^{-3} (cm/h)	Lag Time (h)	Linear range
Caffeine in IPA (finite dose)	3.3 ± 0.9*	2.7 ± 1.1	0.8 ± 0.3	1-3
Caffeine in PG (finite dose)	0.3 ± 0.1	3.2 ± 1.0	4.1 ± 1.5*	4-16

Table 2. Steady state absorption rates, partition coefficients and lag times of caffeine applied to the skin surface as a finite dose in IPA and PG. values are means ± SEM**.** A single asterisk next to a figure denotes that it is significantly different from the remaining figure in the same column ($p<0.05$ with one way ANOVA).

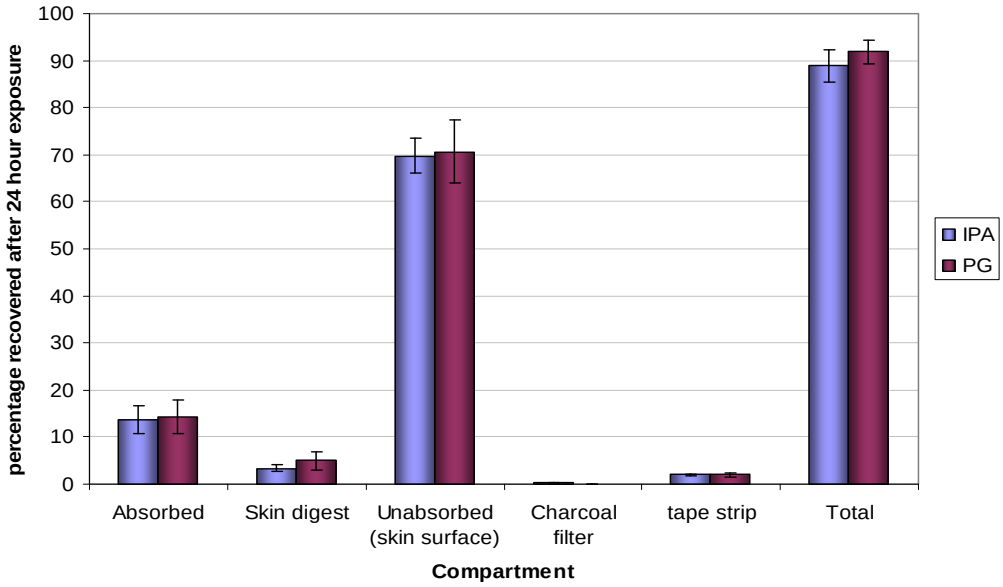

Fig.3.4. Dose distribution of ^{14}C caffeine applied as a finite dose to dermatomed human breast skin. Values are mean ± SEM of 6 cells (2 donors) for IPA, and values for PG are mean ± SEM of 6 cells (2 donors). The absorbed dose accounts for the total amount recovered in the receptor fluid after 24hr exposure. The skin digest represents the amount recovered from the viable epidermis and dermis after tape-stripping. The unabsorbed dose was recovered by swabbing the skin surface with alternate wet (0.5% soap solution) and dry tissue pieces (3 wet and 3 dry swabs). Charcoal filters were placed above the skin surface to trap any volatilised dose. Tape strips (no more than 15 per cell) were taken to remove the stratum corneum for assessment as a separate compartment to the remaining skin. The total is the sum of the absorbed and unabsorbed recoveries.

3.3.3: 24 hour exposure of dermatomed human breast skin to an infinite dose of ^{14}C benzoic acid, using IPA and PG as vehicles

Methods

For this study, 13 flow-through diffusion cells were used, with 6 cells dosed with benzoic acid in IPA (35mg/ml) and 7 cells were dosed with benzoic acid in PG (24mg/ml). The volume applied to the skin surface was 1ml/cm^2 to give an infinite dose exposure. Each dose was left in contact with the skin for 24 hours before terminal procedures were carried out to analyse the distribution

of benzoic acid (receptor fluids and unabsorbed dose) by scintillation counting.

Results

The cumulative absorption profile of benzoic acid applied as a saturated infinite dose in 2 vehicles (IPA and PG) is shown in figure 3.5. Absorption of benzoic acid from IPA was fast from 3 to 5 hours of exposure before tailing off up to 24 hours, despite infinite dosing. However, absorption from PG gave a more classical infinite dose profile, with absorption continuing at an approximately linear rate throughout the 24 hour exposure period.

Despite the fact that absorption after 24 hours was greater from PG than from IPA (1.8 ± 0.7mg/cm^2 and 0.7 ± 0.1mg/cm^2 respectively), the lag time was much shorter from IPA (2.3h ± 0.9) than from PG (9.1h ± 2.1), and the apparent maximum absorption rate was approximately 1.5 times greater from IPA (180.6 ± 60.8µg/cm^2/h) than from PG (120.8 ± 40.3µg/cm^2/h).

The distribution analysis shown in figure 3.6 also indicates the differences in the amount of benzoic acid absorbed from both vehicles after 24 hour exposure. However, it can also be seen that, similarly to the distribution of caffeine after 24 hour exposure, the vast majority of the applied dose was remaining on the skin surface (88.5 ± 18.9% from IPA and 83.4 ± 12.3% from PG).

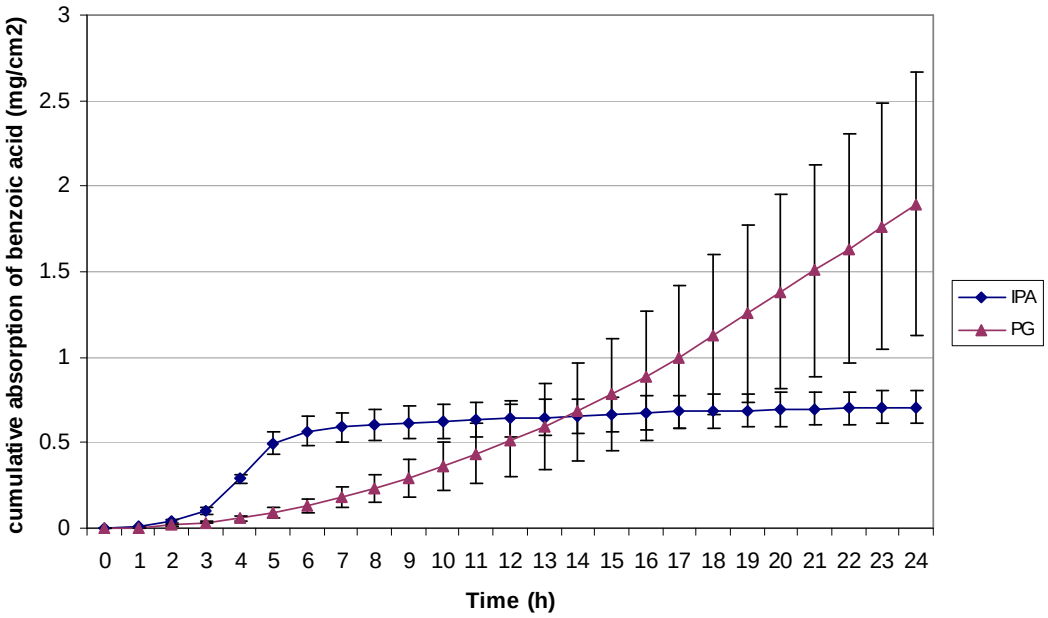

Figure.3.5. 24 hour cumulative absorption profile of an infinite dose of ^{14}C benzoic acid. Values for benzoic acid applied as an infinite dose in IPA are mean ±SEM for 6 cells (2 donors), and 7 cells (2 donors) for benzoic acid applied as a finite dose in PG. ^{14}C benzoic acid (containing approximately 1x10^5 DPM) was applied to the skin surface in an infinite dose (1ml/cm^2) at a concentration of 35mg/ml in IPA and 24mg/ml in PG.

Dose	Flux (µg/cm^2/h)	K_p x 10^{-3} (cm/h)	Lag Time (h)	Linear range
Benzoic acid in IPA (infinite dose)	180.6 ± 60.8	181.4 ± 50.5	2.3 ± 0.9	3-6
Benzoic acid in PG (infinite dose)	120.8 ± 40.3	118.1 ± 30.2	9.1 ± 2.1*	14-24

Table 3. Steady state absorption rates, partition coefficients and lag times of benzoic acid applied to the skin surface as an infinite dose in IPA and PG. values are means ± SEM**.** A single asterisk next to a figure denotes a significant difference from the remaining figure in the same column ($p<0.05$ with one way ANOVA).

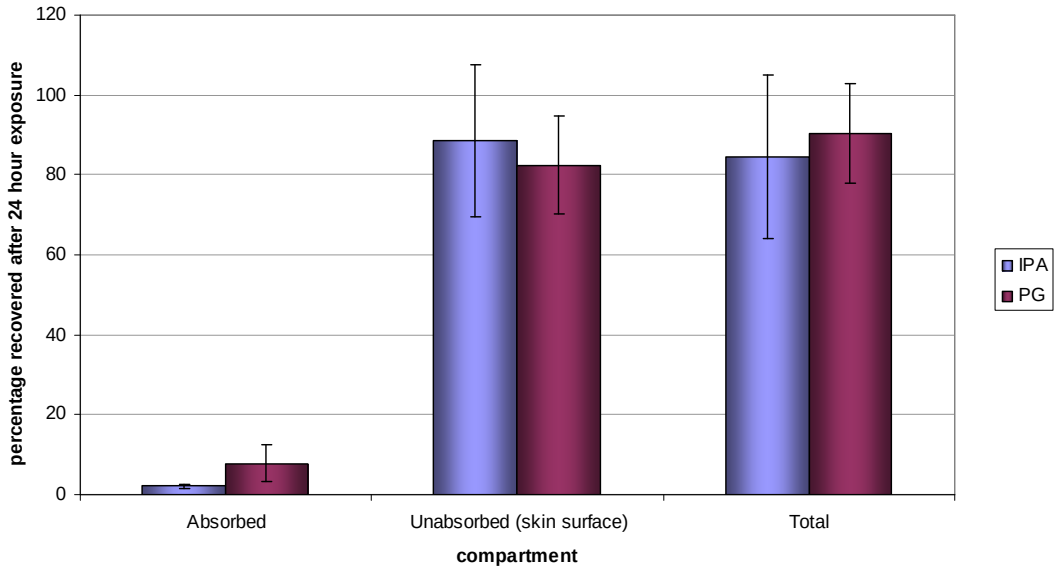

Fig.3.6. Dose distribution of ^{14}C benzoic acid applied as an infinite dose to dermatomed human breast skin. Values are mean ± SEM of 6 cells (2 donors) for IPA, and values for PG are mean ± SEM of 7 cells (2 donors). The absorbed dose accounts for the total amount recovered in the receptor fluid after 24hr exposure. The unabsorbed dose was recovered by swabbing the skin surface with alternate wet (0.5% soap solution) and dry tissue pieces (3 wet and 3 dry swabs). The total is the sum of the absorbed and unabsorbed recoveries.

3.3.4: 24 hour exposure of dermatomed human breast skin to a finite dose of ^{14}C-labelled benzoic acid, using IPA and PG as vehicles

Methods

For this study, 11 flow-through diffusion cells were used. A total of 6 cells were dosed with benzoic acid in IPA (35mg/ml), and 5 cells were dosed with benzoic acid in PG (24mg/ml). Skin samples were taken from 2 individual donors, and the volume of dose applied to the skin surface was 10µl/cm^2 to give a finite exposure. Each dose was left in contact with the skin surface for 24 hours before terminal procedures were carried out to identify the dose distribution.

Results

Figure 3.7 shows the cumulative absorption profile of benzoic acid applied as a finite dose in either IPA or PG vehicles. The finite dose absorption profile from the IPA vehicle followed a similar pattern to the absorption profile of the infinite dose of benzoic acid in IPA (figure.3.5). Absorption from IPA was initially fast over the first 3-4 hours before tailing off rapidly to 24 hours after exposure. There was no apparent lag time for absorption from IPA. The absorption profile of benzoic acid in PG was however, very different, with absorption initially being slow, before reaching steady state absorption after 8 hours of exposure, however, absorption then tailed off rapidly after 15 hours. The apparent lag time for benzoic acid in PG was 5.3 ± 1.4 hours. Despite the absorption profiles of benzoic acid being very different between IPA and PG, the absolute amounts absorbed after 24 hours was very similar from both vehicles (112 ± 23.1µg/cm^2 from IPA, and 108 ± 10.7µg/cm^2 from PG respectively). However, in terms of percentage of dose applied to the skin surface (figure.3.8), a greater amount was absorbed from the PG vehicle (45.5 ± 7.1%) compared with absorption from the IPA vehicle (32.3 ± 6.6%).

Figure 3.8 shows that a large proportion of the applied dose of benzoic acid remained on the skin surface after 24 hour exposure from both vehicles (56.1 ± 7.4% from IPA and 41.1 ± 5.1% from PG). Approximately 3 times more of the applied dose of benzoic acid was found within the skin after 24 hour exposure to the PG vehicle than from IPA (1.1 ± 0.2% from IPA and 3.6 ± 0.8% from PG) (p=>0.05 following 1-way ANOVA); however, similar amounts

were recovered from the stratum corneum tape strips from both vehicles after 24 hours (1.7 ± 0.5% from IPA and 1.1 ± 0.3 % from PG).

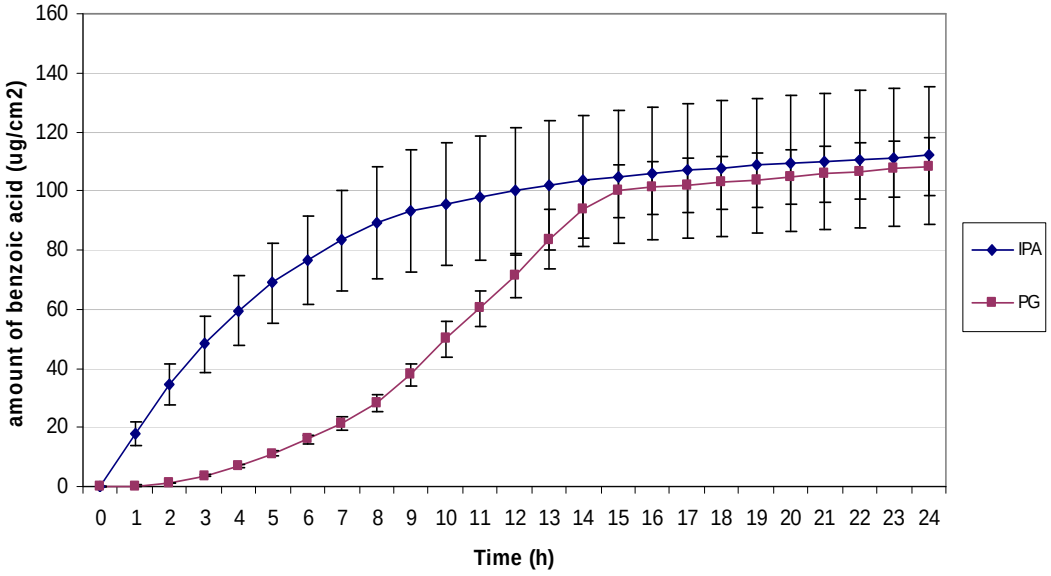

Figure.3.7. 24 hour cumulative absorption profile of a finite dose of ^{14}C benzoic acid. Values for benzoic acid applied as a finite dose in IPA are mean ±SEM for 6 cells (2 donors), and 5 cells (2 donors) for benzoic acid applied as a finite dose in PG. ^{14}C benzoic acid (containing approximately 1x10^5 DPM) was applied to the skin surface in a finite dose (10µl/cm^2) at a concentration of 35mg/ml in IPA and 24mg/ml in PG.

Dose	Flux (µg/cm^2/h)	K_p x 10^{-3} (cm/h)	Lag Time (h)	Linear range
Benzoic acid in IPA (finite dose)	18.5 ± 5.6	17.2 ± 4.3	0	0-2
Benzoic acid in PG (finite dose)	16.6 ± 4.8	13.3 ± 2.6	5.3 ± 1.4*	8-15

Table 4. Steady state absorption rates, partition coefficients and lag times of benzoic acid applied to the skin surface as a finite dose in IPA and PG. Values are means ± SEM**.** A single asterisk next to a figure denotes a statistically significant difference from the remaning figure in the same column ($p<0.05$ with one way ANOVA).

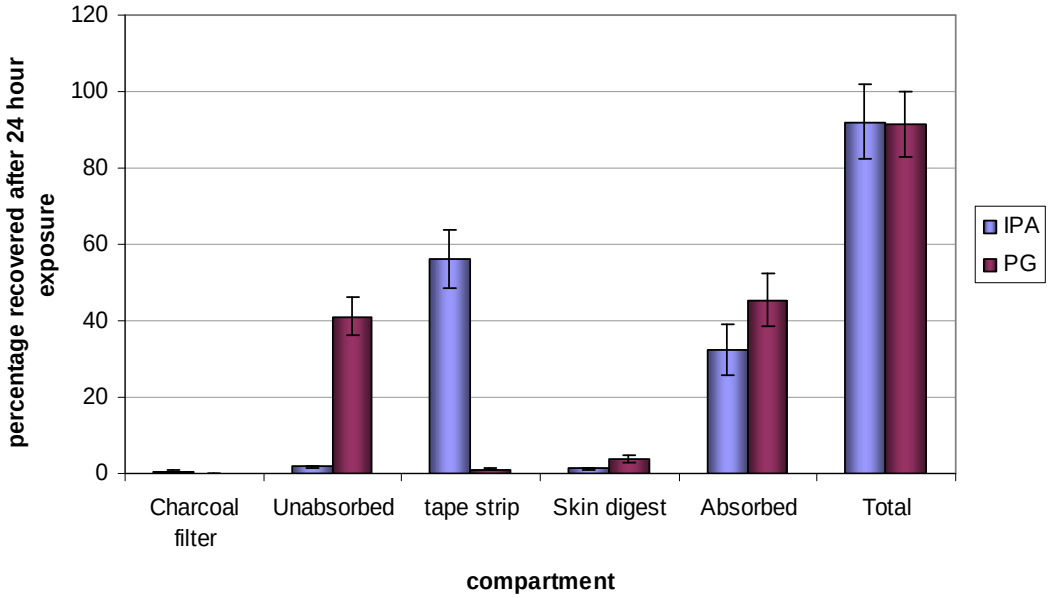

Fig.3.8. Dose distribution of ^{14}C benzoic acid applied as a finite dose to dermatomed human breast skin. Values are mean ± SEM of 6 cells (2 donors) for IPA, and values for PG are mean ± SEM of 5 cells (2 donors). The absorbed dose accounts for the total amount recovered in the receptor fluid after 24hr exposure. The skin digest represents the amount recovered from the viable epidermis and dermis after tape-stripping. The unabsorbed dose was recovered by swabbing the skin surface with alternate wet (0.5% soap solution) and dry tissue pieces (3 wet and 3 dry swabs). Charcoal filters were placed above the skin surface to trap any volatilised dose. Tape strips (no more than 15 per cell) were taken to remove the stratum corneum for assessment as a separate compartment to the remaining skin. The total is the sum of the absorbed and unabsorbed recoveries.

3.4: Discussion

The infinite and finite dose absorption profiles of caffeine and benzoic acid, as expected, were different between application vehicles. The absorption of caffeine applied as a saturated dose in IPA or PG continued to increase up to 24 hours after exposure. This is consistent with a conventional infinite dose absorption curve, as the concentration on the skin surface theoretically remains constant throughout the exposure period. The amount of caffeine absorbed after 24 hours from both infinite and finite doses was small when compared with the amount applied on the skin surface, and the majority of the dose remained on the skin surface after 24 hour exposure for both IPA

and PG. It is probable that this was due to caffeine being a hydrophilic compound, and so penetration into the lipophilic stratum corneum and the upper layers of the skin was limited. As PG is also a hydrophilic solvent with a very low vapour pressure, caffeine would have a greater thermodynamic activity within the PG vehicle than in the stratum corneum lipids. As a result of this, caffeine was more likely to remain partitioned within the PG vehicle rather than penetrate into the upper layers of the skin.

Caffeine absorption from a finite dose in PG continued to increase after a 24 hour exposure period, which was unusual as absorption from a finite dose usually tails off as the applied dose becomes depleted (as seen for caffeine in IPA, figure 3.3). It is thought that the dose applied in PG may have maintained contact with the skin surface for longer than the dose in IPA due to the low volatility of PG. This may have enabled the dose to penetrate more slowly and steadily from the vehicle into the skin and maintain a steady state of absorption throughout exposure.

The cumulative absorption profile of benzoic acid applied as an infinite dose in IPA (figure 3.5) was unusual as it resembled what would be expected from a finite dose. It is thought that this may have been caused by evaporation of volatile IPA. Evaporation of IPA from the skin surface left a solid residue of benzoic acid on the skin surface, which was less able to penetrate through the skin. This explains the high recovery from the skin surface (88.5 ± 18.9% of applied dose figure 3.6), despite the loss of IPA from the skin surface. Because of the volatility of IPA, it was impossible to ascertain a ‘true’

maximum absorption rate for benzoic acid applied to the skin surface in IPA, as a steady state of absorption was not achieved during the 24 hour exposure time. Absorption of benzoic acid applied as an infinite dose in PG followed a more conventional infinite dose profile. As mentioned previously, PG has a low vapour pressure and so remained on the skin surface for the duration of the study.

A greater amount of benzoic acid was absorbed through the skin than caffeine from both vehicles when applied as a finite dose (figure 3.8). This could be explained by the physicochemical properties of benzoic acid and its interaction with the solvent vehicles in which it was applied to the skin surface. Benzoic acid is lipophilic (log p = 1.87), and so is likely to penetrate through the skin more readily than the hydrophilic caffeine. However, application of benzoic acid to the skin surface in a hydrophilic solvent, such as PG, was likely to drive benzoic acid through the skin, as the compound has a greater thermodynamic activity in the lipids of the stratum corneum than it does in the application vehicle. Only a small proportion of the applied finite dose in IPA and PG vehicles was recovered from within the skin (skin digests and tape strips – figure 3.8). This suggests that there would be little opportunity for further absorption of benzoic acid beyond the 24 hour exposure time, as the majority of the applied dose remained on the skin surface.

Chapter 4

Dermal absorption of dichlorvos, chlorpyrifos and phorate

4. Dermal absorption of dichlorvos, chlorpyrifos and phorate

4.1: Introduction

An aim of this project was to define dermal absorption of nerve agents. However there are inherent difficulties and risk associated in working with these agents on our laboratories. Therefore studies were conducted with surrogate organophosphate molecules. Chlorpyrifos, dichlorvos and phorate were selected due to their differing physicochemical properties, with chlorpyrifos being a lipophilic solid (log p = 4.96), dichlorvos a moderately lipophilic liquid (log p = 1.47) and phorate is a lipophilic liquid (log p = 3.56). Dichlorvos is a stable oxon, with chlorpyrifos and phorate both being thiophosphates. These compounds were selected, not only to compare with the absorption profiles of model compounds, but to allow extrapolation from the surrogate compounds to the absorption of the more harmful nerve agents compounds that individuals may become accidentally or deliberately exposed to in the environment following a release.

The study of chlorpyrifos, dichlorvos and phorate in terms of *in vitro* dermal absorption and distribution has been limited. At present, only one study has been conducted to assess chlorpyrifos absorption through skin *in vitro* (Griffin *et al.* 2000), where chlorpyrifos was applied to human skin at a high concentration (18.28mg/ml) from a commercial mixture, and also dissolved in ethanol. In vivo studies have previously been conducted investigating the kinetics of urinary elimination of chlorpyrifos applied to the skin (Griffin *et al.* 1999, Meuling *et al*. 2005), and recently, to investigate chlorpyrifos exposure in Egyptian cotton field workers (Farahat, *et al.* 2010). As chlorpyrifos is still

a widely used organophosphate pesticide in some poorer countries, it has been extensively investigated from an agricultural exposure perspective (Cattani *et al*. 2001**,** Geer *et al*. 2004, Abdel-Rasoul *et al*. 2008). As a result of this, chlorpyrifos was selected to investigate in these studies as it has relevance, not only as a surrogate compound, but also as a harmful chemical in its own right.

To my knowledge, there is little information in the published literature regarding the dermal absorption and distribution of dichlorvos *in vitro*. This makes it an interesting chemical to use in dermal absorption studies. Despite the lack of *in vitro* dermal exposure data, dichlorvos toxicity has been widely studied and reviewed **(**Tungul et al. 1991, Luty et al. 1998, Booth et al. 2007) as a result of being used extensively used as an agricultural insecticide.

Also, little is known regarding the dermal absorption and distribution of phorate. It is still used as a pesticide in many countries and so the possibility of civilians coming into contact with phorate is quite high. Due to the fact that phorate is still used in agriculture, methods for fast detection of serum organophosphates levels as a result of occupational exposure have been implemented using a number of different organophosphates, including phorate (Singh and Dogra, 2009).

The same solvent vehicles used in chapter 3 were chosen for application of chlorpyrifos and dichlorvos to the skin surface. However, in addition, isopropyl myristate (IPM) was also included as a third application vehicle. IPM is a

highly lipophilic solvent (log p = 7.17) with a low vapour pressure (<1mmHg at 25˚C). IPM was used because it has been shown to have similar properties to the lipids of the stratum corneum, and so is less likely to disrupt the barrier integrity of the skin. Other solvent vehicles, such as PG can enhance penetration of a chemical by altering the lipid structure of the stratum corneum, and so using IPM allowed investigation of organophosphate absorption without damaging the stratum corneum. Using IPM also allowed a wider range of exposure scenarios for both organophosphates to be investigated. Initial studies were undertaken to generate data on infinite dose exposures of dichlorvos in IPA, IPM and PG. To do this, dose concentrations of 10mg/ml and 1mg/ml were used. The dose concentrations used in the finite dose studies for chlorpyrifos (500ng/cm^2) and dichlorvos (5µg/cm^2) were selected so that low level exposures to these compounds could be assessed. It is estimated that a dose of 300-400mg/kg of body weight is necessary for severe toxic effects of chlorpyrifos to be seen in humans (FAO/WHO, 2000). The 500ng/cm^2 dose applied to the skin in these studies would be unlikely to result in such high level exposure as this, particularly as absorption would be unlikely to reach 100%, and so the dose used can be termed as low level exposure. Three vehicles (IPA, IPM and PG) were used to identify the effect of application vehicle on dermal absorption, in terms of the effect of the vehicle itself, but also as a result of interaction with the compounds of interest.

Dichlorvos was applied to the skin surface at a higher concentration than chlorpyrifos to allow for detection by GC-MS. Despite the higher

concentration, the dose concentration was still significantly below the limit of dose application (5mg/cm^2) suggested by OECD guideline 428 (OECD, 2004). In a separate study carried out at dstl, finite doses of phorate were applied to excised domestic pig abdomen skin as a neat solution (23mg/cell), and diluted in IPA (25µg/cell). The neat dose of phorate was used because there is little published data regarding dermal absorption of phorate, and so a high dose was applied to some cells to provide a worst case scenario for exposure. Phorate was also applied to the skin as a finite dose in IPA. This was chosen as a vehicle due to the volatility of IPA. This meant following application of a finite dose the solvent would evaporate from the skin surface quickly, and more closely mimic exposure to droplets or a vapour of phorate.

4.2: Aims

The aim of these studies was to generate novel data on the dermal absorption and distribution of chlorpyrifos and dichlorvos exposed to human breast skin samples for 24 hours. Chlorpyrifos and dichlorvos are still widely used in agriculture, and so these are also important to investigate in their own right, as well as using them to predict how bioactive agents with similar physicochemical properties will behave when in contact with the skin.

4.3: Results

4.3.1: 24 hour exposure of dermatomed human breast skin to an infinite dose (1ml/cm^2) of dichlorvos at concentrations of 10mg/ml and 1mg/ml.

Methods

For these studies, a total of 27 flow-through diffusion cells were used. 12 flow-through diffusion cells were used for the 10mg/ml infinite dose study (4 cells for each dose in IPA, IPM and PG), and 15 cells were used for the 1mg/ml infinite dose study (5 cells for each dose in IPA, IPM and PG). Skin was taken from 6 donors in total (3 for each study) to account for interindividual variability. Dichlorvos was applied to the skin as an infinite dose (1ml/cm^2) and dose concentrations of 10mg/ml and 1mg/ml were used. A high dose (10mg/ml) in each vehicle was used instead of using saturated doses to ascertain the infinite dose of dichlorvos in the 3 application vehicles because of the safety issue of handling large quantities of dichlorvos in the laboratory, and also due to the cost implications of using large quantities to produce saturated solutions in each vehicle. The 1mg/ml dose was used to see if there was a linear correlation between dose and absorption. In each study, the dose was left in contact with the skin for 24 hours before analysis of receptor fluid samples (1ml each) and the remaining skin surface dose by GC-MS.

Results

Figure 4.1 shows the cumulative absorption profile of dichlorvos applied to dermatomed human breast skin as an infinite dose (10mg/ml) in three vehicles. As can be seen from this figure, the greatest absorption of dichlorvos was from exposure in IPA, with 75% of the applied dose being absorbed after

24 hours. Absorption was greatest over the first 3 hours of exposure, however, absorption tailed off rapidly from this point up to 24 hours. The lag time for dichlorvos applied in IPA was 0.6 ± 0.1 hours. The absorption profiles of dichlorvos applied in IPM and PG were in keeping with an infinite dosing regime, as absorption continued to increase throughout the 24 hour exposure period. Approximately 27% of the applied dose in PG was recovered from receptor fluid samples after 24 hours, whereas 12% of the applied dose in IPM was absorbed after the same exposure time.

A similar absorption profile was observed for the 1mg/ml infinite dose (figure 4.2) as for the 10mg/ml dose, with absorption of dichlorvos from the IPA vehicle being greater than from the IPM and PG vehicles. Following 24 hour exposure, 688 ± 18µg/cm^2 had been absorbed from the IPA vehicle, (68% of the applied dose). The 10 fold difference in concentration between these 2 infinite dose studies yielded an approximately 10 fold difference in absorption from the IPA vehicle. There was also an approximately 10 fold reduction in maximum flux of dichlorvos between the two studies, with the apparent flux when applied at 10mg/ml in IPA being 1346 ± 298µg/cm^2/h, and 132 ± 28µg/cm^2/h when applied at 1mg/ml in IPA respectively. Absorption from IPA was fastest over the initial 3 hours of exposure before tailing off up to 24 hours after exposure despite infinite dosing. Although absorption from PG was greater than from IPM for the 10mg/ml dose (figure 4.1), this result was found to be reversed following exposure to the 1mg/ml dose. However, absorption from IPM and PG continued to increase throughout the exposure period.

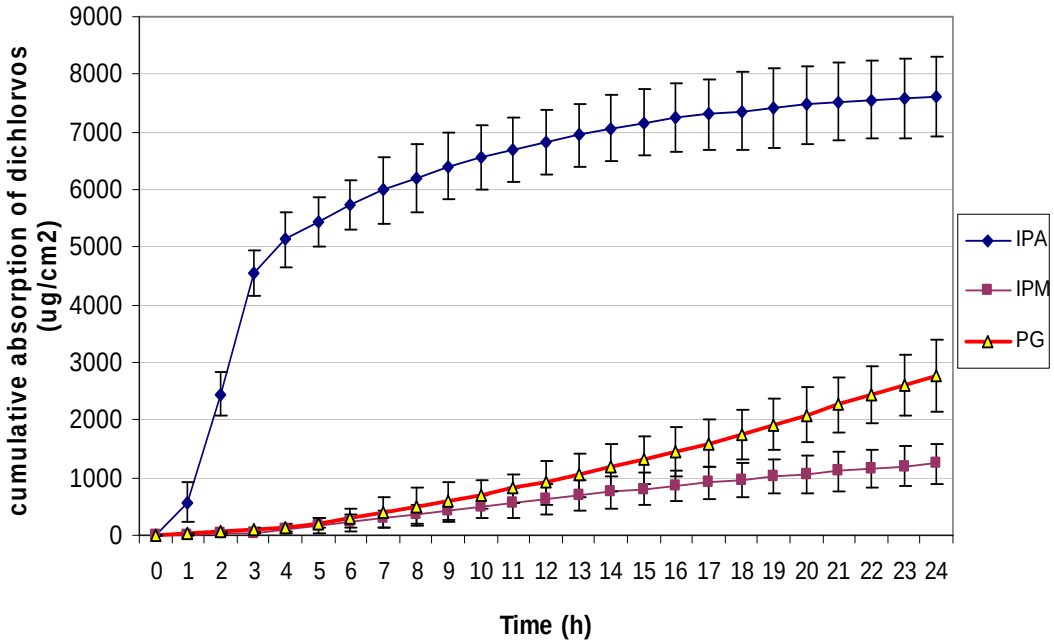

Fig.4.1. 24 hour cumulative absorption profile of an infinite dose of dichlorvos (10mg/ml) in IPA, IPM and PG. Values for dichlorvos applied in IPA, IPM and PG were mean ± SEM for 4 cells (12 cells in total, 3 donors) . Skin sections were mounted in flow through diffusion cells with an exposed area of 0.64cm^2. Dichlorvos was applied to the skin surface as an infinite dose (1ml/cm^2) at a concentration of 10mg/ml.

Dose	Flux (µg/cm^2/h)	K_p x 10^{-3} (cm/h)	Lag Time (h)	Linear range
Dichlorvos in IPA 10mg/ml	1346 ± 298**	1334 ± 220**	0.6 ± 0.1	1-3
Dichlorvos in IPM 10mg/ml	66.4 ± 12.1	69.3 ± 18.1	2.6 ± 0.8*	4-24
Dichlorvos in PG 10mg/ml	108 ± 19.7*	110 ± 20.2*	3.2 ± 1.1*	14-24

Table 5. Observed steady state absorption rates, partition coefficients and lag times of dichlorvos applied to the skin as an infinite dose at a concentration of 10mg/ml. A single asterisk denotes that a figure is significantly different from the lowest figure in the same column. A double asterisk denotes that the figure is significantly different from the remaning two figures in the same column ($p<0.05$ with one way ANOVA).

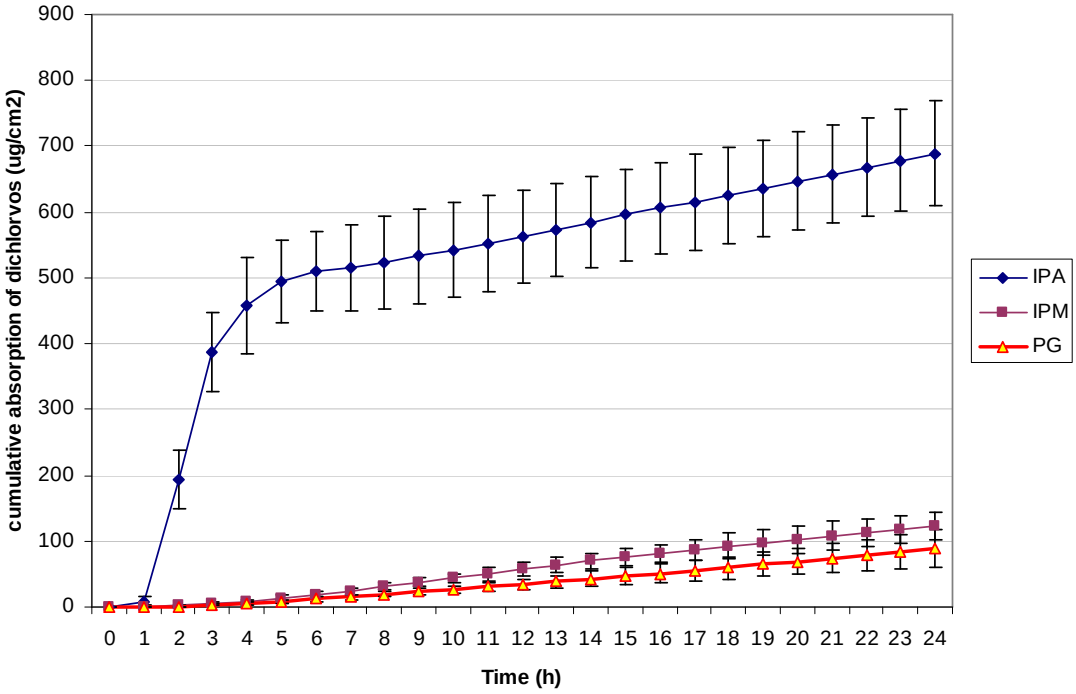

Fig 4.2. 24 hour cumulative absorption profile of an infinite dose of dichlorvos (1mg/ml) in IPA, IPM and PG. Values for dichlorvos applied in IPA, IPM and PG were means ± SEM for 5 cells (15 cells in total, 3 donors). Skin sections were mounted in flow through diffusion cells with an exposed area of 0.64cm^2. Dichlorvos was applied to the skin surface as an infinite dose (1ml/cm^2) at a concentration of 1mg/ml.

Dose	Flux (µg/cm^2/h)	K_p x 10^{-3} (cm/h)	Lag Time (h)	Linear range
Dichlorvos in IPA (1mg/ml)	132.4 ± 28.7**	132 ± 25.1**	0.4 ± 0.2	1-3
Dichlorvos in IPM (1mg/ml)	5.8 ± 1.3	5.5 ± 1.1	2.3 ± 0.6*	6-24
Dichlorvos in PG (1mg/ml)	3.8 ± 0.9	4.1 ± 1.1	2.9 ± 0.7*	3-24

Table 6. Observed steady state absorption rates, partition coefficients and lag times of dichlorvos applied to the skin surface in an infinite dose at a concentration of 1mg/ml. A single asterisk denotes that a figure is significantly different from the lowest figure in the same column. A double asterisk denotes that a figure is significantly different from the remaining two figures in the same column ($p<0.05$ with one way ANOVA).

4.3.2: 24 hour exposure of dermatomed human breast skin to a finite dose of dichlorvos in 3 vehicles.

Methods

For the finite dose studies using dichlorvos, a total of 24 flow-through diffusion cells were used, allowing 8 cells per treatment (in IPA, IPM and PG). Skin sections were taken from 5 separate donors to account for interindividual variability. Each skin sample was dosed with a finite amount (10µl/cm^2) of dichlorvos in each vehicle at a concentration of 5µg/cm^2. Each dose was left in contact with the skin surface for 24 hours before terminal procedures were carried out to determine the dermal distribution of dichlorvos. Sample analysis was carried out using GC-MS. The data shown is pooled from experiments performed in duplicate.

Results

The cumulative absorption profile of dichlorvos applied as a finite dose in three vehicles can be seen in figure 4.3. From this, it can be seen that absorption of dichlorvos was greatest when applied to the skin surface in IPA. The absorption profile of dichlorvos applied in IPA was fastest over the initial 3 hours of exposure, before declining from this point up to 24 hours. Despite the decrease in absorption after 3 hours of exposure, 38% of the applied dose was absorbed from the IPA vehicle after 24 hours. The absorption profiles of dichlorvos applied in IPM and PG were similar, with absorption increasing up to 8 hours after exposure, with the rate of absorption slowing markedly after this point up to 24 hours. Absorption from the PG vehicle was greater than from the IPM vehicle, with 36% of the applied dose in PG, and 31% of the

applied dose in IPM absorbed after 24 hour exposure respectively. Although the cumulative absorption profiles of dichlorvos applied in PG and IPM were very different from the profile of dichlorvos applied in IPA, the total amount of dichlorvos absorbed after 24 hours was not statistically significant between vehicles.

The dose distribution of dichlorvos after 24 hour exposure in IPA, IPM and PG vehicles is shown in figure 4.4. It can be seen that a larger proportion of the applied dose in IPA was found to have evaporated from the skin surface (13.8%), compared with IPM (9.9%) and PG (4.4%). The greatest amount of dichlorvos recovered from the skin surface after 24 hour exposure came from the PG vehicle, with 34.7% of the dose remaining on the skin surface, compared with 19.8% from IPM and 16.6% from IPA. The amount of dichlorvos recovered from the skin surface when applied in PG was significantly different from the amount recovered from the skin surface when applied in IPA or IPM ($p>0.05$ with one-way ANOVA).

Despite comparable amounts of dichlorvos being recovered from the stratum corneum tape strips from all three vehicles (1.2% from IPA, 2.6% from IPM and PG respectively), the amount recovered from within the skin after 24 hour exposure varied greatly between application vehicles. Significantly more dichlorvos was recovered from within the skin membrane after 24 hour exposure when applied in the IPM vehicle (20.1%) compared with 7.1% following application in the IPM vehicle, and 1.6% from the IPA vehicle respectively.

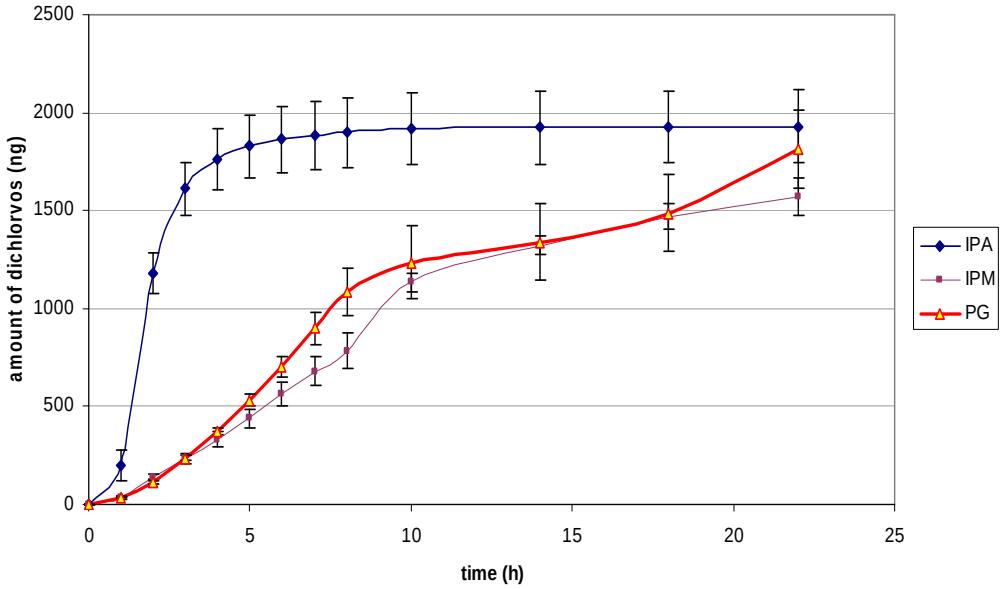

Fig.4.3. 24 hour cumulative absorption profile of dichlorvos applied as a finite dose (10µl/cm^2) in IPA, IPM and PG. Values for dichlorvos applied in IPA, IPM and PG were means ± SEM for 8 cells (24 cells in total, 5 donors). Skin sections were mounted in flow through diffusion cells with an exposed area of 0.64cm^2. Dichlorvos was applied to the skin surface as a finite dose (10µl/cm^2) at a concentration of 5µg/cm^2.

Dose	Flux (ng/cm^2/h)	K_p x 10^{-3} (cm/h)	Lag Time (h)	Linear range
Dichlorvos in IPA (5µg/cm^2)	983.1 ± 121.2**	812 ± 104**	0.6 ± 0.2	1-3
Dichlorvos in IPM (5µg/cm^2)	330.4 ± 65.5*	297 ± 55.1*	0.6 ± 0.1	1-8
Dichlorvos in PG (5µg/cm^2)	163.4 ± 32.7	157 ± 30.2	0.4 ± 0.1	2-8

Table 7. Observed steady state absorption rates, partition coefficients and lag times for dichlorvos applied as a finite dose in IPA, IPM and PG. A single asterisk next to a figure denotes that a figure is significantly different from the lowest figure in the same column. A double asterisk indicates that a figure is significantly different from both remaining figures in the same column ($p<0.05$ with one way ANOVA).

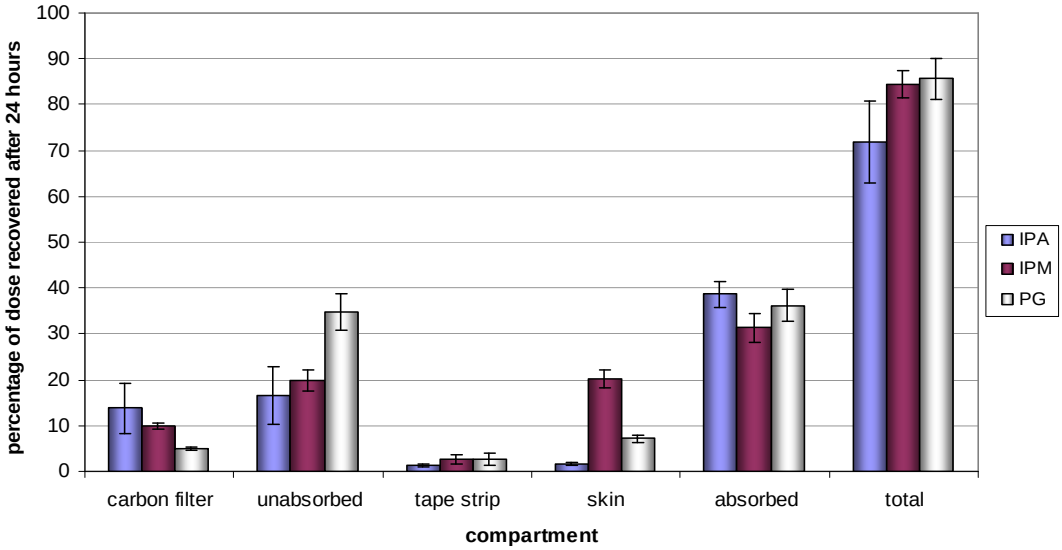

Fig.4.4.Dose distribution of dichlorvos applied as a finite dose to dermatomed human breast skin. Values are means ± SEM for 8 cells for each vehicle (24 cells in total, 5 donors). 'Carbon filter' corresponds to the evaporated dose recovered after 24 hour exposure, 'unabsorbed' is the dose remaining on the skin surface after 24 hours,' tape strip' is the amount of dichlorvos recovered from the stratum corneum tape strips after 24 hours (no more than 15 strips per skin sample), 'skin' is the dose recovered from within the skin membrane after tape stripping, and the absorbed dose accounts for the total amount recovered from the receptor fluid after 24 hour exposure. The total recovery is the sum of all the compartments.

4.3.3: 24 hour exposure of dermatomed human breast skin to a finite dose of ^{14}C-labelled chlorpyrifos in 3 vehicles

Methods

For these studies, a total of 27 flow-through diffusion cells were used, with skin taken from 6 different human breast skin donors. Overall, there were 9 cells per treatment (Chlorpyrifos in IPA, chlorpyrifos in IPM, and chlorpyrifos in PG). Chlorpyrifos was applied to the skin surface as a finite dose (10µl/cm^2), at the same concentration in each vehicle (500ng/cm^2), containing approximately 100,000 DPM/cell of radiolabelled chlorpyrifos. The dose was left in contact with the skin for 24 hours, at which point terminal procedures were undertaken to analyse the dermal distribution of chlorpyrifos after 24 hour exposure. Sample analysis was carried out using liquid scintillation counting.

Results

The cumulative absorption profile of chlorpyrifos applied as a finite dose in IPA, IPM and PG is shown in figure 4.5. It can be seen that chlorpyrifos absorption was greatest following 24 hour exposure to a finite dose in PG, with 19.4% of the applied dose recovered from the receptor fluid compared with 10.3% from the IPA vehicle and 1.9% from the IPM vehicle. Despite more chlorpyrifos being absorbed from the PG vehicle after 24 hour exposure, chlorpyrifos absorption took longer to reach steady state than from either IPM or IPA vehicles, with an observed lag time of 8.6 ± 1.8h, compared with 5.9 ± 1.3h from the IPA vehicle, and 0.3 ± 0.1h from IPM respectively. Although chlorpyrifos applied in IPM gave the shortest apparent lag time, the amount

absorbed after 24 hours was significantly lower than from IPA and PG. Despite finite dosing, absorption or chlorpyrifos through the skin continued to increase steadily over the 24 hour exposure period.

The dose distribution of chlorpyrifos after 24 hour exposure can is shown in figure 4.6. It can be seen that the largest proportion of applied dose was recovered from the skin surface after 24 hour exposure. The greatest amount of chlorpyrifos was recovered from the skin surface following exposure in IPM (68.2%), followed by 57% from IPA and 40.7% from PG. The amount recovered from the skin surface from the PG vehicle was significantly lower than from the other two vehicles following 1-way ANOVA ($p>0.05$). Following 24 hour exposure, a large proportion of the applied dose was recovered from the stratum corneum when applied in all 3 vehicles, with 15% of the applied dose in PG recovered from the stratum corneum tape strips, 13.5% from the IPA vehicle, and 10.5% being recovered from stratum corneum tape strips after exposure in IPM respectively. The greatest amount of chlorpyrifos recovered from within the skin membranes after 24 hour exposure was observed following application of chlorpyrifos in PG (17%), with 8% recovered following application in IPA, and 7% of the applied dose was recovered from within the skin membranes following application of chlorpyrifos in IPM.

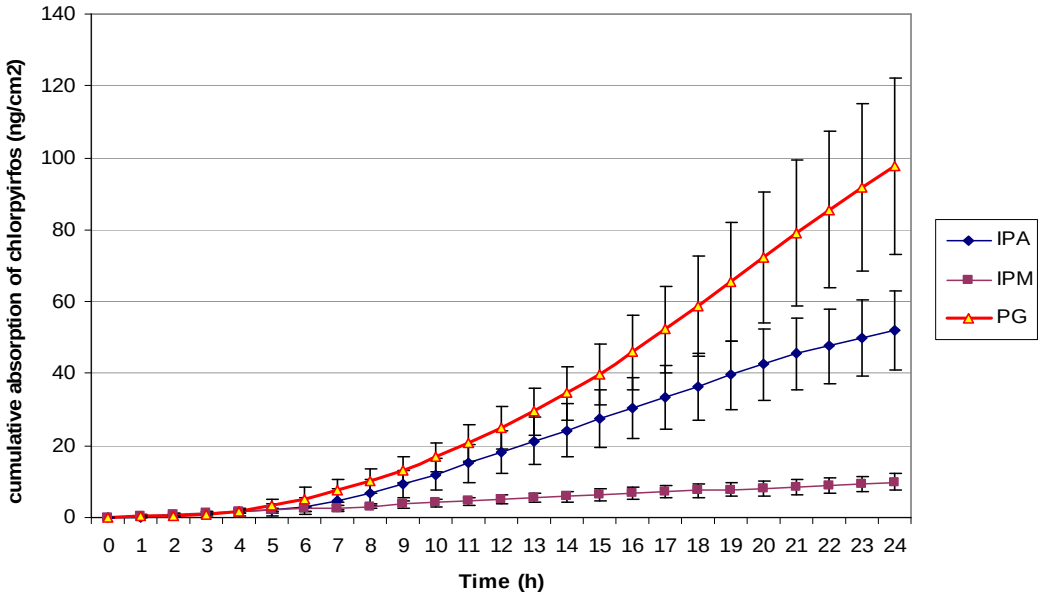

Fig.4.5. 24 hour cumulative absorption profile of chlorpyrifos applied as a finite dose (10µl/cm^2) in IPA, IPM and PG. Values for chlorpyrifos applied in IPA, IPM and PG were means ± SEM for 9 cells (27 cells in total, from 6 donors). Skin sections were mounted in flow through diffusion cells with an exposed area of 0.64cm^2. Chlorpyrifos was applied to the skin surface as a finite dose (10µl/cm^2) at a concentration of 500ng/cm^2.

Dose	Flux (ng/cm^2/h)	K_p x 10^{-3} (cm/h)	Lag Time (h)	Linear range
Chlorpyrifos in IPA (500ng/cm^2)	3.1 ± 1.2*	2.6 ± 1.1	5.9 ± 1.6*	8-21
Chlorpyrifos in IPM (500ng/cm^2)	0.4 ± 0.1	3.9 ± 1.2	0.2 ± 0.04	0-24
Chlorpyrifos in PG (500ng/cm^2)	6.3 ± 1.8*	5.7 ± 1.4*	8.6 ± 2.1*	13-24

Table 8. Observed steady state absorption rates, partition coefficients and lag times for chlorpyrifos applied as a finite dose in IPA, IPM and PG. A single asterisk next to a figure indicates that a figure is significantly different from the lowest figure in the same column. A double asterisk indicates that a figure is significantly different from both remaining figures in the same column (P<0.05 with one way ANOVA).

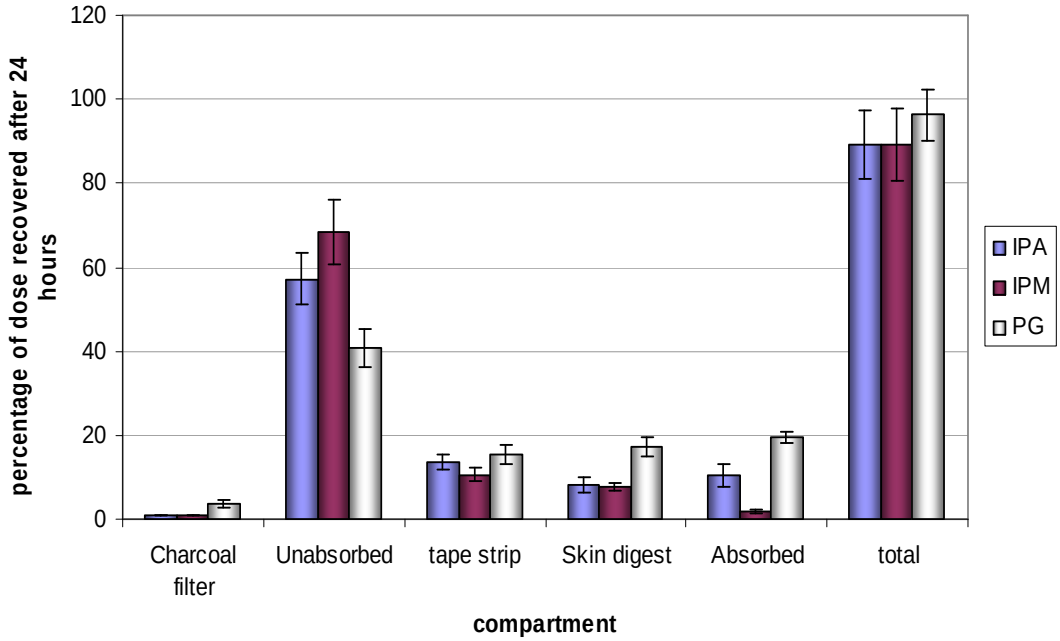

Fig.4.6. Dose distribution of chlorpyrifos applied as a finite dose to dermatomed human breast skin. Values are means ± SEM for 9 cells for each vehicle (27 cells in total, 6 donors). 'Carbon filter' corresponds to the evaporated dose recovered after 24 hour exposure, 'unabsorbed' is the dose remaining on the skin surface after 24 hours,' tape strip' is the amount of chlorpyrifos recovered from the stratum corneum tape strips after 24 hours (no more than 15 strips per skin sample), 'skin' is the dose recovered from within the skin membrane after tape stripping, and the absorbed dose accounts for the total amount recovered from the receptor fluid after 24 hour exposure. The total recovery is the sum of all the compartments.

4.3.4: 24hr exposure of ST pig abdomen skin to a finite dose (20µl) of neat phorate (23mg/cell) and dilute phorate in IPA (25µg/cell)

Methods

For this study, 16 static diffusion cells were used (exposed surface area, 2.54cm^2), taking skin from 4 pig skin donors to account for interindividual variability. Half of the skin samples were exposed to neat phorate and the remaining cells were exposed to dilute phorate in IPA. A finite dose (20µl) was applied to the skin surface with an exposed area of 2.54cm^2. The dose was left in contact with the skin for 24 hours, after which terminal procedures were performed in order to analyse the dermal distribution of phorate. Sample analysis was carried out using GC-MS at dstl, Porton Down.

Results

Absorption of neat phorate continued to increase steadily over the 24 hour exposure period despite finite dosing (20µl), although the absorption rate was fastest over the initial 6 hours of exposure. The lag time for neat phorate through ST pig abdomen skin was 4.4 ± 1.1h. However, despite the increase in absorption over 24hrs (figure 4.7), less than 1% of the applied dose of phorate was absorbed 24hrs after initial exposure to the skin (figure 4.8).

The 24 hour cumulative absorption profile of dilute phorate in IPA is very similar to that of neat phorate in that absorption increases over 24hrs despite finite dosing (Figure 4.9). However, there are some important differences. The lag time for absorption of dilute phorate in IPA (1.4h ± 0.4) was much shorter than for neat phorate. It is also important to note that even though

more phorate was absorbed from neat than from dilute in terms of the actual amount recovered in the receptor fluid, as a percentage of what was applied to the skin surface, far more was absorbed from the dilute dose. Less than 1% of the applied dose of neat phorate was absorbed a 24hrs compared with approximately 18% of the applied dose of dilute phorate in IPA (figures 4.8 and 4.10).

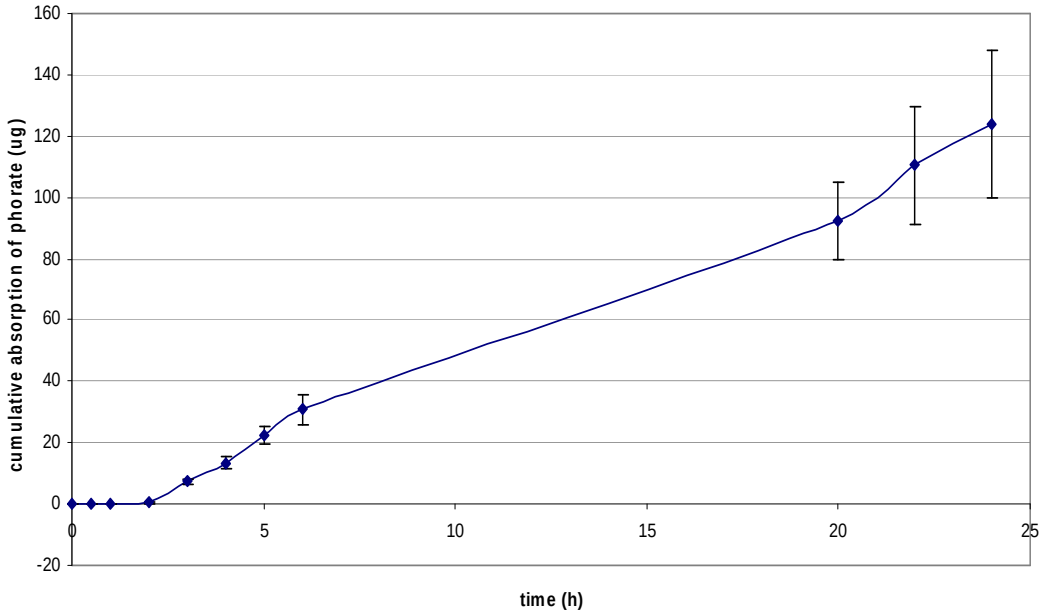

Fig 4.7. 24 hour cumulative absorption profile of neat phorate (23mg/cell (9.05mg/cm^2)) applied as a finite dose to ST pig abdomen skin. Values are means ± SEM of 8 static diffusion cells (4 donors). Skin sections were mounted in static diffusion cells with an exposed area of 2.54cm^2. The dose applied to the skin surface was 20µl/cell. Lag time (4.4 ± 1.1h) was calculated from 3-6 hours after exposure.

Dose	Flux (ng/cm^2/h)	K_p x 10^{-3} (cm/h)	Lag Time (h)	Linear range
Neat phorate (finite dose)	3.9 ± 0.3	3.5 ± 2.1	4.4 ± 1	3-6

Table 9. Observed steady state absorption rate, partition coefficient and lag time for neat phorate applied to pig abdomen skin *in vitro*

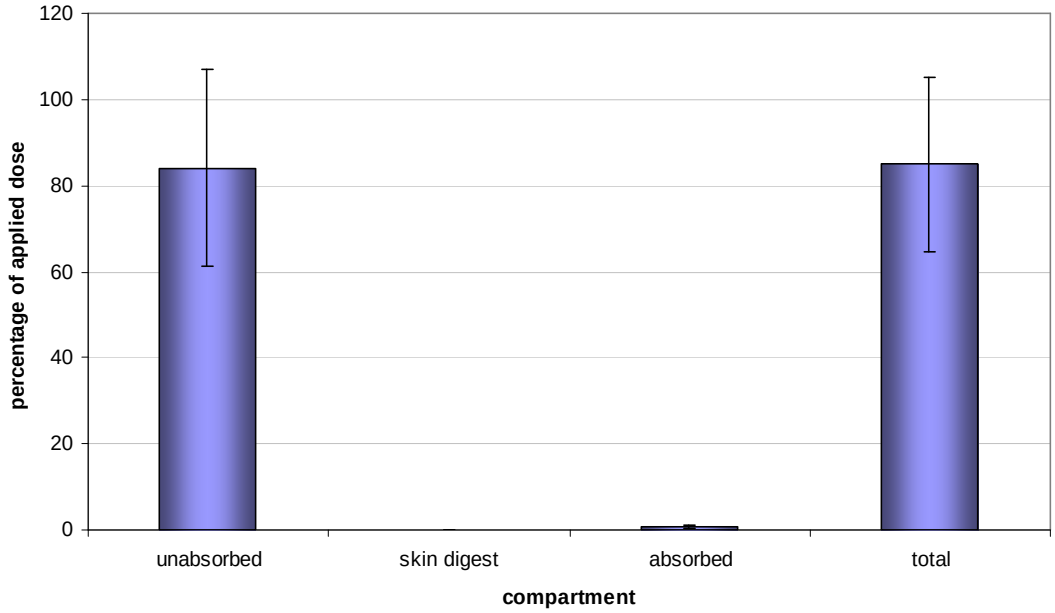

Fig 4.8. Dose distribution of neat phorate (23mg/cell) applied as a finite dose to ST pig abdomen skin. Values are means ± SEM for 8 static diffusion cells (4 donors). 'Unabsorbed' corresponds to the percentage of the applied dose recovered from the skin surface, 'skin digest' is the percentage of applied dose recovered from within the skin, the 'absorbed' dose is the percentage of neat HD recovered from the receptor fluid after 24 hour exposure.

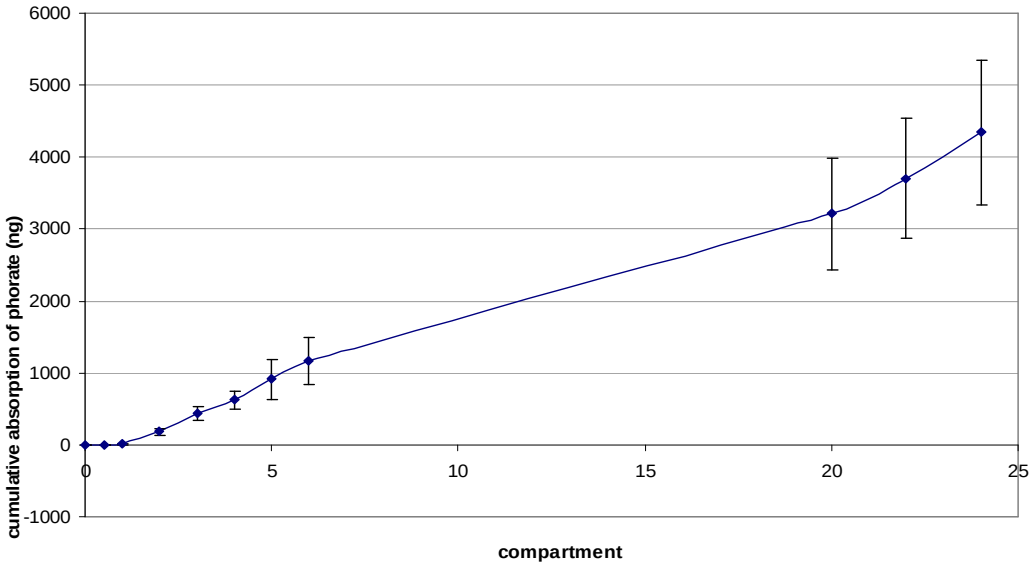

Fig 4.9.24 hour cumulative absorption profile of dilute phorate in IPA (25µg/cell (9.84µg/cm^2)) applied as a finite dose to ST pig abdomen skin. Values are means ± SEM of 8 static diffusion cells (4 donors). Skin sections were mounted in static diffusion cells with an exposed area of 2.54cm^2. The dose applied to the skin surface was 20µl/cell. Lag time (1.4 ± 0.4h) was calculated from 1-6 hours after exposure.

Dose	Flux (ng/cm^2/h)	K_p x 10^{-3} (cm/h)	Lag Time (h)	Linear range
Dilute phorate in IPA (finite dose)	372.3 ± 32.9	359 ± 37.4	1.4 ± 0.4	1-6

Table 10. Observed steady state absorption rate, partition coefficient and lag time of phorate diluted in IPA, applied to pig abdomen skin *in vitro*

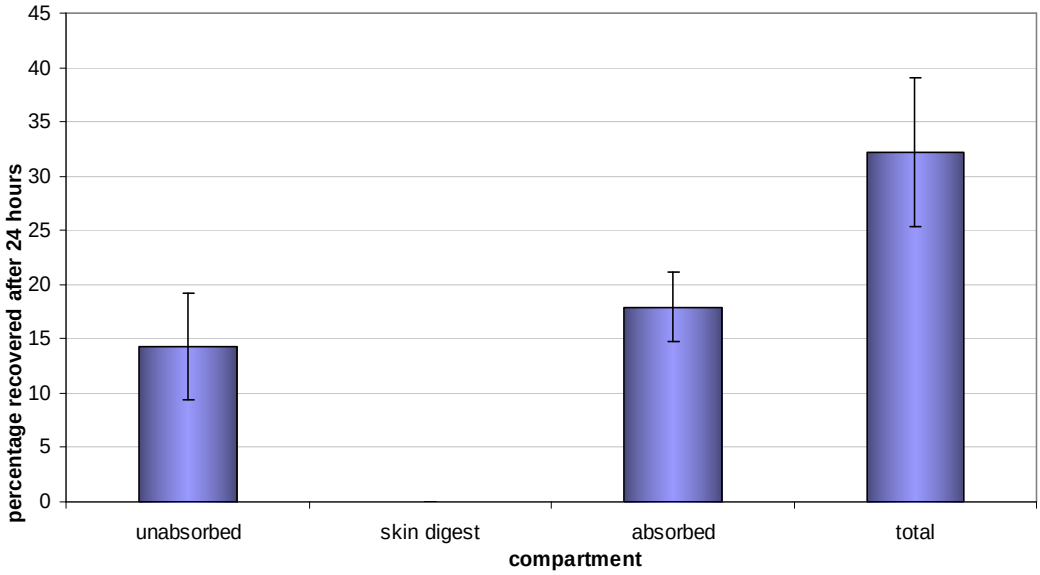

Fig 4.10. Dose distribution of dilute phorate in IPA (25µg/cell) applied as a finite dose to ST pig abdomen skin. Values are means ± SEM for 8 static diffusion cells (4 donors). 'Unabsorbed' corresponds to the percentage of the applied dose recovered from the skin surface, 'skin digest' is the percentage of applied dose recovered from within the skin, the 'absorbed' dose is the percentage of neat HD recovered from the receptor fluid after 24 hour exposure.

4.4: Discussion

4.4.1: Infinite dose dichlorvos

The main purpose of assessing infinite dose exposure is to generate maximum absorption rates, partition coefficients and lag times so that the data can be used to feed into QSAR predictions, in order to rank the chemicals of interest against known marker compounds. Dermal absorption of dichlorvos at high doses (1mg/ml and 10mg/ml) was investigated due to the high levels of dichlorvos required to produce saturated solutions in the vehicles used. Absorption of infinite, saturated solutions of chlorpyrifos were not investigated for similar reasons, however, attempts to investigate high doses under infinite conditions did not work and so are not included in this thesis.

The cumulative absorption profiles of dichlorvos applied as an infinite dose in IPA at both 10mg/ml and 1mg/ml concentrations (figures 4.1 and 4.2) were not typical of what would be expected from an infinite dose absorption profile. The observed flux was fastest over the first 3 hours of exposure (1346.8 ± 298.2μg/cm^2/h), before slowing markedly up to 24 hours. It is possible that the rapid tailing-off in absorption was due to the depletion of IPA from the skin surface, despite infinite dosing. IPA is a highly volatile solvent, and so it is possible that as it evaporated from the skin surface, the surface concentration of dichlorvos may have been increased, leading to an increase in flux. As a result of the volatility of IPA, steady state absorption was not achieved and so true infinite dose conditions were not achieved. Despite dichlorvos being added to the skin surface as an infinite dose in IPA, IPM and PG at 2

concentrations (10mg/ml and 1mg/ml), it was not possible to ascertain the 'true' maximum flux of dichlorvos in the 3 vehicles tested because, in order to do this, the chemical should be saturated in its application vehicle. Also, due to the properties of the 3 vehicles used, the solubility of dichlorvos was different in each vehicle, and so the thermodynamic activity of dichlorvos in each vehicle was not the same. As dichlorvos is a lipophilic compound, it will be closer to saturation in the most hydrophilic solvent (PG), as it is less soluble in PG than in IPA or IPM, which are more lipophilic.

The 10 fold difference in dose concentration of dichlorvos in IPA did however yield an approximately 10 fold difference in the observed flux (1346µg/cm^2/h and 132µg/cm^2/h for 10mg and 1mg/ml doses respectively), meaning that meaning that there was a linear flux-concentration relationship.

4.4.2: Finite exposure to dichlorvos and chlorpyrifos

As expected due to the different chemical properties of the two organophosphates used, the cumulative absorption profiles of dichlorvos (figure 4.3), and chlorpyrifos (figure .4.5) were very different when applied to the skin surface in IPA, IPM and PG. The cumulative absorption profile of dichlorvos applied as a finite dose in IPA (figure.4.3) was similar to the profile observed from the infinite dose studies using dichlorvos in IPA (figure 4.1 and 4.2). From the infinite dose studies, it can be seen that the amount of dichlorvos absorbed after 24 hours was far greater than from the other two vehicles, however, when applied as a finite dose at a low concentration in the same vehicles, there was no significant difference in the amount of dichlorvos

absorbed between the three vehicles used (figure 4.3). This was unexpected and it is possible that the greater volume of IPA on the skin surface for the infinite dose studies allowed absorption to continue at a faster rate for longer than when applied as a finite dose. Therefore, the rapid evaporation of IPA from the skin surface from the finite dose may have prevented absorption by allowing dichlorvos to evaporate. This is supported by the dose distribution in figure 4.4, where more dichlorvos had evaporated from the IPA vehicle than from either IPM or PG.

It was expected that absorption of dichlorvos from a finite exposure would be greatest from the PG vehicle, as this would have had greatest thermodynamic activity. However, it was observed that absorption was marginally greater from the IPA vehicle than from IPM or PG after 24 hours. It is possible that this could also be due to the volatility of IPA. Although the observed flux of dichlorvos in IPA (983 ± 121ng/cm^2/h) was approximately 3 times greater than the observed flux of dichlorvos in IPM (330 ± 65ng/cm^2/h), and 6 times greater than dichlorvos in PG (163 ± 32ng/cm^2/h), the time over which the maximum absorption rate could be calculated was far shorter (2 hours) when applied in IPA. Flux rates from the remaining vehicles were calculated over much longer periods, as IPM and PG are less volatile and maintain contact with the skin for longer, allowing more absorption to occur over a longer period of time. The volatile nature of IPA means that maximum flux can only be measured over a short period of time, and so this makes accurate calculation of steady state flux virtually impossible.

From the dose distribution shown in figure 4.4, it can be seen that a much greater proportion of the applied dose was recovered from within the skin when applied in IPM and PG. Therefore, it may be possible that further absorption from these 2 vehicles could be possible beyond the 24 hour exposure period, and that this could surpass the amount absorbed from IPA, as only a small proportion of the applied dose was recovered from the stratum corneum tape strips and within the skin membranes.

The greatest absorption of chlorpyrifos following 24 hour exposure to the skin came from the PG vehicle (figure 4.5). This was expected due to chlorpyrifos having a greater thermodynamic activity in PG than in either IPA or IPM due to the hydrophilic nature of PG. Absorption continued to increase over 24 hours from all three vehicles despite finite dosing. This was unusual, particularly for IPA given its volatility and rapid evaporation from the skin surface. However, chlorpyrifos is a more lipophilic chemical than dichlorvos, and so it is possible that when this was applied to the skin surface in the moderately amphipathic IPA, that chlorpyrifos partitioned more readily into the skin and from here, could penetrate slowly through the dermis and into the receptor fluid. This appears to be the case when looking at the dose distribution in figure 4.6, as the amount of chlorpyrifos recovered from within the stratum corneum tape strips and skin membrane combined exceeded 20% of the applied dose in IPA. The amount of chlorpyrifos recovered from the tape strips and skin membranes from IPM and PG also exceeded 20% of the applied dose This reservoir may explain the increase in absorption from IPM and PG over the 24 hour exposure period despite finite dosing. Also, IPM and

PG are non volatile and maintain contact with the skin surface for long periods of time compared with IPA, therefore allowing absorption through the skin to occur steadily over time.

When comparing absorption of dichlorvos and chlorpyrifos, it can be seen that absorption of dichlorvos after 24 hour exposure in IPA, IPM and PG was approximately twice as great as absorption of chlorpyrifos from finite dose conditions. This may be explained by differences in their physicochemical properties. Chlorpyrifos is a more lipophilic chemical than dichlorvos, and so will preferentially partition into the stratum corneum, particularly when applied in IPA and PG. From here, penetration through the more hydrophilic dermis into the receptor fluid was much slower. Chlorpyrifos is also a solid at room temperature, and so as the solvent vehicles evaporated, a deposit of chlorpyrifos was left behind which could not be absorbed. This could explain the large proportion of applied dose on the skin surface after 24 hour exposure (figure 4.6). Dichlorvos is less lipophilic, and is also a liquid at room temperature. Therefore, absorption can be maintained for longer on the skin surface even after depletion of the application vehicle from the skin surface.

4.4.3: Phorate absorption through pig abdomen skin

The cumulative absorption profile for neat phorate (figure 4.7) shows that absorption increases over the 24hr exposure period despite finite dosing. It was expected, despite being applied as a small volume to the skin surface in IPA, that phorate would partition readily into the lipophilic upper layers of the

skin, and slowly become absorbed, although the majority of the dose that penetrates the skin surface may not become ‘systemically’ absorbed, due to phorate being a lipophilic liquid (log p = 3.56). Further evidence for this can be seen from the distribution graphs for dilute phorate in IPA (figure 4.10), with 17% of the applied dose of dilute phorate in IPA absorbed following 24 hour exposure. The majority of the applied dose of neat phorate was recovered from the skin surface following 24hr exposure (84%), suggesting that there was little potential for phorate to penetrate the skin beyond the 24hr exposure time. However, recovery of the applied dose of dilute phorate was comparatively poor (32% recovery for dilute phorate, 85% for neat phorate). Unfortunately, no skin distribution data were available due to the poor stability of phorate in soluene, the solvent used to dissolve the skin samples. This may explain the poor recovery of the dilute phorate. However, due to phorate being a lipophilic chemical, it is highly likely that a large proportion of the applied dose would be retained within the skin after 24hr exposure, particularly within the lipids of the stratum corneum in the upper layers of the skin.

Chapter 5

24 hour exposure of human and pig skin to sulphur mustard (HD)

5. 24 hour exposure of human and pig skin to ^{14}C-radiolabelled sulphur mustard (HD)

5.1: Introduction

The purpose of this project was to investigate dermal absorption of chemicals that could be used as potential surrogates for predicting absorption of more harmful, bioactive agents, therefore, it was important to investigate in parallel the dermal absorption of bioactive agents where possible, so that the absorption profiles of these chemicals could be compared with those of the marker and surrogate compounds in order to identify how useful they are for predicting absorption.

Following the absorption studies undertaken with the marker compounds and the organophosphates dichlorvos and chlorpyrifos it would have been informative to study sarin. However this proved impossible. ^{14}C labelled HD was available for a study in collaboration with dstl, and was chosen because it is a potent vesicating agent, meaning the dermal route is of great importance in terms of exposure. HD has previously been studied in terms its potential for high level, military exposure due to its use as a chemical warfare agent (Chilcott *et al*. 2000, Chilcott *et al*. 2001, and Hattersley *et al*. 2008). It has also been extensively reviewed in terms of local HD toxicity and mechanisms of action (Balali-Mood and Hefazi 2005, Saladi *et al* .2005, Shakarjian et al. 2010). Despite this, little is currently known about HD in terms of low level, civilian exposure

HD was applied to the skin surface as a neat, finite dose and also as a finite dose diluted in IPA. Neat doses were applied in order to compare the diluted doses with a 'worst case' scenario in terms of dermal exposure to a finite dose of HD and phorate. The diluted dose in IPA was chosen because IPA is the most volatile of the vehicles tested in previous studies using marker and surrogate compounds, meaning that it more closely mimics exposure to a spray or vapour, which may come into contact with the skin during accidental or deliberate exposure to individuals on the periphery of chemical release.

5.2: Aims

The aim of these studies was to generate 24 hour absorption data for dermal exposure to low levels of HD with the purpose of comparing the data generated with the data obtained from the model and surrogate compounds to identify the usefulness of these chemicals for predicting the dermal absorption of HD.

5.3: Results

5.3.1: 24hr exposure of full thickness human breast skin to neat ^{14}C-labelled HD and ^{14}C-labelled HD diluted in IPA

Methods

For this study, finite doses (20µl/cell) of neat HD (25mg/cell) and HD diluted in IPA (1.25mg/cell) (all containing 0.185MBq/cell of radiolabelled HD) were left in contact with human breast skin in static diffusion cells (exposed area, 2.54cm^2) for 24 hours (6 cells for each dose). Following this, terminal

procedures were performed in order to determine the dermal distribution of HD after 24 hour exposure.

Results

The cumulative absorption profile of neat HD applied to full thickness human breast skin can be seen in figure 5.1. As can be seen from this figure, exposure to neat HD resulted in slow absorption over the initial 3 hours of exposure before an increase in flux up to 20 hours after exposure. This produced a lag time of 2.64 ± 0.61 hours. This profile fits a predicted finite dose curve as the absorption rate tails off towards the end of the exposure period as the applied dose becomes depleted over time.

After 24 hour exposure to neat HD, approximately 25% of the applied dose was absorbed through the full thickness human breast skin into the receptor fluid (figure 5.2). It can also be seen that only a small percentage (8.2 ± 2.7%) of the applied dose was recovered from the skin surface after 24 hour exposure when compared with the absorbed dose, and the dose remaining within the skin. The majority of the applied dose was recovered from within the skin membrane after 24 hours, with 58 ± 8% of the applied dose found in the skin.

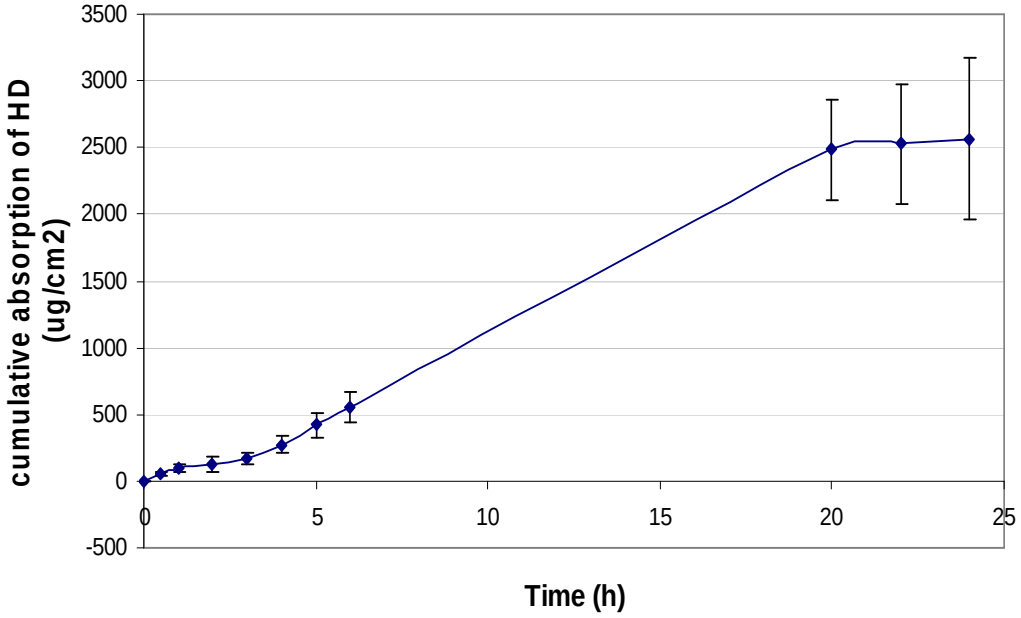

Fig 5.1. 24 hour cumulative absorption profile of neat HD applied as a finite dose (10mg/cm^2) to full thickness human breast skin. Values for neat HD applied to human breast skin were mean ± SEM for 4 static diffusion cells (4 skin donors). Skin sections were mounted in static diffusion cells with an exposed area of 2.54cm^2. Neat HD was applied to the skin surface as a finite dose (20µl/cell).

Dose	Flux (µg/cm^2/h)	K_p x 10^{-3} (cm/h)	Lag Time (h)	Linear range
Neat HD (finite dose)	129.1 ± 14.4	126 ± 10.3	2.6 ± 0.6	3-6

Table 11. Observed steady state absorption rate, partition coefficient and lag time following 24 hour exposure of full thickness human breast skin to neat HD.

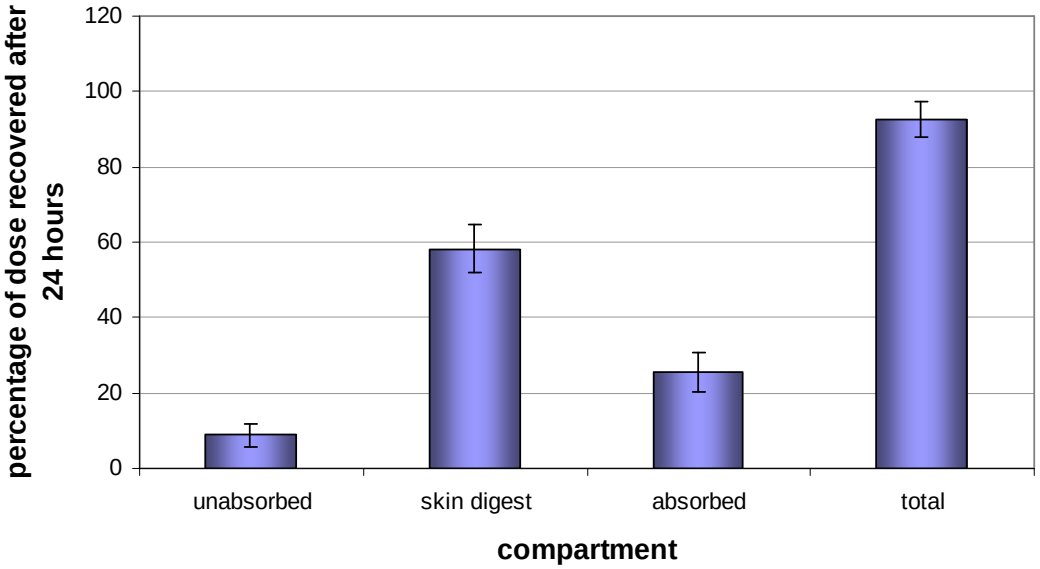

Fig 5.2. Dose distribution of Neat HD applied as a finite dose to full thickness human breast skin. Values are mean ± SEM of 4 static diffusion cells (from 4 donors). 'Unabsorbed' corresponds to the percentage of the applied dose recovered from the skin surface, 'skin digest' is the percentage of applied dose recovered from within the skin, the 'absorbed' dose is the percentage of neat HD recovered from the receptor fluid after 24 hour exposure.

The cumulative absorption profile of HD diluted in IPA through full thickness human breast skin can be seen in figure 5.3. The lag time for dilute HD in IPA was shorter in when compared with that of neat HD (1.8 ± 0.3 hours for HD in IPA, and 2.6 ± 0.6 hours for neat HD). Absorption of dilute HD in IPA was fastest over the first 6 hours of exposure, however, absorption continued to increase from 6 hours up to 24 hours at a slower rate, despite finite dosing.

The dose distribution of dilute HD in IPA shown in figure 5.3 is similar to the distribution profile of neat HD (figure 5.2) in terms of the proportion of the applied dose recovered from each compartment after 24 hour exposure. Again, the percentage of the applied dose recovered from the skin surface was low (7.5 ± 3.2%) when compared to the percentage absorbed (24.2 ± 6.2%) and the percentage retained within the skin after 24 hours (62.2 ± 9.8%).

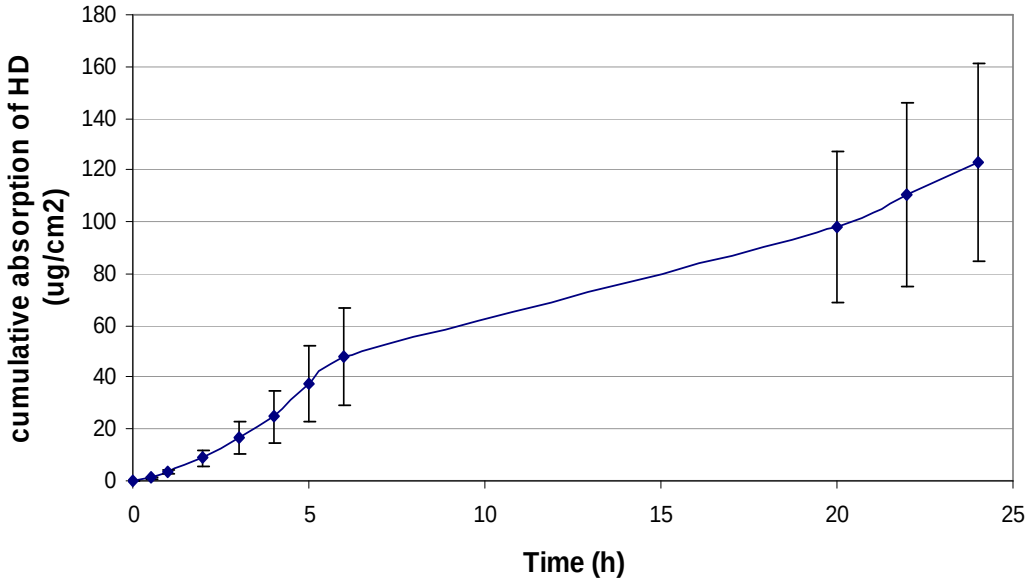

Fig 5.3. 24 hour cumulative absorption profile of dilute HD applied in IPA as a finite dose (492µg/cm^2) to full thickness human breast skin. Values for neat HD applied to human breast skin were mean ± SEM for 8 static diffusion cells (4 skin donors). Skin sections were mounted in static diffusion cells with an exposed area of 2.54cm^2. Dilute HD in IPA was applied to the skin surface as a finite dose (20µl/cell). Lag time was calculated from 4-6 hours after exposure.

Dose	Flux (µg/cm^2/h)	K_p x 10^{-3} (cm/h)	Lag Time (h)	Linear range
Dilute HD in IPA (finite dose)	11.63 ± 4.03	10.4 ± 3.1	1.8 ± 0.3	4-6

Table 12. Observed steady state absorption rate, partition coefficient and lag time following 24 hour exposure of full thickness human breast skin to HD diluted in IPA

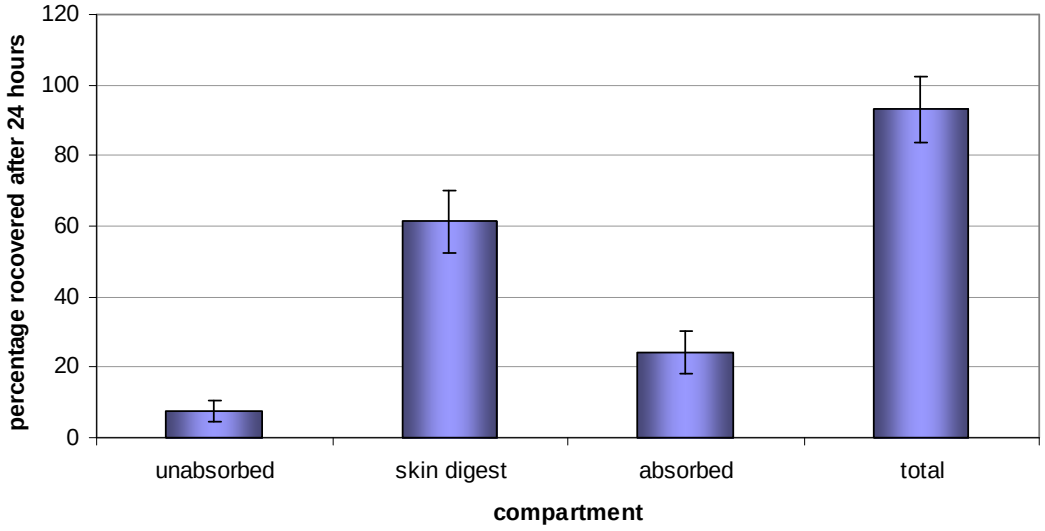

Fig 5.4. Dose distribution of dilute HD in IPA applied as a finite dose to full thickness human breast skin. Values are mean ± SEM of 8 static diffusion cells (from 4 donors). 'Unabsorbed' corresponds to the percentage of the applied dose recovered from the skin surface, 'skin digest' is the percentage of applied dose recovered from within the skin, the 'absorbed' dose is the percentage of neat HD recovered from the receptor fluid after 24 hour exposure.

5.3.2: 24 hour exposure of full thickness (FT) and split thickness (ST) pig abdomen skin to finite doses of neat ^{14}C-radiolabelled HD and ^{14}C-radiolabelled HD diluted in IPA

Methods

For these studies, a total of 20 static diffusion cells were used, meaning 5 cells were available for each treatment:

1 – Full thickness pig abdomen skin exposed to neat HD

2 – Split thickness pig abdomen skin exposed to neat HD

3 – Full thickness pig abdomen skin exposed to dilute HD in IPA

4 – Split thickness pig abdomen skin exposed to dilute HD in IPA

Neat HD (25.4mg/cell) was applied as a finite dose (20µl) to the skin, and dilute HD in IPA (1.25mg/cell) was also applied to the skin surface as a finite dose. Each dose contained approximately 0.185MBq/cell of radiolabelled HD. After 24 hour exposure, terminal procedures were undertaken to assess the dermal distribution of HD.

Results

The cumulative absorption of neat HD through full thickness and split thickness pig abdomen skin following 24 hour exposure is shown in figure 5.5. From this figure, it can be seen that absorption of neat HD continued to increase through both full thickness and split thickness pig abdomen skin for 24 hours despite finite dosing. The amount of HD absorbed through split thickness pig skin was significantly greater than through full thickness pig abdomen skin, with more than double the amount being absorbed after 24

hour exposure. The lag time for absorption through split thickness skin was also much shorter than through full thickness pig skin (1.7h ± 0.2 through split thickness skin and 4.1 ± 0.6 through full thickness skin).

From the dose distribution profile of neat HD applied to full thickness and split thickness pig abdomen skin shown in figure 5.6, it can be seen that a greater proportion of the applied dose was recovered from the skin surface with full thickness pig skin (16.6 ± 5.2%) compared with split thickness pig skin (8.9 ± 2.1%). The amount of HD recovered from within the skin after 24 hour exposure was also greater in full thickness pig abdomen skin (52.5 ± 6.2%) compared with the amount recovered from split thickness pig abdomen skin (33.7 ± 4.4%).

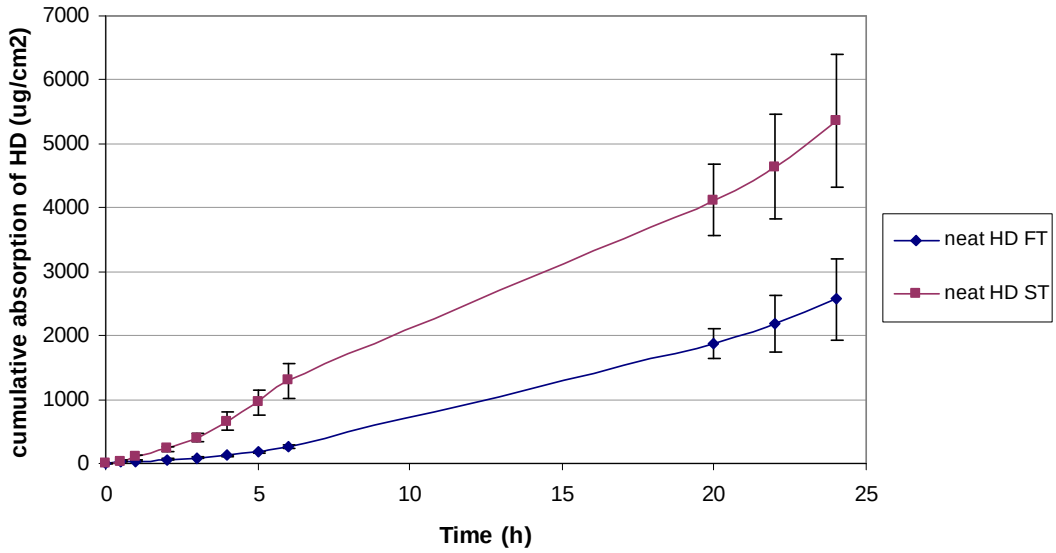

Fig 5.5 24 hour cumulative absorption profile of neat HD (10mg/cm^2) applied as a finite dose to full and split thickness pig abdomen skin. Values for neat HD FT are mean ± SEM of 5 diffusion cells (5 donors), and values for neat HD ST are means ± SEM of 5 cells (5 donors). Skin sections were mounted in static diffusion cells with an exposed area of 2.54cm^2. The dose applied to the skin surface was 20µl/cell. The lag time for neat HD FT was calculated from 4-6 hours, and the lag time for neat HD ST was calculated from 3-6 hours

Dose	Flux (µg/cm^2/h)	K_p x 10^{-3} (cm/h)	Lag Time (h)	Linear range
neat HD ST pig skin (finite dose)	268.4 ± 10.6*	259.1 ± 10.6*	1.7 ± 0.2	2-6
neat HD FT pig skin (finite dose)	82.4 ± 14.7	80.4 ± 10.1	4.1± 0.6*	4-6

Table 13. Observed steady state absorption rates, partition coefficients and lag times of HD applied to full and split thickness pig abdomen skin *in vitro*. A single asterisk next to a figure indicates a significant difference ($p<0.05$ with one way ANOVA).

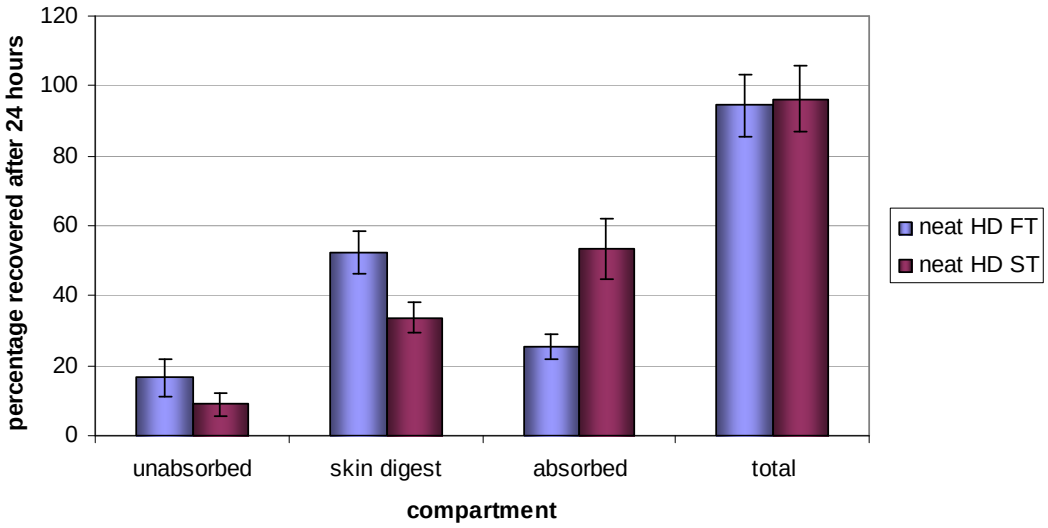

Fig 5.6. Dose distribution of neat HD applied as a finite dose to full and split thickness pig abdomen skin. Values for neat HD FT are mean ± SEM of 5 static diffusion cells (5 donors), and values for neat HD ST are means ± SEM of 5 static diffusion cells (5 donors). 'Unabsorbed' corresponds to the percentage of the applied dose recovered from the skin surface, 'skin digest' is the percentage of applied dose recovered from within the skin, the 'absorbed' dose is the percentage of neat HD recovered from the receptor fluid after 24 hour exposure.

The cumulative absorption profile of dilute HD in IPA through full thickness pig abdomen skin differs greatly to that of dilute HD through split thickness pig abdomen skin (figure 5.7). As can be seen from this figure, absorption through full thickness pig skin continues to increase steadily throughout the 24 hour exposure period, despite application of a finite dose. However, absorption through split thickness pig skin was much faster over the first 6 hours of exposure, but then slowed dramatically up to the 24 hour time point. Despite this, the amount of HD absorbed through split thickness pig abdomen skin was significantly greater than through full thickness pig skin, with more than double the amount being absorbed through split thickness pig skin after 24 hours.

The dose distribution of dilute HD in IPA applied to full and split thickness pig abdomen (figure 5.8) follows a similar pattern to the dose distribution of neat HD through full and split thickness pig skin (figure 5.6) in the sense that a greater proportion of the applied dose was recovered from the skin surface of full thickness pig skin (17.3 ± 4.7% from full thickness skin compared with 10.2 ± 3.5% from split thickness skin), and also a greater proportion of the applied dose was recovered from within full thickness skin compared with split thickness skin (56.1 ± 10.2% for full thickness skin and 35.8 ± 7.3% for split thickness skin respectively).

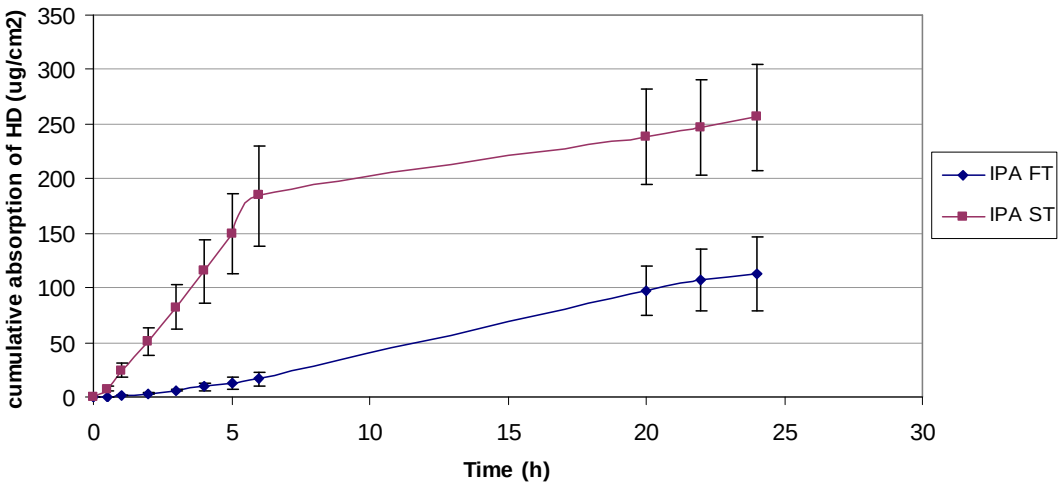

Fig 5.7. 24 hour cumulative absorption profile of dilute HD in IPA (492µg/cm^2) applied as a finite dose to full and split thickness pig abdomen skin. Values for dilute HD in IPA (IPA FT) are mean ± SEM of 5 diffusion cells (5 donors), and values for dilute HD in IPA (IPA ST) are means ± SEM of 5 cells (5 donors). Skin sections were mounted in static diffusion cells with an exposed area of 2.54cm^2. The dose applied to the skin surface was 20µl/cell.

Dose	Flux (µg/cm^2/h)	K_p x 10^{-3} (cm/h)	Lag Time (h)	Linear range
HD in IPA FT pig skin (finite dose)	5.99 ± 0.50	2.1 ± 0.5	2.86 ± 0.67*	4-6
HD in IPA ST pig skin (finite dose)	33.37 ± 3.14*	31.5 ± 3.1*	0.5 ± 0.03	1-6

Table 14. Observed steady state absorption rates, partition coefficients and lag times of HD applied to full and split thickness pig abdomen skin in IPA. A single asterisk next to a figure indicates a significant difference ($p<0.05$ with one way ANOVA).

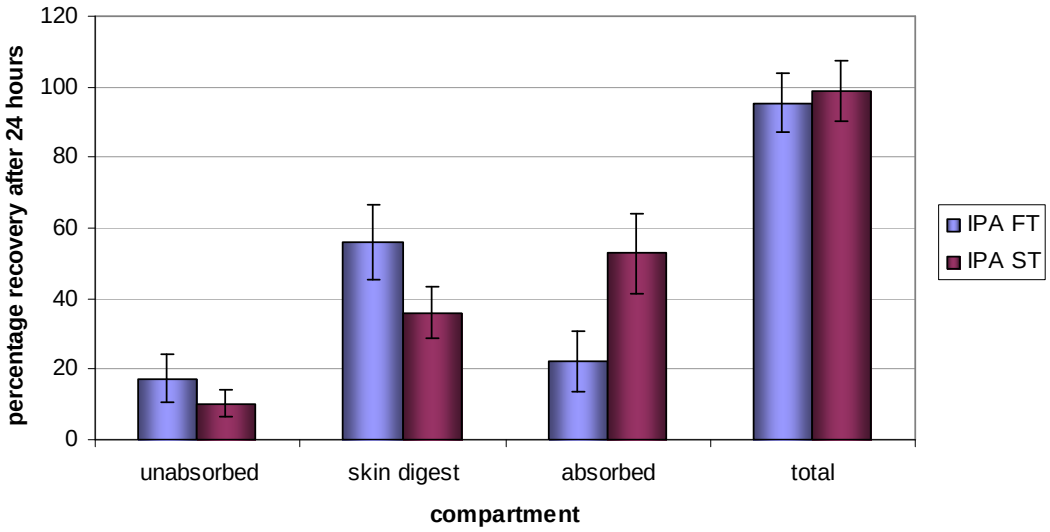

Fig 5.8. Dose distribution of dilute HD in IPA (492µg/cm^2) applied as a finite dose to full and split thickness pig abdomen skin. Values for dilute HD in IPA (IPA FT) are mean ± SEM of 5 static diffusion cells (5 donors), and values for dilute HD in IPA (IPA ST) are means ± SEM of 5 static diffusion cells (5 donors). 'Unabsorbed' corresponds to the percentage of the applied dose recovered from the skin surface, 'skin digest' is the percentage of applied dose recovered from within the skin, the 'absorbed' dose is the percentage of neat HD recovered from the receptor fluid after 24 hour exposure.

5.4: Discussion

Although the 24 hour cumulative absorption profiles of neat HD and dilute HD in IPA through full thickness human breast skin were very different (figures 5.1 and 5.3), the amount of HD absorbed through the skin in terms of percentage applied to the skin surface was similar (25.2 ± 4.3% absorbed from neat HD and 24.2 ± 6.2% from dilute HD in IPA respectively). The lag time for HD applied in IPA (1.8 ± 0.3h) was similar to that of neat HD (2.6 ± 0.6h). However, the observed reduction in lag time may be explained by the vehicle effect of IPA on HD absorption. HD is a lipophilic compound and so will have a greater affinity for the lipids of the stratum corneum than for the IPA vehicle, leading to an increase in absorption initially while the vehicle evaporated from the skin surface. It can be seen from the cumulative absorption profiles that absorption of HD is greater over the first 6 hours of exposure when applied in IPA than as a neat dose (as a proportion of the applied dose).

It is important to note from the dermal distribution graphs shown in figures 5.2 and 5.4 that the majority of the applied dose of neat HD and dilute HD in IPA was recovered from within the skin after 24 hour exposure (58 ± 8.6% after exposure to neat HD and 62.2 ± 9.8% following exposure to dilute HD in IPA). This suggests that HD preferentially partitions within the skin, and is slow to be further absorbed. This confirms the presence of a HD skin reservoir from which it can elicit local, chronic toxic effects as described by Hattersley *et al*. 2008. It is possible that some of the dose remaining within the skin may have the potential to become absorbed, however, it has been suggested that at least part of the applied dose of HD becomes fixed within the skin and is non-

extractable, and that this is the cause of the vesication within the skin (Chilcott *et al*. 2000, Hattersley *et al*. 2008). It has also been suggested that binding of HD to various skin membrane proteins, including actin, annexin A2 and keratin 9 may contribute to HD pathology, as these proteins all play an important role in maintaining skin membrane structure (Sayer *et al*. 2009).

The amount of HD absorbed through full thickness pig abdomen skin after 24hr exposure for both neat HD and dilute HD in IPA was very similar to the amount absorbed through full thickness human breast skin. However, absorption through split thickness pig abdomen skin was approximately 2 fold higher for neat HD and HD applied in IPA than through full thickness skin. This suggests that split thickness pig abdomen skin was not as good a model for absorption through human skin as full thickness pig abdomen skin. Despite this, it is interesting to see that approximately 35% of the applied dose for both neat HD and dilute HD were retained within the split thickness pig abdomen skin (figures 5.6 and 5.8). Even though a large proportion of the applied dose of HD was retained within full thickness human skin (figures 5.2 and 5.4), the amount found in split thickness pig abdomen skin after 24hr exposure may further suggest that HD can be readily absorbed into the skin and can form a ‘reservoir’ from which to cause prolonged local toxic effects. It is possible that this could also be the case for split thickness human skin as well as for split thickness pig abdomen skin.

Chapter 6

The effect of clothing and skin surface decontamination on dermal absorption of organophosphates

6. The effect of clothing and skin surface decontamination on dermal absorption of organophosphates

6.1: Introduction

The effect of covering the skin with everyday clothing and decontamination of the skin surface following exposure to chemicals was investigated to identify how effective they can be at reducing absorption. The approach was to compare dermal absorption of organophosphates following 24 hour exposure with that following decontamination and when the skin was protected with clothing.

Due to the fact that organophosphates (OPs) are widely used in agriculture, the possibility of workers and civilians becoming exposed to these chemicals is high. As a result of this, exposure to various OPs from an occupational perspective has been widely investigated, with many studies being carried out in vivo to assess pesticide worker exposure and the effectiveness of personal protective equipment (PPE) for reducing exposure, in particular with respect to the protection provided by gloves (Creely and Cherrie, 2001, Rawson *et al*. 2001, Nielsen and Andersen, 2001, Cherrie *et al*. 2004), but also with respect to protection provided by PPE worn by workers (Baldi *et al*. 2006, Marchera *et al*. 2009, Protano *et al*. 2009). The investigation carried out by Protano *et al*. 2009 not only investigated PPE such as rubber boots, Tyvek suits and gloves, but also long sleeved cotton shirts and cotton shorts. In this study, it was found that PPE gave >97% protection against five different pesticides (azinphos-methyl, terbutylazine, alachlor, dimethoate and dicamba), whereas cotton clothing gave protection in the range of 84.1% to 92.5%, indicating that

clothing designed for protective purposes is more effective that cotton clothing for reducing exposure to chemicals used in agriculture. Studies undertaken by Marchera *et al*. 2009 investigated the effect of different designs (woven cotton design vs water repellent cotton/polyester) of coverall for reducing exposure of pesticide applicators, and found that cotton/polyester material gave approximately 5.5 times the protection of woven cotton material coveralls. However, both types of coverall were deemed to be sufficiently protective against exposure for use.

Exposure of the hands to various hazardous chemicals has been extensively investigated as exposure to hands has been shown to account for between 50% and 90% of total body exposure (Karr *et al*. 1992, Archibald *et al*. 1995). A study by Creely and Cherrie, 2001 showed that internal glove contamination occurred frequently (25 out of 30 occasions) when using a permethrin-based pesticide based on the use of a novel method for assessing glove protection, where cotton gloves were worn underneath, and over the top of protective gloves to assess the amount of pesticide that would deposit on the skin surface. Despite internal glove contamination occurring so frequently, all gloves tested were found to be impermeable after 8 hours of exposure. Nielsen and Andersen, 2001 also investigated protective gloves (latex and nitrile), as well as the protective nature of nonylphenolethoxylate (NPE), a detergent widely used in pesticide formulations, against absorption of methiocarb, paclobutrazol and pirimicarb. This study showed that NPE decreased absorption of the 3 pesticides, and also that nitrile gloves gave better general protection against absorption than latex, although the degree of

protection was found to decrease over time (nitrile gave only 18 hours of protection against pirimicarb). Nitrile and similar protective material gloves have generally been shown to provide greatest resistance against pesticide exposure, whereas natural rubber has been found to provide limited protection in comparison (Ehntholt *et al*. 1989, Schwope *et al*. 1992, and Raheel and Dai, 1997).

Despite the extensive research into occupational exposure relating to pesticides, very little is known regarding the capability of everyday clothing worn by workers or civilians to provide protection against exposure to hazardous chemicals. It is a distinct possibility that bystanders may become exposed to low levels of chemicals used in agriculture following application to crops, and so it is important to identify the level of protection obtained from wearing everyday clothing. Of relevance to this project t is important to be able to quantitate the effects of every-day clothing worn by those exposed in an incident to protect them.

Studies investigating the effects of decontamination on the dermal absorption of chemicals have also primarily focused on military exposure. In relation to organophosphate exposure, the most common chemical used to investigate the effects of decontamination is the chemical warfare agent VX (Hamilton *et al*. 2004, Bide *et al*. 2005, Taysse *et al*. 2007, Bjarnason *et al*. 2008). The majority of decontamination studies have been carried out using animal models *in vivo*, in particular the domestic pig and guinea pig, with the most common decontamination procedures being application of Fuller’s Earth or

reactive skin decontamination lotion (RSDL). Fuller's Earth is frequently used as it is widely available and cheap to produce. It is generally an effective absorbent of a variety of chemical warfare agents; however, it does not detoxify agents, and also provides a dust hazard if being used outdoors. As a result of this, liquid skin surface decontaminants have become preferable, and led to the production of RSDL. The first formulation of RSDL was a solution of 2, 3 butanedione mono-oximate and diacetyl mono-oxime in MPEG2, and is now commercially available, and used by a number of armies worldwide (Taysse *et al*. 2007). It has been commonly found that decontamination of pig skin *in vivo* after exposure to VX is effective at reducing clinical manifestations of VX exposure. The study by Hamilton *et al*. 2004 showed that decontamination of pig ear skin with RSDL 15 minutes after exposure resulted in arrested development of clinical symptoms of VX poisoning. Fuller's Earth and RSDL have commonly been used as decontaminants for VX exposure and have both been shown to prevent cholinesterase inhibition as a result of VX exposure (Taysse *et al*. 2007). These results were supported by Bjarnason *et al*. 2008, who found that decontamination of pig skin with both RSDL and Fuller's Earth 45 minutes after exposure to 5 times the LD50 for the domestic pig resulted in 100% survival. However, RSDL was found to be more effective at reducing clinical symptoms, as 50% of the surviving pigs decontaminated with Fuller's Earth displayed classical symptoms of VX exposure. This study also found that decontamination of the skin surface with soapy water following VX exposure was completely ineffectual. However, decontamination of guinea pig skin with RSDL following VX exposure was

less effective, with only 36% of guinea pigs surviving after only a 1 minute exposure to VX (Bide *et al*. 2005).

There is little in the published literature aimed specifically at civilian exposure, with the majority of studies using animal models *in vivo*, aimed at military exposure to chemical warfare agents. Therefore, high level exposures for short exposure times have traditionally been used. As a result of this, one of the main aims of these studies was to assess the effectiveness of decontamination using human skin *in vitro*, as this is widely regarded as the best model for human exposure *in vivo*, following low level exposure to surrogate organophosphate compounds.

6.2: Aims and Methods

The aims of these studies were to generate novel data regarding low level exposure of human skin to surrogate compounds in *vitro* in order to assess the ability of everyday clothing (cotton shirt material) to reduce dermal absorption of surrogate compounds (dichlorvos and chlorpyrifos), and also to identify the effect of decontaminating the skin surface using a simple soap solution (5% v/v in water) in relation to skin exposure to surrogate compounds.

For the chlorpyrifos studies, 14C-labelled chlorpyrifos (500ng/cm^2) was applied as a finite dose (10µl/cm^2) and for the dichlorvos studies; dichlorvos was applied as a finite dose (10µl/cm^2) at a concentration of 5µg/cm^2. Clothing (cotton shirt material, 1cm^2) was held in place above the skin surface

by screwing in the donor chamber attachment over the piece of shirt material, creating an approximately 1mm air gap between the clothing and the skin surface (figure 6).

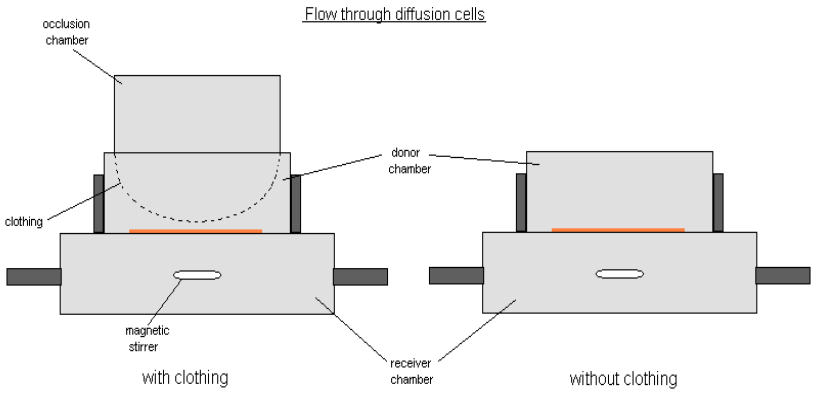

Fig.6. Schematic diagram of the flow through diffusion cell with clothing

After exposure of clothed skin to ^{14}C-labelled chlorpyrifos (4 hours) and dichlorvos (30 minutes), the donor chamber attachment was removed and the clothing was removed. Some of the diffusion cells had no clothing, and were decontaminated at the same time as the removal of clothing from the remaining diffusion cells. Decontamination was carried out by swabbing the skin surface with alternate wet and dry tissues (6 swabs in total), with the initial wet swab containing 0.5% soap solution (v/v), and the remaining wet swabs were carried out using water (to mimic washing with soap and water). Some of the cells had clothing removed and were also decontaminated at the same time, whereas others had clothing removed and were not decontaminated until 24 hours after the initial exposure. All cells were left for 24 hours before terminal procedures were carried out to determine dermal distribution of the test compounds.

6.3: Results

6.3.1: 4 hour exposure of dermatomed human breast skin (clothed and unclothed) to ^{14}C-labelled chlorpyrifos in IPA and PG

Methods

For this study, a total of 18 flow-through diffusion cells were used for 2 *in vitro* flow-through diffusion cell experiments. 6 cells were left unclothed, but were decontaminated after 4 hour exposure to ^{14}C-labelled chlorpyrifos applied in IPA or PG at a concentration of 500ng/cm^2 (finite dose, 10µl/cm^2). 6 cells were clothed, with removal and decontamination of the skin surface after 4 hours, and 6 cells were clothed, with removal at 4 hours after exposure, but no decontamination of the skin surface was carried out until after 24 hours. Samples were analysed by scintillation counting.

Results

The 24 hour cumulative absorption profile in figure 6.1 shows the absorption of chlorpyrifos (applied in IPA) following 4 hour exposure to clothed and unclothed skin. From this figure, it can be seen that decontamination of the unclothed skin surface with 5% soap solution after 4 hour exposure was the least effective at reducing dermal absorption of chlorpyrifos, with 11.6 ± 0.9ng/cm^2 being absorbed. The highest flux was also observed following exposure to unclothed skin compared with both clothed treatments (0.50 ± 0.24ng/cm^2/h for unclothed, 0.14 ± 0.06ng/cm^2/h for clothed 4 hour removal and decontamination, and 0.26 ± 0.1ng/cm^2/h for clothed, 4 hour removal and 24 hour decontamination respectively) However, despite removal of the dose

from the skin surface after 4 hours, absorption continued to increase steadily over 24 hours.

Although a higher flux was observed following removal of clothing at 4 hours followed by 24 hour decontamination of the skin surface, the actual amounts absorbed through the skin at 24 hours were not significantly different, with 5.2 ± 1.1ng/cm^2 absorbed following removal of clothing at 4 hours and decontamination at 24 hours, and 4.9 ± 0.9ng/cm^2 being absorbed following removal of clothing and decontamination at 4 hours respectively. Despite the presence of clothing up to 4 hours after exposure, absorption continued to increase over 24 hours with or without the decontamination step at 4 hours. Even though absorption continued to increase after all 3 treatments, absorption was significantly reduced when compared with the amount absorbed following 24 hour exposure to a finite dose chlorpyrifos in IPA (chapter 4), where 51.9 ± 11.1ng/cm^2 was absorbed. This means that an approximately 5 fold reduction in absorption was observed following decontamination of unclothed skin after 4 hours, and an approximately 10 fold reduction in absorption was observed in the presence of clothing (with or without decontamination at 4 hours).

The distribution profile (table 16 and figure 6.2) shows that the majority of the dose applied to clothed skin was retained within the cotton shirt material after 4 hour exposure, as 86.1 ± 6.3% was recovered from clothing – 4 hour decontamination, and 79.3 ± 4.1% recovered from clothing – 24 hour decontamination respectively. Also, the majority of the applied dose was

recovered from the skin surface of unclothed skin following 4 hour decontamination (84 ± 5.2% recovered in the skin surface wash). Results indicated that significantly more of the applied dose was recovered from the tape strips of unclothed skin compared with clothed skin ($p<0.05$ with one way ANOVA). More of the applied dose was also recovered from the skin digests and receptor fluid samples (absorbed) following 4 hour decontamination of unclothed skin compared with both clothed treatments. However, the differences here did not reach significance.

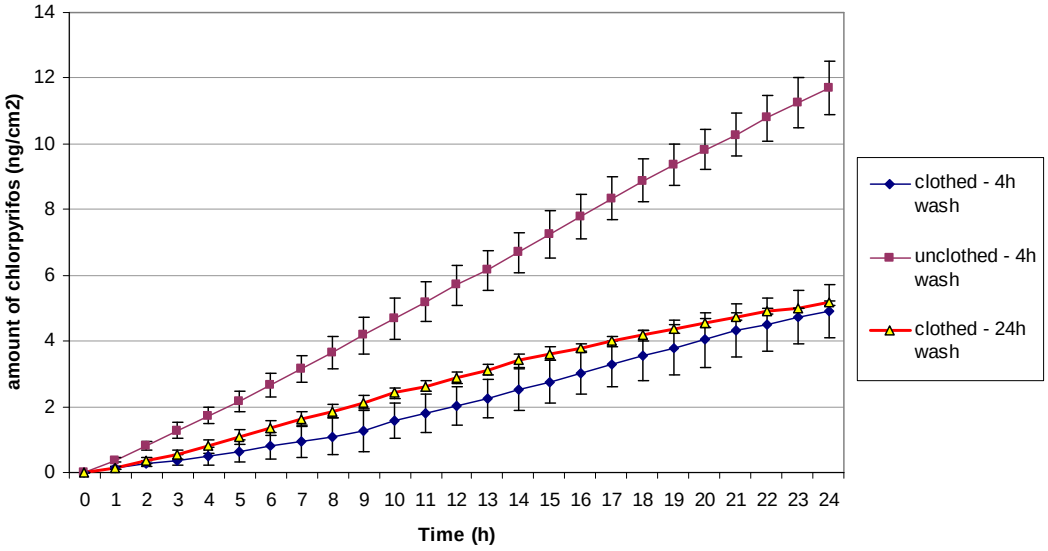

Figure 6.1. 24 hour cumulative absorption profile of chlorpyrifos applied in IPA to clothed and unclothed skin following 4 hour exposure. Values are mean ± SEM of 6 cells per treatment (18 cells in total, taken from 4 skin donors). Skin sections were mounted in flow through diffusion cells with an exposed area of 0.64cm^2. Chlorpyrifos was applied to both clothed and unclothed dermatomed human breast skin surface as a finite dose (10µl/cm^2) at a concentration of 500ng/cm^2. Clothing was removed after 4 hour exposure and the skin either decontaminated using 5% (v/v) soap solution at 4 hours or 24 hours after exposure. Unclothed skin samples were decontaminated after 4 hour exposure.

Dose	Flux (ng/cm^2/h)	K_p x 10^{-3} (cm/h)	Lag Time (h)	Linear range
Chlorpyrifos in IPA:unclothed - 4 hour wash	0.50 ± 0.24	0.05 ± 0.002	0.58 ± 0.38	1-24
Chlorpyrifos in IPA:clothed - 4 hour removal and decontamination	0.26 ± 0.10	0.02 ± 0.01	0.34 ± 0.12	1-9
Chlorpyrifos in IPA:clothed - 4 hour removal , 24 hour decontamination	0.14 ± 0.06	0.002 ± 0.001	0.80 ± 0.26	4-14

Table 15. Observed steady state absorption rates, partition coefficients and lag times following absorption of chlorpyrifos applied in IPA to clothed and unclothed skin, with removal of clothing at 4 hours and decontamination at 4 or 24 hours

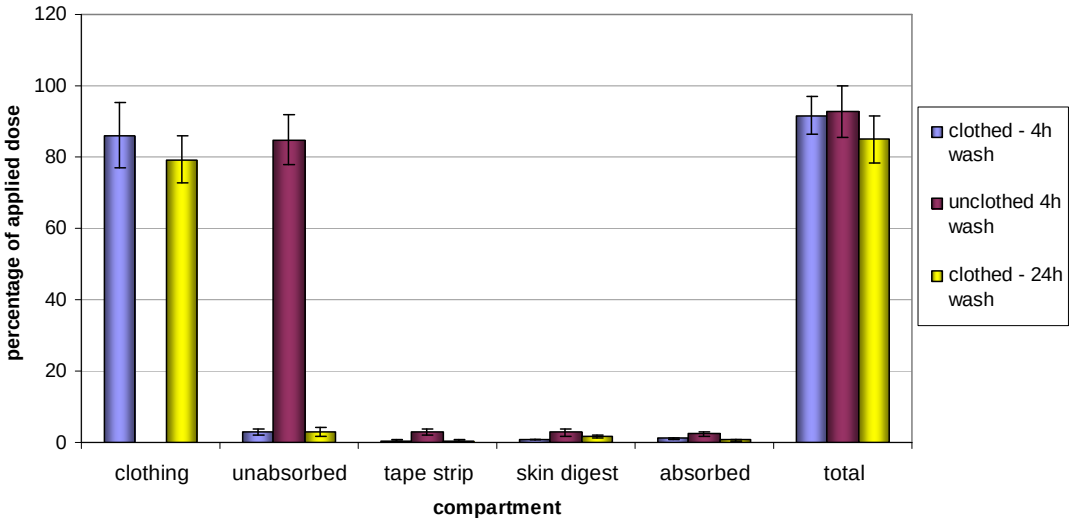

Figure 6.2. Dose distribution of chlorpyrifos applied to clothed and unclothed skin in IPA. Values are mean ± SEM of 6 cells per treatment (18 cells in total from 4 skin donors) over 2 studies. 'clothing' relates to the percentage of dose recovered from within the clothing after 4 hour exposure, 'unabsorbed' is the dose remaining on the skin surface after 4 or 24 hour exposure, 'tape strip' is the dose recovered from the stratum corneum tape strips (no more than 15 per cell) after 24 hours, 'skin digest' is the percentage of dose recovered from within the skin membrane after 24 hours, and the absorbed dose is the percentage of the applied dose recovered from the receptor fluid samples after 24 hours.

	Clothing (%)	Unabsorbed (%)	tape strip (%)	skin digest (%)	Absorbed (%)	Total (%)
clothed - 4h wash	**86.1**	**2.98**	**0.51**	**0.86**	**1.08**	**91.5**
SEM	6.33	1.02	0.21	0.12	0.33	8.36
unclothed 4h wash		**84.8***	**2.79***	**2.85**	**2.34**	**92.8**
SEM		7.01	0.86	0.94	0.45	9.92
clothed - 24h wash	**79.3**	**2.88**	**0.56**	**1.59**	**0.72**	**85.0**
SEM	4.12	1.32	0.21	0.32	0.11	7.41

Table 16. Table showing figures for the dose distribution of chlorpyrifos applied to clothed and unclothed skin in IPA (as shown in figure 6.2 above). Figures are expressed as percentage of dose applied to the skin surface. An asterisk (*) next to a figure denotes a statistically significant difference ($p<0.05$ with one way ANOVA).

The cumulative absorption profile of chlorpyrifos applied to clothed and unclothed skin in PG is shown in figure 6.3. This profile is similar to the profile of chlorpyrifos in IPA (figure 6.1), as the greatest absorption was seen when chlorpyrifos was applied to unclothed skin, followed by decontamination at 4 hours (11.2 ± 1.6ng/cm^2 absorbed after 24 hours). The lowest level of absorption was observed when clothing was removed and the skin surface decontaminated after 4 hours, with 1.3 ± 0.2ng/cm^2 absorbed at 24 hours. A significant difference in absorption was observed between the two clothed skin treatments from the PG vehicle, the same was not seen following absorption from the IPA vehicle (figure 6.1). Absorption following 4 hour exposure to clothed skin followed by 24 hour decontamination led to approximately double the amount being absorbed compared with absorption through the skin following removal of clothing and skin surface decontamination after 4 hours (2.5 ± 0.4ng/cm^2 absorbed through clothed skin - 24 hour wash, 1.3 ± 0.2ng/cm^2 absorbed through clothed skin – 4 hour wash respectively) ($p<0.05$ with one way ANOVA).

Despite a greater amount of chlorpyrifos absorption through the skin following removal of clothing at 4 hours with decontamination at 24 hours compared with 4 hour clothing removal and decontamination, the lag time for absorption was significantly longer following 24 hour decontamination (2.5 ± 0.9h), compared with 0.4 ± 0.2h following removal of clothing and decontamination at 4 hours. Although absorption took approximately 5 times longer to reach steady state flux without decontamination immediately after removal of clothing, the steady state flux was approximately 2 fold greater without

decontamination following removal of clothing after 4 hour exposure (table 16).

The dose distribution at 24 hours after the initial exposure shown in figure 6.4 and table 17 is similar to the distribution following exposure of clothed and unclothed skin to chlorpyrifos in IPA (figure 6.2). Again, the majority of the applied dose was retained within the cotton shirt material following 4 hour exposure to chlorpyrifos in PG (86.1 ± 8.1 for clothed – 4 hour wash, and 83.3 ± 7.3 for clothed – 24 hour wash). Significantly more chlorpyrifos was recovered from the stratum corneum tape strips taken from unclothed skin decontaminated after 4 hours following termination of the study at 24 hours after the initial exposure (5.9 ± 1.6% of the applied dose in the stratum corneum, compared with 0.5 ± 0.2% from clothed – 4 hour wash and 1.5 ± 0.4% from clothed – 24 hour wash respectively). A greater percentage of the applied dose was also recovered from within the skin membrane at 24 hours from the unclothed skin compared with the two clothed skin treatments; however, this was not statistically significant.

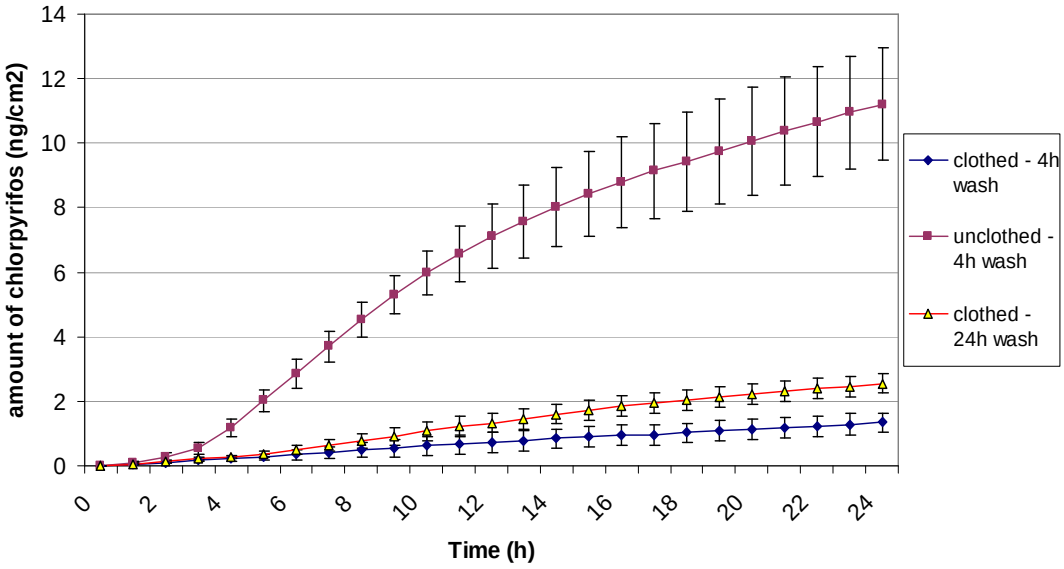

Figure 6.3. 24 hour cumulative absorption profile of chlorpyrifos applied in PG to clothed and unclothed skin following 4 hour exposure. Values are means ± SEM of 7 cells per treatment (21 cells in total, taken from 5 skin donors) over 2 studies. Skin sections were mounted in flow through diffusion cells with an exposed area of 0.64cm^2. Chlorpyrifos was applied to both clothed and unclothed dermatomed human breast skin surface as a finite dose (10µl/cm^2) at a concentration of 500ng/cm^2. Clothing was removed after 4 hour exposure and the skin either decontaminated using 5% (v/v) soap solution at 4 hours or 24 hours after exposure. Unclothed skin samples were decontaminated after 4 hour exposure.

Dose	Flux (ng/cm^2/h)	K_p x 10^{-3} (cm/h)	Lag Time (h)	Linear range
Chlorpyrifos in PG:unclothed - 4 hour wash	0.81 ± 0.23**	0.02 ± 0.01	2.4 ± 0.8*	3-9
Chlorpyrifos in PG:clothed - 4 hour removal and decontamination	0.14 ± 0.05	0.002 ± 0.001	0.4 ± 0.2	1-10
Chlorpyrifos in PG:clothed - 4 hour removal , 24 hour decontamination	0.06 ± 0.02	0.003 ± 0.001	2.5 ± 0.9*	6-12

Table 17. Observed steady state absorption rates, partition coefficients and lag times of chlorpyrifos applied to clothed and unclothed skin in a PG vehicle. An asterisk (*) next to a figure denotes a statistically significant difference from the remaining figures in each column (one way ANOVA, p<0.05). A double asterisk denotes that that figure is statistically significant from the remaining 2 figures in the column.

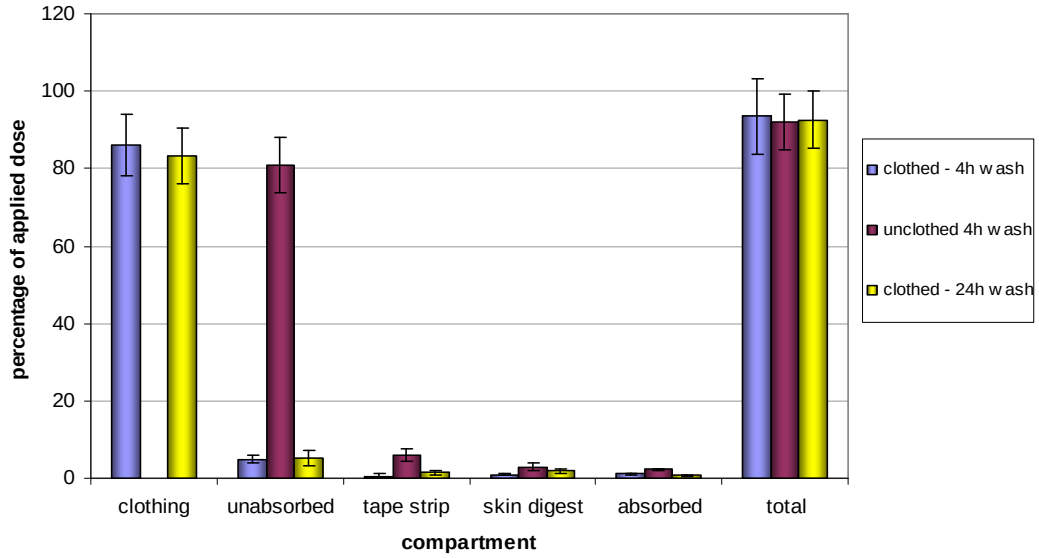

Figure 6.4. Dose distribution of chlorpyrifos applied to clothed and unclothed skin in PG. Values are means ± SEM of 7 cells per treatment (21 cells in total from 5 skin donors) over 2 studies. 'clothing' relates to the percentage of dose recovered from within the clothing after 4 hour exposure, 'unabsorbed' is the dose remaining on the skin surface after 4 or 24 hour exposure, 'tape strip' is the dose recovered from the stratum corneum tape strips (no more than 15 per cell) after 24 hours, 'skin digest' is the percentage of dose recovered from within the skin membrane after 24 hours, and the absorbed dose is the percentage of the applied dose recovered from the receptor fluid samples after 24 hours.

	clothing	unabsorbed	tape strip	skin digest	absorbed	total
clothed - 4h wash	**86.1**	**4.9**	**0.5**	**0.9**	**1.1**	**93.5**
SEM	8.09	1.12	0.20	0.16	0.09	9.21
unclothed 4h wash		**81.01****	**5.8****	**2.9***	**2.2***	**92.1**
SEM		7.09	1.60	0.85	0.35	8.32
clothed - 24h wash	**83.3**	**5.3**	**1.4**	**1.8**	**0.6**	**92.5**
SEM	7.32	2.05	0.46	0.63	0.12	7.81

Table 18. Figures for the distribution of chlorpyrifos applied to clothed and unclothed human skin in a PG vehicle (as shown in figure 6.4 above). An asterisk (*) next to a figure denotes a significant difference with the lowest figure in each column, but not both remaining figures. A double asterisk denotes a significant difference with both remaining figures in the column ($p<0.05$ with one way ANOVA).

6.3.2: 30 minute exposure of dermatomed human breast skin (clothed and unclothed) to dichlorvos in IPA

Methods

For the purposes of this study, 12 flow-through diffusion cells were used containing skin from 2 human breast skin donors. The finite dose of dichlorvos in IPA (10µl/cm^2, concentration - 5µg/cm^2) was applied to the skin under unclothed conditions, and to the clothing under clothed conditions. After a 30 minute exposure, the clothing was removed from the skin surface. Of the 12 cells used, 4 cells had clothing removed and also had the skin surface decontaminated using 5% soap solution (v/v), 4 cells had clothing removed but without decontamination until 24 hours after exposure, and 4 unclothed cells were decontaminated at 30 minutes using 5% soap solution. Following removal of clothing and decontamination at 30 minutes, all cells were left for 24 hours, where terminal procedures were undertaken to assess the dermal distribution of dichlorvos applied to the skin. Sample analysis was carried out by GC-MS.

Results

The cumulative absorption of dichlorvos applied to clothed and unclothed dermatomed human breast skin in IPA is shown in figure 6.5. From this figure, it can be seen that absorption of dichlorvos applied in IPA was significantly greater through unclothed skin compared with clothed skin ($p<0.05$ with one way ANOVA). Despite skin surface decontamination at 30 minutes after exposure, 501.7 ± 113.5ng/cm^2 of dichlorvos was absorbed through unclothed skin after 24 hours. This was approximately 10% of the

applied dose. The rate of absorption from the IPA vehicle after decontamination with 5% soap solution was fastest over the first 2 hours (220 ± 26.3ng/cm^2/h, table 19), before rapidly tailing off up to 24 hours. This was despite absorption through unclothed skin generating the longest observed lag time of all the treatments (0.6 ± 0.3h, compared with 0.3 ± 0.1h for clothed – 30 minute decontamination, and 0.2 ± 0.1h for clothed – 24 hour decontamination, shown in table 19). From the two clothing treatments, it can also be seen that approximately double the amount of dichlorvos was absorbed following removal of clothing at 30 minutes followed by 24 hour skin surface decontamination compared with absorption after removal of clothing at 30 minutes with decontamination at 30 minutes (129.2 ± 16.6ng/cm^2 through clothed – 24 hour wash, and 63.2 ± 13.6ng/cm^2 through clothed – 30 minute wash) ($p<0.05$ with one way ANOVA). When compared with 24 hour exposure of human breast skin to dichlorvos in IPA (figure 4.3, chapter 4), it can be seen that absorption was greatly reduced for all 3 treatments. Absorption through unclothed skin decontaminated after 30 minutes was reduced by approximately a third when compared with 24 hour exposure, whereas absorption through clothed skin was reduced by 15 fold through clothed skin with decontamination at 24 hours, and by approximately 30 fold through clothed skin with decontamination at 30 minutes after initial exposure.

From the dose distribution graph shown in figure 6.6, it can be seen that the majority of the applied dose of dichlorvos was recovered from the cotton shirt material following removal of clothing at 30 minutes after exposure (74.3 ± 8.3% from clothed – 30 minute wash, and 70.8 ± 7.6% from clothed – 24 hour

wash respectively). The majority of the applied dose of dichlorvos was also recovered from the surface of the unclothed skin following 30 minute decontamination (73.4 ± 7.2%). Despite the presence of clothing on some of the cells, approximately 15% of the applied dose was still recovered from the skin surface swabs following decontamination at both 30 minutes and 24 hours after the initial exposure. Significantly more of the applied dose of dichlorvos was recovered from the stratum corneum tape strips, the skin digests and receptor fluid (absorbed) of unclothed skin decontaminated at 30 minutes after exposure ($p<0.05$ with one way ANOVA).

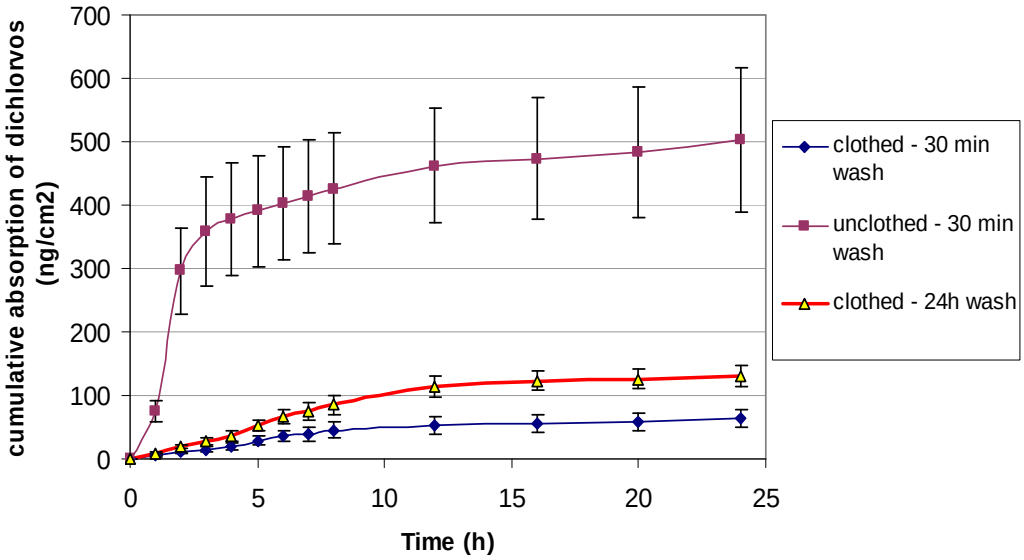

Figure 6.5. 24 hour cumulative absorption profile of dichlorvos applied in IPA to clothed and unclothed skin following 0.5 hour exposure. Values are mean ± SEM of 4 cells per treatment (12 cells in total, taken from 2 skin donors). Skin sections were mounted in flow through diffusion cells with an exposed area of 0.64cm^2. Dichlorvos was applied to both clothed and unclothed dermatomed human breast skin surface as a finite dose (10µl/cm^2) at a concentration of 5µg/cm^2. Clothing was removed after 0.5 hour exposure and the skin either decontaminated using 5% (v/v) soap solution at 0.5 hours or 24 hours after exposure. Unclothed skin samples were decontaminated after 0.5 hour exposure.

Dose	Flux (ng/cm^2/h)	K_p x 10^{-3} (cm/h)	Lag Time (h)	Linear range
Dichlorvos in IPA: unclothed 30 min decontamination	220.0 ± 26.3**	214.1 ± 21.10**	0.66 ± 0.26*	1-2
Dichlorvos in IPA: clothed 30 min decontamination	5.8 ± 1.2	5.16 ± 1.4	0.31 ± 0.07	0-7
Dichlorvos in IPA: clothed 24 hour decontamination	10.8 ± 2.1	10.2 ± 1.8	0.22 ± 0.05	0-6

Table 19. Observed steady state absorption rates, partition coefficients and lag times following exposure of clothed and unclothed skin to dichlorvos in IPA. A single asterisk denotes that the figure is significantly different from the lowest figure in the same column. A double asterisk denotes that that figure is statistically significant compared with the remaining two figures in the column. ($p<0.05$ with one way ANOVA).

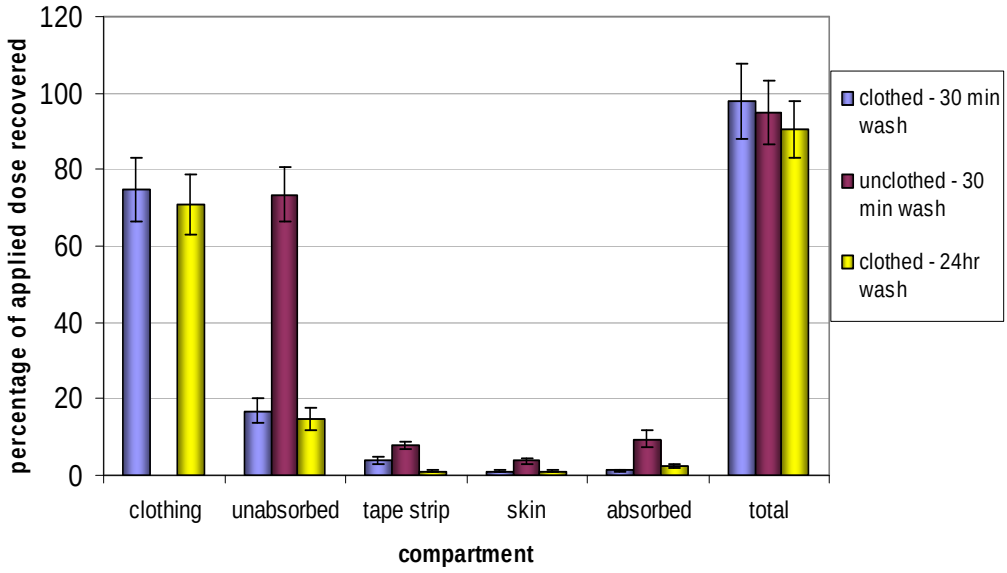

Figure 6.6. Dose distribution of dichlorvos applied to clothed and unclothed skin in IPA. Values are mean ± SEM of 4 cells per treatment (12 cells in total from 2 skin donors). 'clothing' relates to the percentage of dose recovered from within the clothing after 0.5 hour exposure, 'unabsorbed' is the dose remaining on the skin surface after 0.5 or 24 hour exposure, 'tape strip' is the dose recovered from the stratum corneum tape strips (no more than 15 per cell) after 24 hours, 'skin digest' is the percentage of dose recovered from within the skin membrane after 24 hours, and the absorbed dose is the percentage of the applied dose recovered from the receptor fluid samples after 24 hours.

	Clothing (%)	Unabsorbed (%)	tape strip (%)	Skin (%)	Absorbed (%)	Total (%)
clothed - 30 min wash	**74.3**	**16.9**	**3.80****	**1.13**	**1.26**	**97.9**
SEM	8.37	3.11	1.07	0.11	0.18	10.1
unclothed - 30 min wash		**73.3****	**7.97****	**3.83****	**9.55****	**94.7**
SEM		7.22	1.03	0.84	2.32	8.32
clothed - 24hr wash	**70.8**	**14.8**	**1.08**	**1.17**	**2.58**	**90.5**
SEM	7.66	2.87	0.15	0.18	0.51	9.36

Table 20. Figures for the distribution of dichlorvos applied to clothed and unclothed human skin in an IPA vehicle (as shown in figure 6.6 above). A double asterisk denotes that a figure is statistically significant from both of the remaining figures in the same column ($p<0.05$ with one way ANOVA).

6.3.3: 30 minute exposure of dermatomed human breast skin (clothed and unclothed) to dichlorvos in IPM

Methods

For this study, 12 flow-through diffusion cells were used, containing human breast skin from 2 different donors. A finite dose of dichlorvos in IPM (10µl/cm^2, concentration at 5µg/cm^2) was applied to the skin surface under unclothed conditions, and directly to the clothing under clothed conditions. Following 30 minute exposure, the 4 unclothed cells were decontaminated with 5% soap solution (v/v), 4 clothed cells had clothing removed and the skin surfaces were decontaminated immediately using soap solution, and the remaining clothed cells had clothing removed but the skin surfaces were not decontaminated until 24 hours after exposure. All cells were left in the flow-through diffusion system for 24 hours at which point, terminal procedures were undertaken to assess the dermal distribution of dichlorvos applied to the skin.

Results

The cumulative absorption profile of dichlorvos applied to clothed and unclothed skin in IPM was different from the profile shown with dichlorvos applied in IPA as can be seen in figure 6.7. Once again, absorption through the skin was significantly greater through unclothed skin decontaminated at 30 minutes, compared with the two clothed treatments ($p<0.05$ with one way ANOVA). Approximately 6.5 ± 2.1% (322.5 ± 63.2ng/cm^2) was absorbed through unclothed skin at 24 hours following 30 minute skin surface decontamination. Absorption through unclothed skin was approximately 6 fold

greater than through clothed skin decontaminated at 30 minutes (56.9 ± 5.2ng/cm^2), and approximately 4 fold greater than through clothed skin decontaminated at 24 hours (81.83 ± 10.42ng/cm^2). The rate of absorption through unclothed skin was greater than through skin for either of the clothed treatments (19.2 ± 5.6ng/cm^2/h through unclothed skin, 3.62 ± 0.81ng/cm^2/h through clothed skin – 30 minute wash, and 6.4 ± 1.9ng/cm^2/h through clothed skin – 24 hour wash). The significantly higher absorption and absorption rate through unclothed skin was observed despite a marginally longer lag time in comparison to the clothed skin treatments (0.35 ± 0.13h for unclothed, 0.14 ± 0.04h for clothed – 30 minute wash, and 0.24 ± 0.07h for clothed – 24 hour wash) (table 21). No significant differences were observed in the amount of dichlorvos absorbed through clothed skin decontaminated at 30 minutes, or 24 hours after initial exposure, although a numerical decrease was observed.

From the dose distribution graph shown in figure 6.8, and the dose distribution table (table 22), it can be seen that the majority of the applied dose was either recovered from within the clothing (77.2 ± 8.4% for clothed – 30 minute wash, 73.6 ± 9.3% for clothed – 24 hour wash), or from the skin surface swabs following 30 minute decontamination of unclothed skin (83.3 ± 11.6%). It can also be seen that approximately 12-14% of the applied dose of dichlorvos was recovered from the skin surface of clothed skin following decontamination of the skin surface after 30 minutes or 24 hours. A greater proportion of the applied dose was recovered within the stratum corneum tape strips of unclothed skin (3.6 ± 0.9%) compared with clothed skin (1.34 ± 0.5% from clothed – 30 minute decontamination, and 2.5 ± 1% from clothed – 24 hour

decontamination). A greater proportion of the applied dose of dichlorvos was also recovered from within the skin membranes of unclothed skin following 30 minute decontamination (1.57 ± 0.36%) compared with 0.87 ± 0.12% from clothed skin decontaminated at 30 minutes, and 1.55 ± 0.44% from clothed skin decontaminated at 24 hours. Despite the greater recovery from the tape strips and skin membranes from the unclothed treatment compared with the two clothed treatments, the results obtained were not statistically significant.

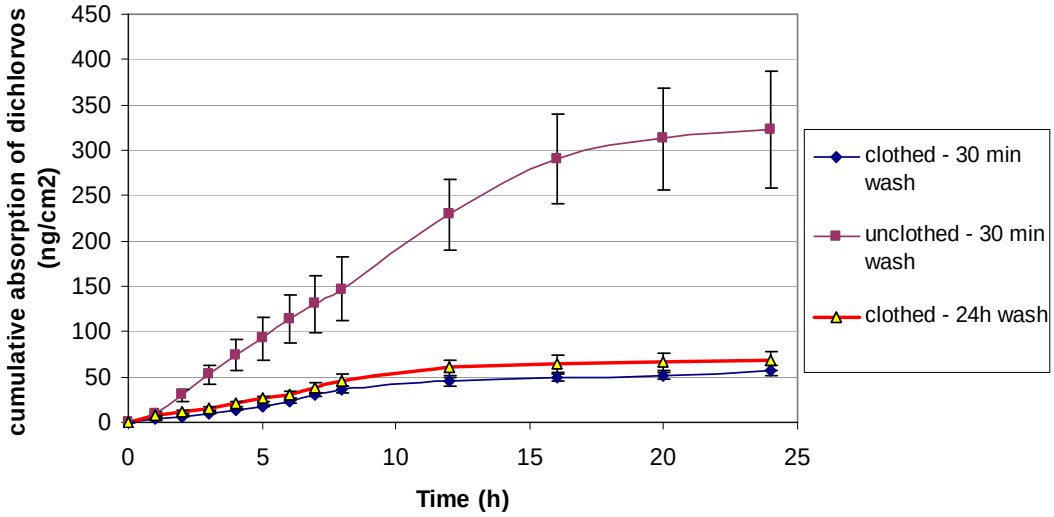

Figure 6.7. 24 hour cumulative absorption profile of dichlorvos applied in IPM to clothed and unclothed skin following 0.5 hour exposure. Values are mean ± SEM of 4 cells per treatment (12 cells in total, taken from 2 skin donors). Skin sections were mounted in flow through diffusion cells with an exposed area of 0.64cm^2. Dichlorvos was applied to both clothed and unclothed dermatomed human breast skin surface as a finite dose (10µl/cm^2) at a concentration of 5µg/cm^2. Clothing was removed after 0.5 hour exposure and the skin either decontaminated using 5% (v/v) soap solution at 0.5 hours or 24 hours after exposure. Unclothed skin samples were decontaminated after 0.5 hour exposure.

Dose	Flux (ng/cm^2/h)	K_p x 10^{-3} (cm/h)	Lag Time (h)	Linear range
Dichlorvos in IPM: unclothed 30 min decontamination	19.25 ± 5.62**	20.8 ± 5.32*	0.35 ± 0.13*	0-8
Dichlorvos in IPM: clothed 30 min decontamination	3.62 ± 0.81	2.71 ± 0.25	0.14 ± 0.04	0-5
Dichlorvos in IPM: clothed 24 hour decontamination	6.42 ± 1.91	6.29 ± 1.12*	0.24 ± 0.07	1-8

Table 21. Observed steady state absorption rates, partition coefficients and lag times following exposure of clothed and unclothed human skin to dichlorvos in IPM. A single asterisk denotes that a figure is statistically significant compared with the lowest figure in the same column. A double asterisk denotes that a figure is statistically significant from both of the remaining figures in the same column ($p<0.05$ with one way ANOVA).

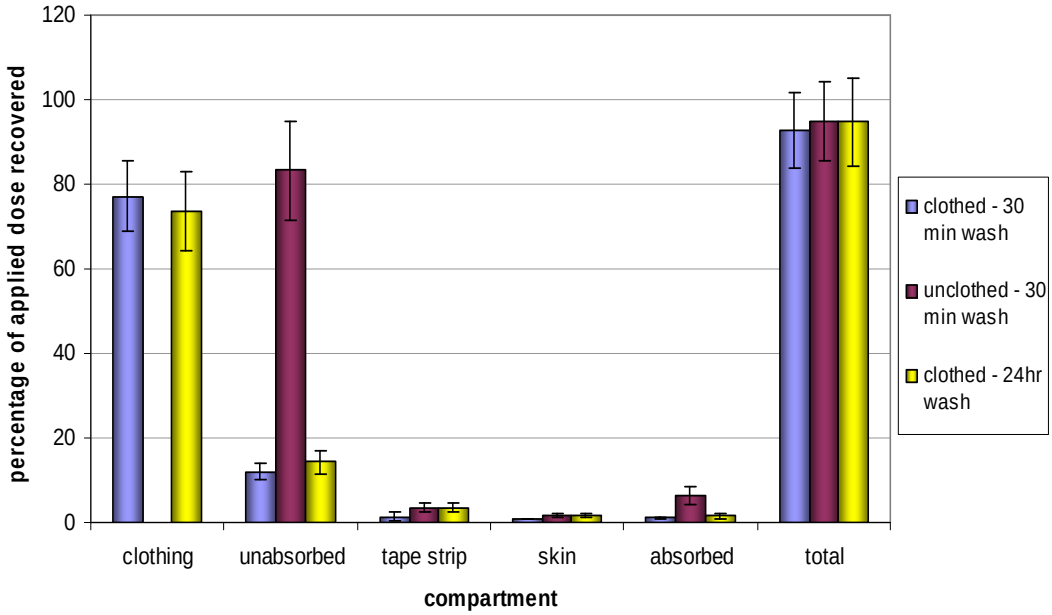

Figure 6.8. Dose distribution of dichlorvos applied to clothed and unclothed skin in IPM. Values are mean ± SEM of 4 cells per treatment (12 cells in total from 2 skin donors). 'clothing' relates to the percentage of dose recovered from within the clothing after 0.5 hour exposure, 'unabsorbed' is the dose remaining on the skin surface after 0.5 or 24 hour exposure, 'tape strip' is the dose recovered from the stratum corneum tape strips (no more than 15 per cell) after 24 hours, 'skin digest' is the percentage of dose recovered from within the skin membrane after 24 hours, and the absorbed dose is the percentage of the applied dose recovered from the receptor fluid samples after 24 hours.

	clothing	unabsorbed	tape strip	skin	absorbed	total
clothed - 30 min wash	**77.23**	**12.12**	**1.34**	**0.87**	**1.13**	**92.69**
SEM	8.37	2.11	0.47	0.12	0.28	8.96
unclothed - 30 min wash		**83.32****	**3.59**	**1.57**	**6.44****	**94.92**
SEM		11.64	0.97	0.36	2.11	9.31
clothed - 24hr wash	**73.61**	**14.32**	**2.46**	**1.55**	**1.62**	**94.7**
SEM	9.32	2.66	1.03	0.44	0.56	10.31

Table 22. Table of figures for the dermal distribution of dichlorvos applied to clothed and unclothed human skin in an IPM vehicle (as shown in figure 6.8 above). A double asterisk next to a figure denotes that this figure is significantly different compared with the remaining two figures in the same column 9p<0.05 with one way ANOVA).

6.3.4: 30 minute exposure of dermatomed human breast skin (clothed and unclothed) to dichlorvos in PG

Methods

For this study, 12 flow-through diffusion cells were used, containing human breast skin from 2 different donors. A finite dose of dichlorvos in PG (10µl/cm^2, concentration at 5µg/cm^2) was applied to the skin surface under unclothed conditions, and directly to the clothing under clothed conditions. Following 30 minute exposure, the 4 unclothed cells were decontaminated with 5% soap solution (v/v), 4 clothed cells had clothing removed and the skin surfaces were decontaminated immediately using soap solution, and the remaining clothed cells had clothing removed but the skin surfaces were not decontaminated until 24 hours after exposure. All cells were left in the flow-through diffusion system for 24 hours at which point, terminal procedures were undertaken to assess the dermal distribution of dichlorvos applied to the skin.

Results

The cumulative absorption profiles shown in figure 6.9 are in keeping with all of the absorption profiles of dichlorvos through clothed and unclothed skin shown previously throughout this chapter. It can be seen that absorption of dichlorvos applied in a PG vehicle was greater through unclothed skin decontaminated after 30 minutes (446.59 ± 51.33ng/cm^2) than through clothed skin (53.60 ± 7.44ng/cm^2 absorbed through clothed skin decontaminated at 30 minutes, and 107.64ng/cm^2 absorbed through clothed

skin decontaminated at 24 hours). The amount of dichlorvos absorbed at 24 hours was significantly different between all 3 treatments ($p<0.05$ with one way ANOVA). The lag times were short despite the presence of clothing (0.12 ± 0.04h for clothed skin decontaminated at 30 minutes and 0.13 ± 0.02h for clothed skin decontaminated at 24 hours after exposure) (table 22). Absorption continued to increase up to 24 hours after the initial exposure to dichlorvos despite removal of the majority of the applied dose after 30 minutes of exposure. Despite this increase, the amounts absorbed through the skin were significantly lower compared to the amount absorbed following 24 hour exposure of human breast skin to dichlorvos in a PG vehicle (figure 4.3, chapter 4). Here, it was shown that 36.2 ± 3.41% of the applied dose was absorbed, meaning that a 4–fold reduction in absorption was observed through unclothed skin decontaminated at 30 minutes after exposure, an approximately 16-fold decrease in absorption through clothed skin decontaminated at 24 hours, and a 30-fold reduction in absorption was observed through clothed skin decontaminated after a 30 minute exposure.

The dose distribution of dichlorvos applied in a PG vehicle can be seen in figure 6.10. Once again, this follows a very similar pattern to the dose distribution of dichlorvos in both the IPA and the IPM vehicle, with the majority of the applied dose recovered either from within the cotton shirt material (69.1 ± 10.3% from clothed – 30 minute wash, and 62.3 ± 7.61% from clothed – 24 hour wash), or from the skin surface of unclothed skin decontaminated at 30 minutes after exposure (68.3 ± 7.32%). Also, between 11 and 15% of the

applied dose was recovered from the skin surface after 30 minute and 24 hour decontamination, despite the presence of clothing for both treatments.

It can also be seen that the percentage of the applied dose of dichlorvos recovered from the stratum corneum tape strips and the skin membranes was greater for unclothed skin compared with clothed skin. However, the amount of dichlorvos recovered from the tape strips of the stratum corneum from both clothed treatments was greater following application in a PG vehicle than from either the IPA or IPM vehicles. 3.95 ± 0.66% was recovered from tape strips from clothed skin decontaminated at 30 minutes, and 4.22 ± 0.73% was recovered from tape strips of clothed skin decontaminated at 24 hours respectively.

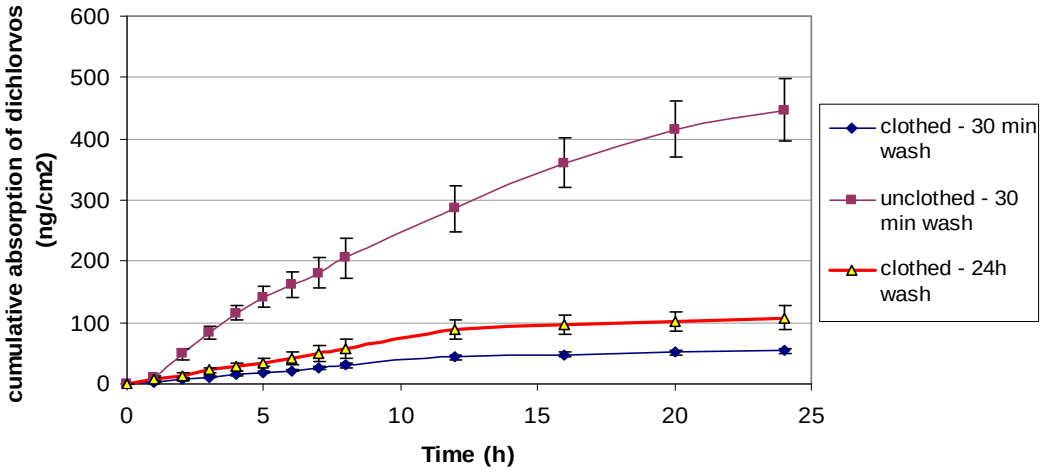

Figure 6.9. 24 hour cumulative absorption profile of dichlorvos applied in PG to clothed and unclothed skin following 0.5 hour exposure. Values are means ± SEM of 4 cells per treatment (12 cells in total, taken from 2 skin donors). Skin sections were mounted in flow through diffusion cells with an exposed area of 0.64cm^2. Dichlorvos was applied to both clothed and unclothed dermatomed human breast skin surface as a finite dose (10µl/cm^2) at a concentration of 5µg/cm^2. Clothing was removed after 0.5 hour exposure and the skin either decontaminated using 5% (v/v) soap solution at 0.5 hours or 24 hours after exposure. Unclothed skin samples were decontaminated after 0.5 hour exposure.

Dose	Flux (ng/cm^2/h)	K_p x 10^{-3} (cm/h)	Lag Time (h)	Linear range
Dichlorvos in PG: unclothed 30 min decontamination	30.1 ± 7.33**	27.6 ± 6.2**	0.28 ± 0.11*	0-5
Dichlorvos in PG: clothed 30 min decontamination	3.77 ± 0.91	3.8 ± 1.2	0.12 ± 0.04	0-8
Dichlorvos in PG: clothed 24 hour decontamination	7.12 ± 2.10	6.36 ± 1.9	0.13 ± 0.02	0-8

Table 23. Observed steady state absorption rates, partition coefficients and lag times of dichlorvos applied to the skin surface in a PG vehicle. A single asterisk next to a figure denotes that this figure is statistically significant from the lowest figure in the same column. A double asterisk denotes that a figure is significantly different from the remaning two figures in the same column ($p<0.05$ with one way ANOVA).

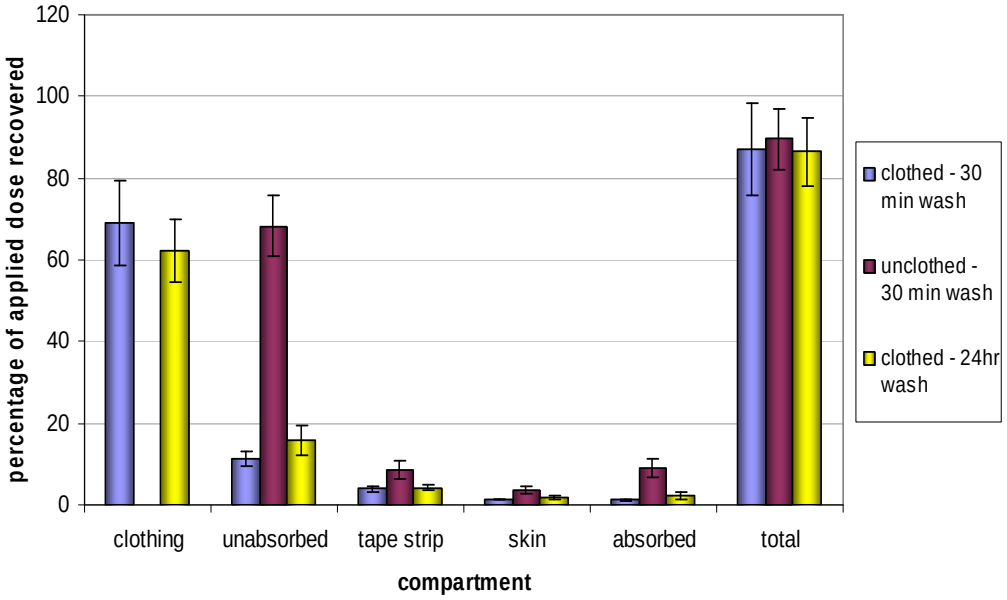

Figure 6.10. Dose distribution of dichlorvos applied to clothed and unclothed skin in PG. Values are means ± SEM of 4 cells per treatment (12 cells in total from 2 skin donors). 'clothing' relates to the percentage of dose recovered from within the clothing after 0.5 hour exposure, 'unabsorbed' is the dose remaining on the skin surface after 0.5 or 24 hour exposure, 'tape strip' is the dose recovered from the stratum corneum tape strips (no more than 15 per cell) after 24 hours, 'skin digest' is the percentage of dose recovered from within the skin membrane after 24 hours, and the absorbed dose is the percentage of the applied dose recovered from the receptor fluid samples after 24 hours.

	clothing	unabsorbed	tape strip	skin	absorbed	total
clothed - 30 min wash	**69.1**	**11.3**	**3.95**	**1.42**	**1.23**	**86.9**
SEM	10.30	1.86	0.66	0.07	0.21	11.24
unclothed - 30 min wash		**68.3****	**8.62***	**3.69****	**8.92****	**89.5**
SEM		7.32	2.35	0.97	2.14	7.66
clothed - 24hr wash	**62.3**	**15.9**	**4.22**	**1.92**	**2.14**	**86.5**
SEM	7.61	3.65	0.67	0.52	0.84	8.32

Table 24. Table of figures for the dermal distribution of dichlorvos applied to clothed and unclothed human skin in a PG vehicle (as shown in figure 6.10 above). A single asterisk next to a figure denotes that a figure is significantly different from the lowest figure in the same column. A double asterisk next to a figure denotes that a figure is significantly different from the remaining two figures in the same column ($p<0.05$ with one way ANOVA).

6.4: Discussion

6.4.1: Chlorpyrifos

The time of 4 hours for removal of clothing and decontamination of the skin surface following exposure to chlorpyrifos was chosen based on the lag times of chlorpyrifos applied in IPA (5.91 ± 1.36h) and PG (8.4 ± 2.9h) following 24 hour exposure. This time point would allow some absorption to occur prior to steady state absorption being reached, and also provided a reasonable time frame in which an individual may remove decontaminated clothing in a real life scenario.

Decontamination of chlorpyrifos from the surface of unclothed skin at 4 hours was the least effective method for reducing dermal absorption measured at 24 hours after exposure. This was expected; as it was hypothesised that everyday cotton shirt material would provide more of a barrier to absorption than decontamination with 5% soap solution alone. Two clothing treatments were used, removal of clothing at 4 hours after exposure supplemented with decontamination of the skin surface at 4 hours, and removal of clothing at 4 hours after exposure with washing of the skin surface at 24 hours. There was no difference in the amount of chlorpyrifos absorbed at 24 hours between the two clothing treatments when applied to the skin in IPA, however, a significant reduction in absorption was seen when removal of clothing at 4 hours was supplemented with skin surface decontamination at 4 hours when chlorpyrifos was applied in a PG vehicle. It was expected that decontamination of the skin surface and removal of clothing carried out at the same time would help to reduce absorption as it would be a more thorough decontamination

procedure. It is possible that the skin surface decontamination may not have been as necessary when removing the dose applied in the IPA vehicle due to the volatility of the vehicle. This would mean that less of the applied dose would soak through the clothing and reach the skin surface to become available for dermal absorption.

As expected, the clothing retained the majority of the applied dose applied in IPA and PG; however, the amount recovered from the skin surface following removal of the clothing following application in the IPA vehicle was approximately half of the amount of chlorpyrifos recovered from the skin surface following application in PG. It is possible that the non-volatile PG vehicle may have kept the cotton shirt material wet for longer than when applied in IPA, and therefore may have resulted in longer contact with the skin surface to allow deposition of chlorpyrifos on the skin surface.

Despite absorption being significantly higher following application of chlorpyrifos in both IPA and PG to unclothed skin decontaminated at 4 hours compared with the two clothed skin treatments, all 3 of the decontamination regimes were effective at reducing absorption compared with 24 hour exposure to the chlorpyrifos in IPA and PG (chapter 4). Absorption of chlorpyrifos applied as a finite dose in IPA, and left in contact with the skin for 24 hours resulted in absorption of 10.38 ± 2.60% of the dose, and 19.55 ± 2.36% of the applied dose in PG was absorbed at 24 hours. Absorption of chlorpyrifos was greatest through unclothed skin when applied in both IPA (2.34 ± 0.46%), and PG (2.24 ± 0.35%). Although the amount of chlorpyrifos

absorbed through unclothed skin decontaminated at 4 hours was similar between vehicles, the reduction in absorption from the PG vehicle was far greater than from the IPA vehicle following decontamination at 4 hours, when compared with 24 hour exposure. Absorption from the IPA vehicle following decontamination of unclothed skin at 4 hours was reduced by approximately 5 fold, whereas absorption from the PG vehicle was reduced by approximately 9 fold. It is possible that the greater reduction in absorption through clothed skin from the PG vehicle compared with 24 hour exposure is likely to be due to the physicochemical properties of PG. As PG has been shown to enhance penetration through the skin, it is possible that the presence of clothing greatly reduces the ability of PG to perturb the lipid formation of the stratum corneum, and so the difference in absorption would be greater when compared with absorption from the IPA vehicle, which evaporates rapidly from the skin surface.

6.4.2: Dichlorvos

The lag times observed following 24 hour exposure to dichlorvos in IPA, IPM and PG were shorter than for exposure to chlorpyrifos in the same vehicles, and so the clothing removal and decontamination time was altered to 30 minutes after exposure for dichlorvos. It was decided that the decontamination times would be set around the time at which dichlorvos had been seen to reach steady state flux, to identify how removal of the dose at this point would affect absorption.

Similar results to the chlorpyrifos data were obtained following 30 minute exposure of clothed and unclothed skin to dichlorvos in IPA, IPM and PG vehicles. As expected, absorption was found to be significantly higher following decontamination of unclothed skin at 30 minutes after exposure when compared with absorption through clothed skin regardless of the application vehicle. It was expected that absorption would be greatest from the PG vehicle as this was the most hydrophilic of the vehicles used, however, the greatest absorption was observed following exposure of unclothed skin to dichlorvos in the IPA vehicle. It is possible that the rapid evaporation of IPA may have caused an increase in concentration of dichlorvos on the skin surface and resulted in faster absorption within the first 2 hours of exposure. Due to skin surface decontamination being carried out using an aqueous soap solution, it is likely that removal of the dose in PG would be more successful than removal with IPA and IPM, as PG is a hydrophilic solvent.

Despite the amount of dichlorvos absorbed being greater through unclothed skin following decontamination at 30 minutes after application in IPA, the actual reduction in absorption compared with 24 hour exposure to dichlorvos in IPA, IPM and PG was similar for all vehicles. An approximately 4 fold reduction in absorption from IPA and PG was seen following skin decontamination at 30 minutes, and an approximately 5 fold reduction was observed following exposure of unclothed skin to dichlorvos in IPM. This suggests that decontamination of the skin with an aqueous soap solution was successful regardless of the application vehicle used.

These studies indicate that removal of contaminated clothing and skin surface decontamination within 4 hours of exposure to chlorpyrifos, and within 30 minutes of exposure to dichlorvos can significantly reduce the amount of chemical being absorbed through the skin. From a real life exposure perspective, an approximate 4 hour window of opportunity to significantly reduce absorption following exposure to chlorpyrifos gives a greater opportunity to reduce any potential toxic effects resulting from systemic absorption. However, due to the rapid absorption of dichlorvos into the skin, particularly from the IPA vehicle, decontamination of the skin surface would potentially have to occur immediately after exposure in order to prevent significant absorption of dichlorvos occurring.

These studies indicate that, although everyday clothing is not primarily designed for protective purposes, it could potentially help to reduce chemical to skin contact. This in turn may be vitally important in reducing local and systemic toxic effects that can occur as a result of dermal absorption.

Chapter 7

Effect of clothing and decontamination on dermal absorption of neat ^{14}C-labelled HD and dilute ^{14}C-labelled HD in IPA

7. Effect of clothing and decontamination on dermal absorption of neat ^{14}C-labelled HD and dilute ^{14}C-labelled HD in IPA.

7.1: Introduction

Following the 24 hour absorption studies carried out at Dstl using neat HD, and diluted HD in IPA; further studies were conducted to investigate how effective everyday clothing (cotton shirt material) was at reducing dermal absorption of neat HD and dilute HD in IPA under similar conditions. Comparison was also made with the effect of clothing on dermal absorption of surrogate compounds

Previous studies have investigated the effect of decontamination using fuller's earth (used in laboratories to clean up spillages of HD), Ambergard (a decontaminating agent used in military exposure scenarios), and BDH spillage granules in response to exposure to neat HD (Chilcott *et al*. 2001). This study also investigated the differences in absorption and decontamination between human breast, and pig ear skin. Other studies have also investigated the effect of barrier creams at reducing absorption of neat HD through human skin *in vitro* (Chilcott *et al*. 2002), and also through pig skin *in vivo* and *in vitro* (Chilcott *et al*. 2007). These studies have all been undertaken from the perspective of military personnel becoming exposed to high levels of HD. The influence of clothing on HD absorption has been investigated previously using man-in-simulant testing (MIST) as reported by Duncan and Gudgin Dickson, 2003. Individuals were exposed to methyl salicylate, as an HD surrogate, whilst wearing military protective equipment, Data was compared with archived data for military exposure to HD (Gudgin Dickson, 2008).

At present, there is little published data regarding the protective qualities of ‘everyday’ clothing against HD absorption. In particular, with reference to low level exposure of civilians on the periphery of a chemical release. Historically, HD has been used as a chemical warfare agent, and existing knowledge on HD skin exposure, and protection against it, has primarily focused on military scenarios. As a result of this, it was decided that it would be useful to generate novel data for low level exposure to HD (neat and diluted in a solvent vehicle (IPA)) of clothed human skin in vitro using ‘everyday’ cotton shirt material

7.2: Results

7.2.1: 1hour exposure of clothed full thickness (FT) human breast skin to neat HD

Methods

For this study, 12 static diffusion cells were used. The static diffusion cells used had an exposed surface area of 2.54cm^2. All skin samples were covered with a small piece of cotton shirt material onto which the dose was applied. Half of the cells dosed with 25.4mg/cell of neat HD, and the remaining 6 cells were dosed with 1.25mg/cell of dilute HD in IPA applied as a finite dose (20µl). Each dose contained approximately 0.185MBq or radiolabelled HD per static cell. The cotton shirt material was placed on top of the skin on a 1mm x 1mm steel washer to create a 1mm air gap to simulate how clothing would be worn in a real life scenario. The clothing was removed from all cells after 1 hour exposure. For half of the cells, clothing was removed and the skin

surface was decontaminated using 5% soap solution immediately after removal of clothing. For the remaining cells, clothing was removed after 1 hour, with decontamination of the skin surface being carried out at the end of the experiment (24 hours).

Results

From figure 7.1, it can be seen that removal of clothing and skin decontamination at 1 hour reduced the cumulative absorption of neat HD compared with just removal of clothing at 1 hour. A similar outcome was observed when HD diluted in IPA was used instead of neat HD (figure 7.3). Neat HD absorbed to the receptor fluid continued to increase over 24 hours despite the fact that the clothing upon which the dose was applied was removed after 1 hour exposure, and that the dose was finite (20µl). However, although absorption from both clothing treatments continued to increase, the amount absorbed following dose deposition on clothing (cotton shirt) was significantly reduced when compared with 24 hour exposure. Following 24 hour exposure to neat HD, 25.3 ± 5.2% of the applied dose was recovered from the receptor fluid, and 58.3 ± 6.5% of the applied dose was recovered from within the skin membrane following digestion in soluene.

The dose distribution graph for neat HD (figure 7.2) shows that the majority of the applied dose of neat HD was retained within the clothing after 1 hour exposure. Following application to clothed skin, absorption was significantly reduced when compared with the percentage of applied dose absorbed after 24 hour exposure to neat HD (8.4 ± 2.9% absorbed for 1 hour removal with 24

hour decontamination, and 5.9 ± 1.7% absorbed following 1 hour removal of clothing and 1 hour decontamination respectively). The presence of clothing on the skin surface also reduced the amount of HD recovered from within the skin membrane from 58.3 ± 6.5%, to 18.6 ± 4.1% following skin surface decontamination at 1 hour, and 6.1 ± 3.2% following decontamination at 24 hours.

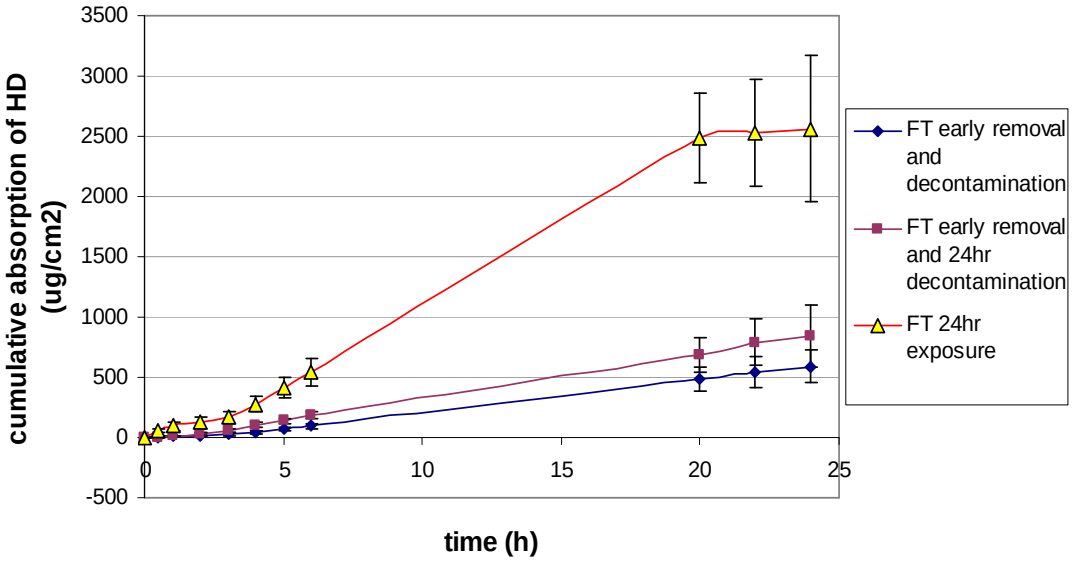

Figure 7.1. 24 hour cumulative absorption profile of neat HD (10mg/cm^2) applied to clothed, full thickness human breast skin. Values were means ± SEM of 3 cells (3 skin donors) for each of the clothing treatments (6 static diffusion cells in total). Clothing was removed at 1 hour after exposure to HD in both treatments, but skin surface decontamination was carried out at either 1 hour or 24 hours. Skin was mounted in static diffusion cells with an exposed area of 2.54cm^2. HD was applied at a concentration of 10mg/cm^2 in a finite dose (20µl).

Dose	Flux (ng/cm^2/h)	K_p x 10^{-3} (cm/h)	Lag Time (h)	Linear range
full thickness, 1hr removal and decontamination	23.3 ± 6.33	23.9 ± 7.3	1.91 ± 0.57	3-6
full thickness, 1hr removal and 24hr decontamination	39.0 ± 9.52	41.1 ± 9.3	0.32 ± 0.10	2-6
full thickness, 24hr exposure	129 ± 19.6**	127 ± 20.1**	1.77 ± 0.52	3-6

Table 25. Observed steady state absorption rates, partition coefficients and lag times of neat HD applied to clothed and unclothed full thickness human breast skin *in vitro*. A double asterisk next to a figure indicates that a figure is significantly different from the remaining 2 figures in the same column ($p<0.05$ with one way ANOVA).

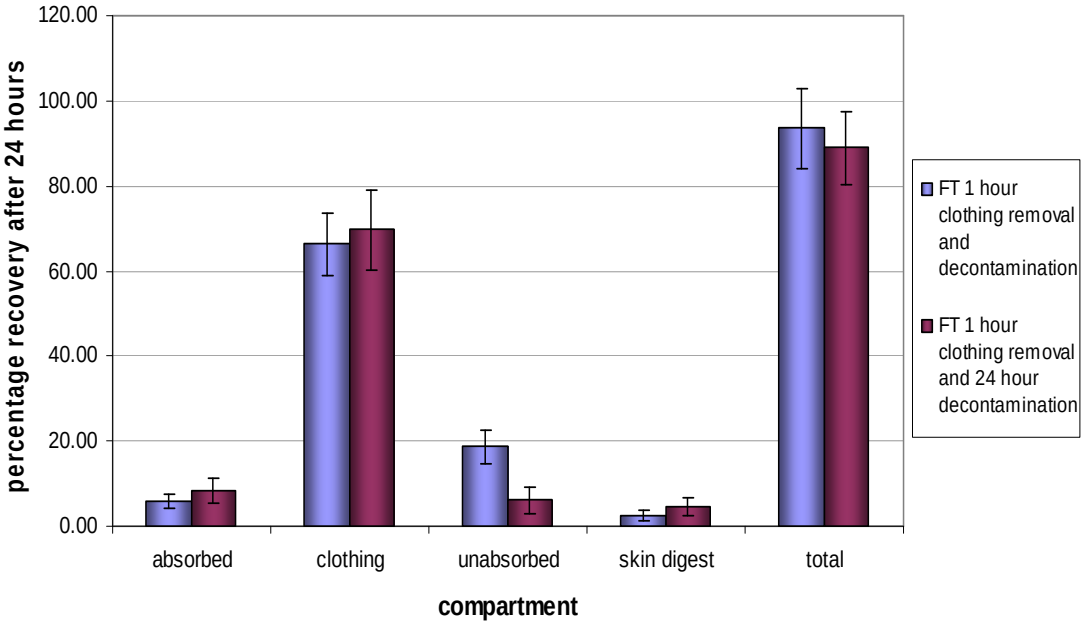

Figure 7.2. Dose distribution at 24 hours following 1 hour exposure of clothed full thickness human breast skin to neat HD (10mg/cm^2). Absorbed represents the percentage dose recovered from receptor fluid samples either after 1hour removal and decon or 1hr removal with 24hour decon, clothing represents the percentage of applied dose recovered from the clothing after 1hour exposure, unabsorbed was the percentage dose removed from the skin surface after either 1hour decon or 24 hour decon, and skin digest represents the percentage recovered from within the skin at 24 hours following 1hr removal and decon or 1hr removal with 24 hour decon respectively.

7.2.2: 1 hour exposure of clothed, full thickness human breast skin to dilute ^{14}C-labelled HD in IPA (492µg/cm^2)

The cumulative absorption profile of dilute HD in IPA (figure 7.3) shows that removal of contaminated clothing (cotton shirt material) from the skin surface after 1 hour followed by immediate decontamination reduced the cumulative absorption of HD by approximately 20µg/cm^2 when compared with removal of clothing alone (with decontamination at the end of the experiment at 24 hours). Absorption continued to increase up to 24 hours, despite the presence of clothing above the skin for 1 hour after dosing. However, as can be seen from this figure, absorption was reduced by approximately 50% following removal of clothing with immediate skin surface decontamination compared with 24 hour exposure. Absorption following removal of clothing with immediate decontamination was lower than with 24 hour decontamination, despite having a shorter apparent lag time (0.49 ± 0.11h, compared with 1.14 ± 0.55) (table 26). A lower apparent maximum flux was also observed following removal of clothing and decontamination at 1 hour compared with removal of clothing alone (3.82 ± 0.89 µg/cmµ^2/h, compared with 5.62 ± 1.13µg/cm^2/h respectively) (table 26). However, the overall reduction in absorption compared with 24 hour exposure was not statistically significant, despite there being a significantly greater observed maximum flux following 24 hour exposure to neat HD compared with the flux observed following 1 hour removal of clothing with immediate decontamination (table 28).

The dose distribution of dilute HD in IPA (figure 7.4) shows a very similar pattern to the dose distribution for neat HD. Here, the clothing had also

retained the majority of the applied dose after 1 hour exposure. Approximately 11% of the applied dose was recovered from the skin surface after removal of clothing and decontamination at 1hour. This is much more than what was recovered from the skin surface at 24 hours (2.5%). Despite this difference, the amount of HD retained within the skin was similar for both treatments (approximately 7%). However, this represents a significant reduction in skin retention of HD compared with 24 hour exposure to dilute HD in IPA, where 61.2 ± 8.8% of the dose was found within the skin after 24 hour exposure ($p<0.05$ with one way ANOVA). Absorption of dilute HD in IPA was approximately double compared with absorption of neat HD in terms of percentage of dose applied to the skin surface.

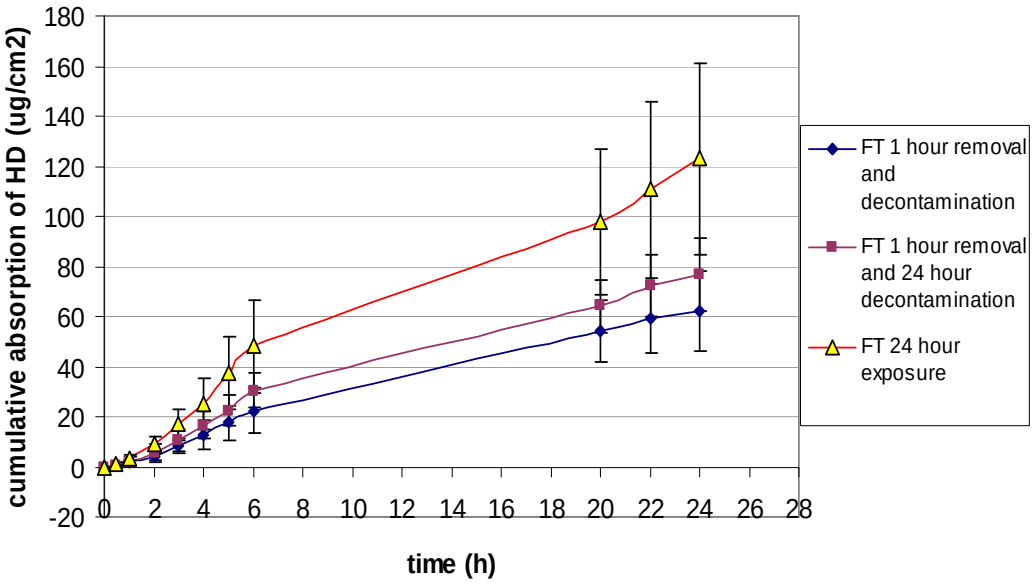

Figure 7.3. 24 hour cumulative absorption profile of dilute HD in IPA (492µg/cm^2) applied to clothed, full thickness human breast skin. Values were means ± SEM of 3 cells (3 skin donors) for each of the clothing treatments (6 static diffusion cells in total). Clothing was removed at 1 hour after exposure to HD in both treatments, but skin surface decontamination was carried out at either 1 hour or 24 hours. Skin was mounted in static diffusion cells with an exposed area of 2.54cm^2. HD was applied at a concentration of 10mg/cm^2 in a finite dose (20µl).

Dose	Flux (ng/cm^2/h)	K_p x 10^{-3} (cm/h)	Lag Time (h)	Linear range
full thickness, 1hr removal and decontamination	3.82 ± 0.89	3.74 ± 1.1	0.49 ± 0.11	0-6
full thickness, 1hr removal and 24hr decontamination	5.62 ± 1.13	5.5 ± 1.2	1.03 ± 0.37	2-5
full thickness, 24hr exposure	9.35 ± 2.74*	9.1 ± 3.5	1.14 ± 0.55*	2-5

Table 26. Observed steady state absorption rates, partition coefficients and lag times of dilute HD in IPA following application to clothed and unclothed full thickness human breast skin *in vitro*. A single asterisk next to a figure indicates that it is significantly different from the lowest figure in the same column.

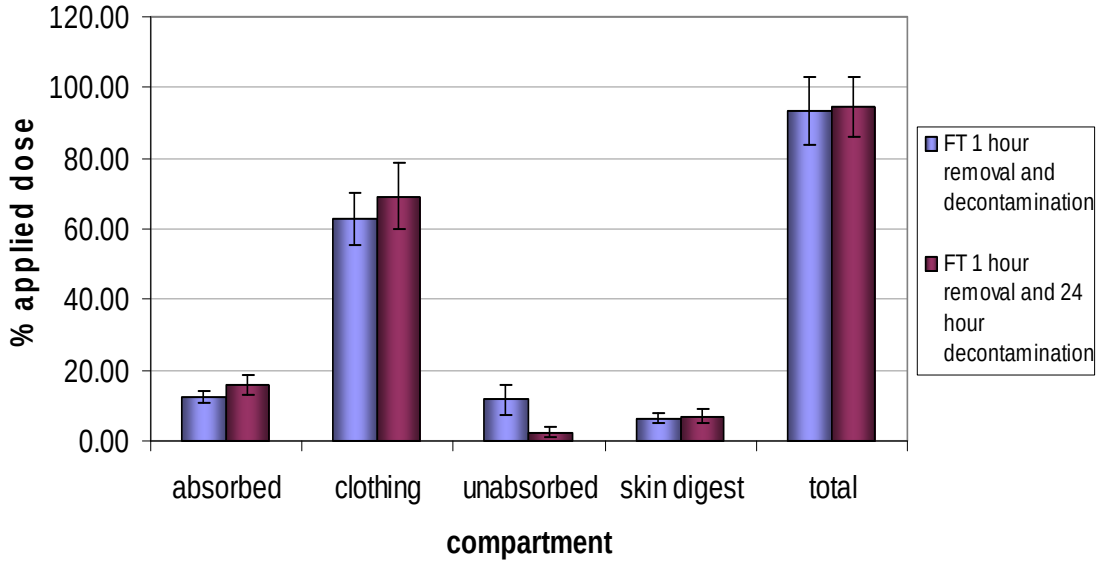

Figure 7.4. Dose distribution at 24 hours following 1hour exposure of clothed full thickness human breast skin to dilute HD in IPA (492µg/cm^2). Absorbed represents the percentage dose recovered from receptor fluid samples either after 1hour removal and decon or 1hr removal with 24hour decon, clothing represents the percentage of applied dose recovered from the clothing after 1hour exposure, unabsorbed was the percentage dose removed from the skin surface after either 1hour decon or 24 hour decon, and skin digest represents the percentage recovered from within the skin at 24 hours following 1hr removal and decon or 1hr removal with 24 hour decon respectively.

7.3: Discussion

The purpose of these studies was to investigate the effectiveness of everyday clothing (cotton shirt) at reducing dermal absorption of neat HD and dilute HD through human breast skin which was used full thickness in static diffusion cells. Dermal absorption of neat HD was reduced by cotton shirt clothing compared to unclothed skin, suggesting that 'every day' clothing can provide a significant barrier to dermal absorption of chemicals. Absorption of neat HD following removal of clothing and skin surface decontamination at 1 hour was reduced compared with removal of clothing only although the difference was not significant.

It is clear that removal or clothing supplemented with immediate skin surface decontamination can help to further reduce the amount of HD being absorbed into the skin. This is supported by the lower absorption of HD through the skin following immediate decontamination after removal of clothing compared with removal of clothing alone. Although this was not a statistically significant reduction, it is a numerical one and this could potentially be important with regard to decontamination procedures in real life scenarios.

Removal of clothing with immediate decontamination resulted in more of the applied dose being recovered from the skin surface compared with the amount recovered from the skin surface with removal of clothing alone. This suggests that a significant proportion of the applied dose can still come into contact with the skin despite the presence of clothing, and even though clothing was only in contact with the skin for 1 hour after exposure. This may

suggest that, from a real life exposure perspective, skin surface decontamination and removal of clothing as soon as possible following exposure to a chemical is advantageous for minimising the amount of chemical coming into contact with the skin, and also the amount of time in which the chemical has to penetrate through the stratum corneum.

Similar results were obtained when clothed; full thickness human breast skin was exposed to dilute HD in IPA Absorption was approximately halved following removal of clothing and decontamination at 1 hour compared with the amount of HD absorbed following 24 hour exposure, and by approximately a third when clothing was removed at one hour without decontamination. The amount of HD recovered from the skin surface following 1 hour decontamination after removal of clothing was also significantly greater than following 24 hour decontamination. This adds further evidence to the proposal that removal of clothing supplemented with skin surface decontamination as early as possible after exposure can help to reduce absorption of HD through the skin. Despite the presence of clothing and a short exposure time, the amount of HD absorbed through the skin was still high. This may be an effect of the application vehicle, with IPA leading to greater penetration of HD into the stratum corneum, particularly with occlusion from the clothing above the skin surface.

Following exposure of clothed, full thickness human breast skin to both neat HD, and HD diluted in IPA, it can be seen that ‘everyday’ cotton shirt material provides an effective barrier to absorption despite not being designed specifically for protective purposes. The amount of HD retained within the

clothing at 1 hour following exposure ranged from 62-69% of the applied dose. From a real life exposure perspective, this suggests that if contaminated clothing is removed from the skin surface as soon as possible after exposure, then the amount of chemical reaching the skin surface, and also the amount being absorbed through the skin can be significantly reduced. This is important to consider for chemicals like HD, which elicits its major toxic effects locally within the skin, but also for chemicals which exert their effect systemically.

Chapter 8

Predictions of dermal absorption using a mathematical model

8. Predictions of dermal absorption using a mathematical model

8.1: Introduction

It is important to investigate dermal absorption of chemicals from a toxicological risk assessment perspective in order to estimate the amount of a chemical which may become internally available following exposure to the skin. As shown in previous chapters, *in vitro* dermal absorption studies can be undertaken to predict *in vivo* exposure. Also, many *in vivo* experiments have been undertaken using animal models to predict exposure outcomes for human exposure *in vivo*. However, cost implications, as well as the desire to reduce the number of animals used in dermal absorption studies, are limiting factors when implementing the *in vivo* approach. *In vitro* experiments also have flaws, particularly as individual experiments implement highly specific parameters for absorption of a particular chemical. This means that data obtained may not reflect the outcomes under different exposure settings.

As of the end of mid-2007, new European Union legislation on the registering of chemicals was agreed, known as REACH (Registration, Evaluation, Authorisation and Restriction of Chemicals). This states that over 50,000 known chemicals will need to be evaluated for environmental and occupational safety regarding the way they are produced, used and disposed of by the end of 2017. These issues have stimulated this area of research, and have led to a variety of pharmacokinetic models being established to predict dermal absorption of chemicals, to attempt to reduce the time and

financial costs needed to rank chemicals for risk assessment purposes (European Commission, Joint Research Centre website).

QSAR models have traditionally been used to quantify the relationship between the chemical structure and the pharmacological activity of a chemical. Most available QSAR models predict only the permeability coefficient (K_p) of a chemical from an infinite dose, under steady state conditions. An extensive overview of most of the available QSAR models has been published recently (Bouwman *et al*. 2008). This review came to the conclusion that none of the available QSARs were suitable for accurate risk assessment of chemical absorption through skin. The permeability coefficient of a chemical across the skin is expressed as cm/h, and from this parameter, the steady state flux can be calculated under infinite dose conditions. Under these conditions, the dose concentration of a chemical on the skin surface does not reduce markedly over time, however, for 'real life' exposure scenarios, finite dose conditions are more likely to occur. Many '*in silico*' methods do not take the depletion in dose concentration across the skin into account, and so generally lead to poor prediction of dermal absorption.

For the purposes of this chapter, a novel pharmacokinetic model has been implemented, using infinite and finite dose parameters from the experimental data obtained in order to identify whether predicted outcomes correlate well with experimental outcomes from finite dose studies. The model used for this purpose was described by Buist *et al*. 2010. This model was developed to predict cumulative absorption from finite dose conditions based on the permeability coefficients, lag times and the stratum corneum/water partition

coefficients ($K_{sc/w}$) obtained from infinite dose data. This model incorporates a distribution factor, which accounts for the depletion of the surface dose concentration after distribution of the test chemical into the stratum corneum, and so may lead to more accurate prediction of dermal absorption. Cumulative absorption was predicted using the following equation:

$$M_t = M_0(1-e^{f(-KpA\ (t-tlag)/V)}) \quad (1)$$

Here, M_t is the cumulative amount of chemical absorbed at time t, M_0 is the amount of chemical applied to the skin surface at time 0 (µg), f is the distribution factor, K_p is the permeability coefficient (cm/h), A is the application area (cm^2), tlag is the experimental lag time (h) (under infinite dose conditions) and V is the volume applied to the skin surface (ml). Without the distribution factor (f), the model would assume that the dose concentration remained unchanged during absorption, until the entire dose was exhausted by the absorption process.

The distribution factor was calculated using the following equation:

$$F = \frac{V_{DL}/ (V_{DL} + K_{SC,\ V} * V_{SC})}{V_{DH}/ (V_{DH} + K_{SC,\ V} * V_{SC})} \quad (2)$$

Here, V_{DL} and V_{DH} are applied volumes (µl) for finite and infinite dose conditions respectively, $K_{SC,\ V}$ is the stratum corneum: vehicle partitioning coefficient, and V_{SC} is the volume of stratum corneum (1.23µl for an exposed area of 0.64cm^2).

For aqueous vehicles, the value for $K_{SC, V}$ can be calculated using a QSAR. For the purposes of the data set obtained from the experiments in this project, non aqueous vehicles were used for application of chemicals to the skin. Therefore, the following equation was used to calculate $K_{SC, V}$ for any vehicle:

$$K_{SC, V} = [tlag*6K_p]/h \quad (3)$$

Here, h is the distance through the stratum corneum (20μm).

The amount of chemical present in the stratum corneum can be predicted using the following equation:

$$M_{SC} = (M_0-M_P) * (1-f) \quad (4)$$

Here, M_{SC} is the amount of chemical present in the stratum corneum, M_0 is the amount applied to the skin surface (μg), and M_P is the cumulative amount absorbed in the receptor fluid (this was determined using the equation 1).

The experimental data obtained from human breast skin exposure to infinite dose and finite doses of the chemicals outlined in chapters 3 and 4 was used to correlate with the pharmacokinetic model described by Buist *et al.* 2010, in order to establish comparisons between experimental data and predicted outcomes. Data taken from infinite dose exposure experiments (experimental lag time, permeability coefficient (K_P), and stratum corneum: vehicle partition coefficient ($K_{SC, W}$)) was used to predict the experimental outcome based on a finite dose exposure. The experimental data shown in each cumulative

absorption graph is from a finite dose exposure. The data used to input into the Buist model is shown in table 27 below.

application dose	dose concentration	finite dose applied volume (µl)	infinite dose experimental lag (h)	Partition coefficient	Ksc,w
Caffeine in IPA	10mg/ml	6.4	2.4 hours	0.0427cm/h	307
Caffeine in PG	12mg/ml	6.4	1.7 hours	0.0168 cm/h	85.7
Benzoic acid in IPA	35mg/ml	6.4	2.3 hours	0.0014 cm/h	9.66
Benzoic acid in PG	24mg/ml	6.4	9.1 hours	0.0011 cm/h	30
Dichlorvos in IPA	500µg/ml	6.4	0.6 hours	0.133 cm/h	240
Dichlorvos in IPM	500µg/ml	6.4	2.6 hours	0.0693 cm/h	541
Dichlorvos in PG	500µg/ml	6.4	3.2 hours	0.110 cm/h	1060

Table 27. Table of infinite dose data used to predict finite dose absorption based on the Buist pharmacokinetic model. A shorter lag time for caffeine in IPA was used here compared to the data shown in chapter 3 (12.1 hours). The shorter lag time of 2.4 hours was selected based on the early linear phase of the cumulative absorption graph, as the later increase in absorption may have been due to evaporation of the application vehicle.

8.2: Results

8.2.1: Caffeine applied in IPA and PG

The cumulative absorption profile of caffeine applied as a finite dose in IPA can be seen in figure 8.1, with the predicted outcome also shown based on the partition coefficient calculated from equation 3, using the K_P and lag time measured under infinite dose conditions (table 27). The results show that the model described by Buist *et al* over predicted absorption compared with experimental data, despite the assumption that no absorption occurred before the lag time. Absorption at 24 hours showed an approximately 4 fold over estimate of absorption compared with experimental data. Absorption of caffeine applied in IPA was faster over early time points, and then tailed off up to 24 hours. As a result of this, the predicted outcome prior to the lag time (2.4 hours) does not correlate well with the experimental data.

Caffeine applied as a finite dose in PG gave an unusual cumulative absorption profile, with slow initial absorption, followed by an increase at later time points (19-24 hours). As a result of this, the predicted cumulative absorption significantly over estimated absorption of caffeine applied as a finite dose in PG (approximately 7 fold higher than the experimental value).

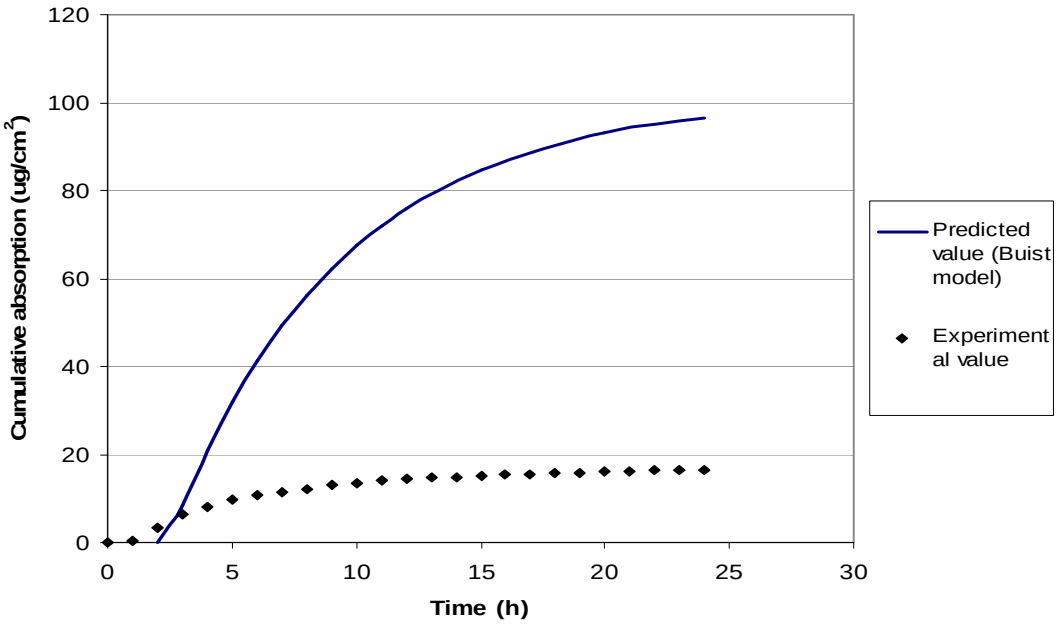

Fig 8.1. Cumulative absorption graph comparing predicted outcomes for a finite exposure with experimental data obtained from exposure of skin to finite dose of caffeine in IPA. Predictions were made based on the partition coefficient (K_p), and lag time measured under infinite dose conditions, with correction for distribution into the stratum corneum.

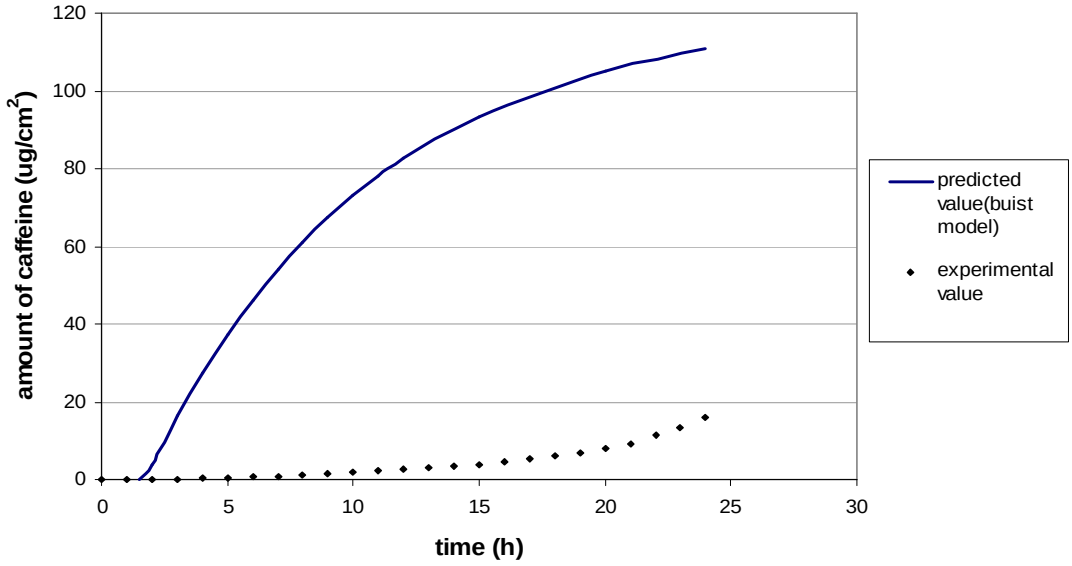

Fig 8.2. Cumulative absorption graph comparing predicted outcomes for a finite exposure with experimental data obtained from exposure of skin to finite dose of caffeine in PG. Predictions were made based on the partition coefficient (K_p), and lag time measured under infinite dose conditions, with correction for distribution into the stratum corneum.

8.2.2: Benzoic acid applied in IPA and PG

As can be seen from the cumulative absorption profile in figure 8.3, the predicted absorption of benzoic acid applied as a finite dose in IPA more closely followed the experimental values than for caffeine. The predicted and experimental values after 7 hours of exposure were similar (predicted value = 86μg/cm^2, experimental value = 83μg/cm^2). However, after this time point, the predicted values continued to over estimate absorption, with predicted absorption being approximately double that of the experimental values at 24 hours.

In contrast to the previous predictions leading to an over estimate of absorption, the predicted absorption of benzoic acid from a finite dose in PG led to an underestimation compared with the experimental value, despite the long lag time (9.1 hours) (figure 8.4). Benzoic acid applied as a finite dose in PG was initially slow to be absorbed, until reaching steady state absorption between 8 and 14 hours after exposure, before tailing off up to 24 hours. The experimental value was approximately double that of the predicted value at 24 hours.

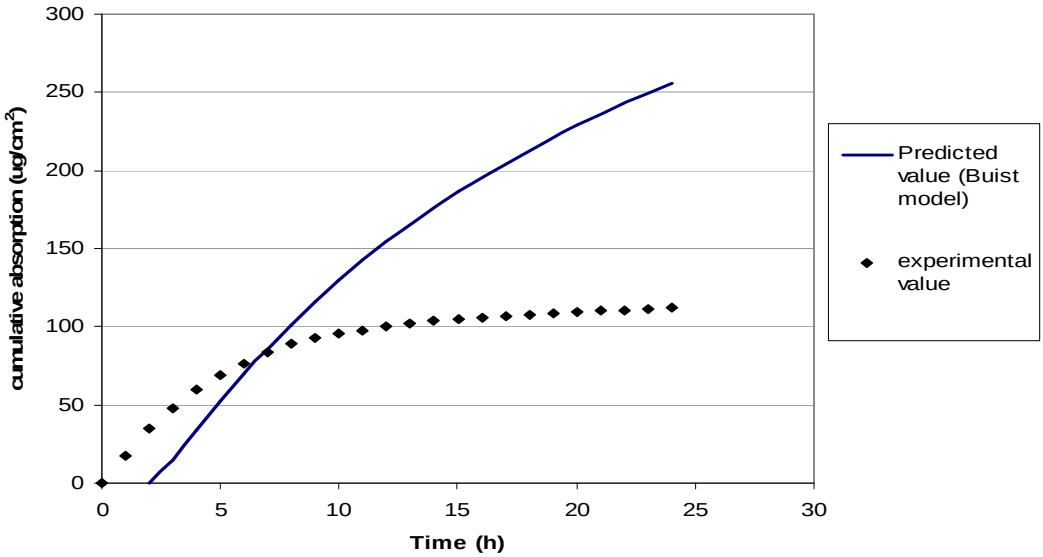

Fig 8.3. Cumulative absorption graph comparing predicted outcomes for a finite exposure with experimental data obtained from exposure of skin to finite dose of benzoic acid in IPA. Predictions were made based on the partition coefficient (K_p), and lag time measured under infinite dose conditions, with correction for distribution into the stratum corneum.

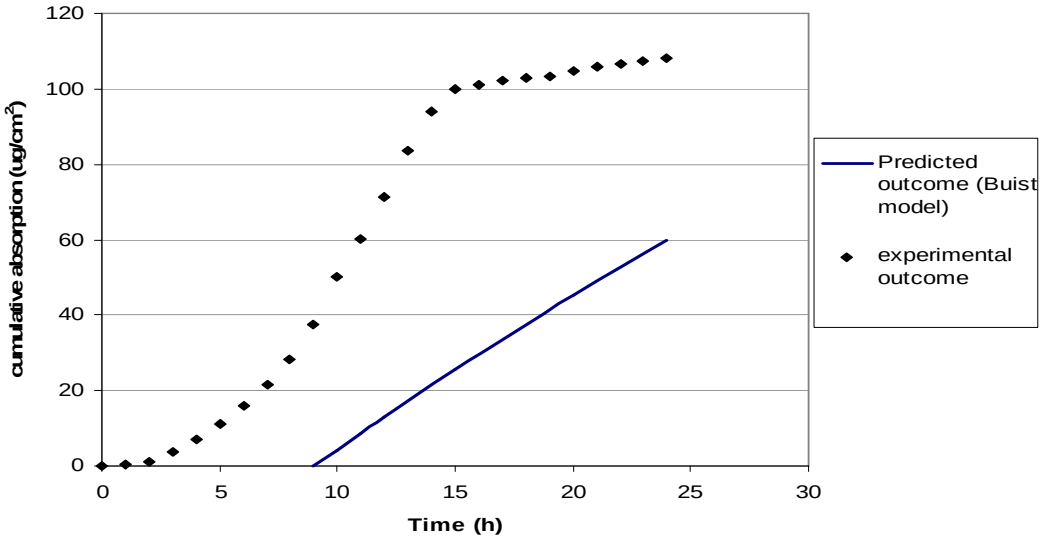

Fig 8.4. Cumulative absorption graph comparing predicted outcomes for a finite exposure with experimental data obtained from exposure of skin to finite dose of benzoic acid in PG. Predictions were made based on the partition coefficient (K_p), and lag time measured under infinite dose conditions, with correction for distribution into the stratum corneum.

8.2.3: Dichlorvos applied in IPA, IPM and PG

As can be seen from the predicted cumulative absorption values shown in figures 8.5, 8.6 and 8.7 (for IPA, IPM and PG respectively), the predicted model for cumulative absorption of dichlorvos from all three vehicles significantly over predicted absorption compared with the experimental values obtained from finite dose studies for dichlorvos applied in IPA, IPM and PG, with absorption being over predicted by approximately 2-fold after 24 hours. The predicted cumulative absorption profile of dichlorvos in IPA and IPM were similar in terms of the shape of the profile curve. The predicted cumulative absorption of dichlorvos in IPA closely matched the experimental values for the first 2-3 hours, but then absorption tailed off rapidly and the difference between predicted and experimental values became greater.

A short lag time (0.6 hours) was observed when dichlorvos was applied in IPM, with absorption reaching a steady state in the early time points (1-8 hours) before tailing off up to 24 hours. Absorption of dichlorvos from PG was also approximately linear from 2-8 hours after exposure, with a lag time of 3.2 hours. The predicted values for absorption from all three vehicles showed rapid absorption over the initial time points after the experimental lag time, with absorption tailing off up to 24 hours.

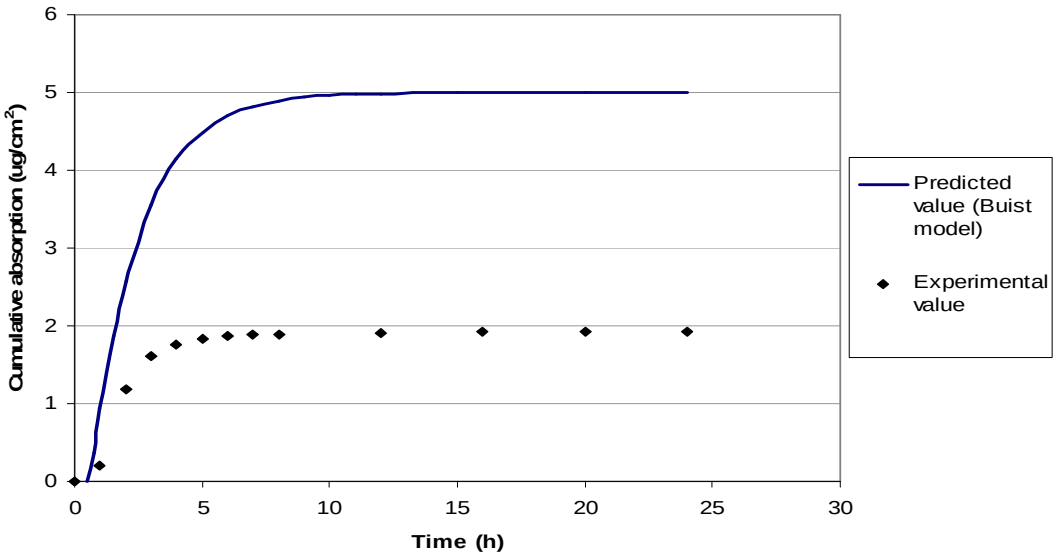

Fig 8.5. Cumulative absorption graph comparing predicted outcomes for a finite exposure with experimental data obtained from exposure of skin to finite dose of dichlorvos in IPA. Predictions were made based on the partition coefficient (K_p), and lag time measured under infinite dose conditions, with correction for distribution into the stratum corneum.

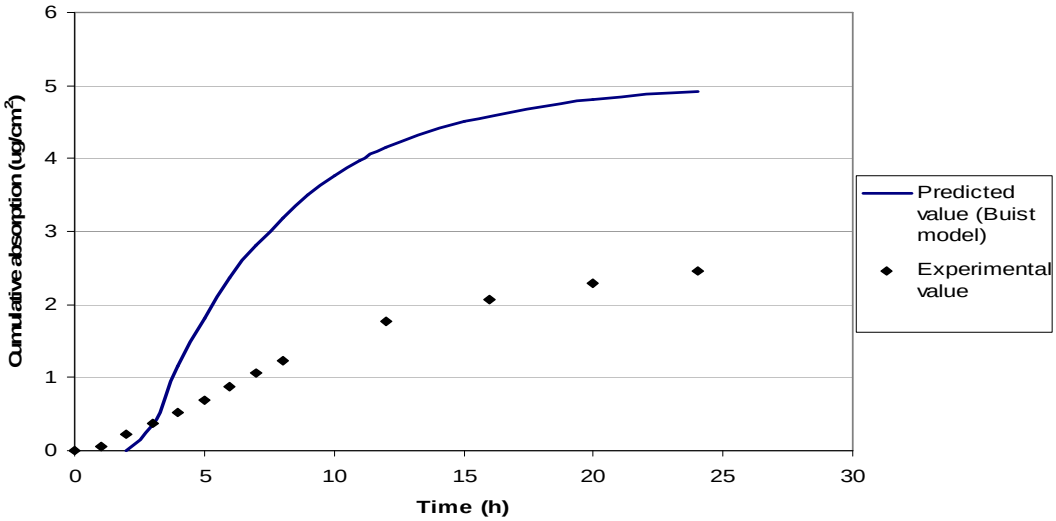

Fig 8.6. Cumulative absorption graph comparing predicted outcomes for a finite exposure with experimental data obtained from exposure of skin to finite dose of dichlorvos in IPM. Predictions were made based on the partition coefficient (K_p), and lag time measured under infinite dose conditions, with correction for distribution into the stratum corneum.

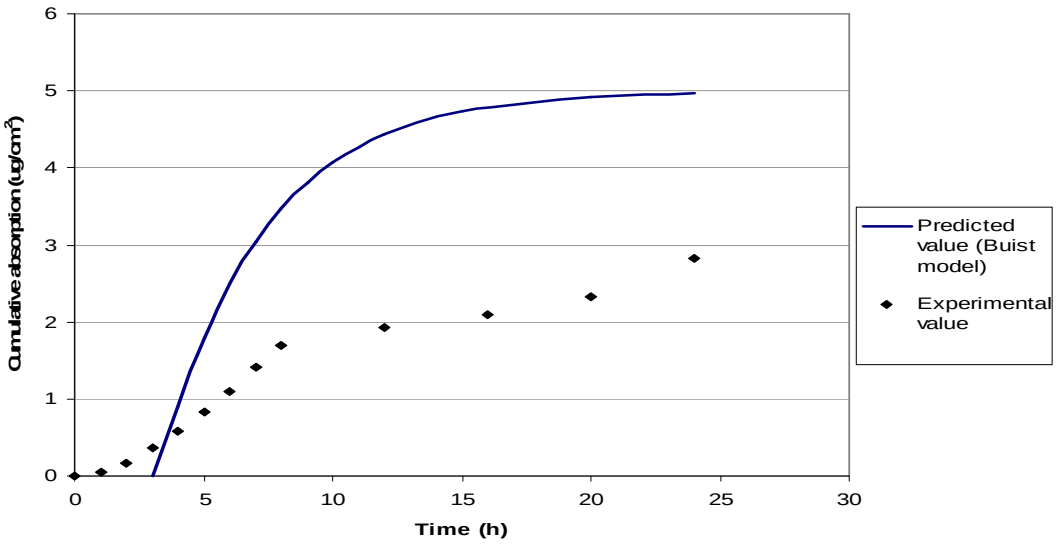

Fig 8.7. Cumulative absorption graph comparing predicted outcomes for a finite exposure with experimental data obtained from exposure of skin to finite dose of dichlorvos in PG. Predictions were made based on the partition coefficient (K_p), and lag time measured under infinite dose conditions, with correction for distribution into the stratum corneum.

8.3: Discussion

The results show that the model described by Buist *et al.* does not correlate well with the finite dose experimental data obtained during this project. Very few predictive models are available that attempt to predict absorption from non aqueous vehicles. The majority of models focus on absorption from aqueous vehicles due to the lack of availability of $K_{SC,\ W}$ values. One of the main problems with the Buist predictive model is that it does not recognise any absorption before the experimental lag time. However, the lag time is calculated based on the extrapolation of the linear portion of the cumulative absorption curve to the x-axis, and is therefore not represented by the amount of time taken for a chemical to partition into the skin. During *in vivo* and *in vitro* studies, a chemical applied to the skin will undergo some absorption prior to the measured lag time. As a result of this, the model described by Buist *et al*.2010 will almost certainly be a poor predictor of absorption, particularly during early time points. With the exception of benzoic acid applied in IPA, this is certainly true of the data shown in this chapter.

It is also possible that the lag times may not be accurately calculated, particularly with the dichlorvos studies where the dose concentration on the skin surface was not saturated (meaning that true infinite dose conditions were not obtained). It is also unlikely that calculating the lag time by extrapolating the line of best fit through the linear portion of the cumulative absorption curve to the x-axis may not be an accurate measure of the 'true' lag time. Inaccuracies in measurement of experimental lag time will lead to error in the calculation of $K_{SC,\ W}$ values.

Also, the model tends to predict that all compounds that are absorbed through the skin under finite conditions will fit a classical finite dose cumulative absorption curve (fast absorption during early time points followed by tailing off up to 24 hours). However, the experimental data used in these predictions show that this is not always the case. For instance, the cumulative absorption profile of caffeine applied to the skin as a finite dose in PG began with a slow absorption rate over the initial 10 hours of exposure, followed by an increase in absorption rate up to 24 hours. Therefore, it is likely that chemicals which do not fit this particular profile will not fit well with the predictive model. The best fit observed from the experimental data came from benzoic acid in IPA, which gave an expected finite dose cumulative absorption curve, however, absorption was still over predicted by approximately double at 24 hours.

However, it is clear from the data shown in this chapter that the predicted absorption more closely matched the experimental data when using a chemical that more readily partitions into the stratum corneum (dichlorvos), compared with experimental data obtained using a chemical which is less able to penetrate into the stratum corneum (caffeine). This is shown in particular from the predicted absorption of dichlorvos from IPA, as predicted absorption closely matched observed absorption over early time points. It is possible that better predictions for absorption of chemicals that readily penetrate the stratum corneum are due to the Buist model taking into consideration partitioning into the stratum corneum, and not absorption through the skin as a whole. It is possible that if predictions were made to identify the amount of a test chemical within the skin at a given time point, that the amount penetrated

and the amount absorbed combined may more closely match the amount absorbed based on the predictive model described by Buist *et al*.

There are complex interactions between chemicals and the vehicles in which they are applied to the skin surface, and to take this into consideration, as well as the complexities of skin structure, make it extremely difficult to produce mathematical models which will be suitable for risk assessment for dermal exposure to chemicals. It could be argued that in order to validate mathematical models, experimental data will need to be produced in parallel, and so the argument for using mathematical models as a cost effective tool for compliance with the REACH programme may not be entirely valid. However, models that reliably over predict absorption may possibly be useful for a ‘worst case scenario’ for dermal exposure to chemicals.

Further work on mathematical models of dermal absorption is clearly needed if the predicted data is to be trusted without having to validate it by producing experimental data.

Chapter 9

General Discussion

9. General Discussion

9.1: Discussion and conclusion

The main aim of this project was to increase the understanding of the dermal absorption of chemical agents in man and to assess the influence of different exposure scenarios, including application vehicle, and the influence of everyday clothing with decontamination on the dermal absorption of a series of chemicals, including marker chemicals, organophosphates and HD. To do this, skin mounted in static and flow through diffusion cells was used to provide information *in vitro* and to extrapolate these results to dermal absorption of chemicals *in vivo*. It has previously been shown that in vitro studies with human skin predict absorption in vivo under similar exposure conditions for a range of model compounds (Williams *et al*. 2006).

9.1.1: Choice of Surrogate compounds for chemical agents and vehicle effects on dermal absorption

Initially, caffeine and benzoic acid were used for in vitro diffusion studies as model compounds as they represent a range of physico chemical properties, and the influence of vehicle on their dermal absorption was assessed (chapter 3). These chemicals were used as they had been extensively studied in the laboratory in Newcastle as reference compounds in dermal absorption studies. Including these compounds as references allowed ranking of absorption studies with organophosphates, which could be considered chemical agents in their own right as well as surrogates for nerve agents, and with a chemical agent (HD). The main purpose of conducting the *in vitro* finite dose exposure experiments outlined in this project was to understand the

absorption profile of a range of chemicals and to use this data to predict absorption *in vivo* for specific exposure scenarios.

Caffeine (applied to the surface of dermatomed human breast skin as a finite (10µl/cm^2), saturated dose in IPA (10mg/ml) or in PG (12mg/ml) resulted in approximately 16µg/cm^2 of caffeine absorbed at 24 hours after exposure, despite differences between the two absorption profiles. This was despite a longer lag time being observed following application of caffeine in PG, and also a greater observed maximum flux being observed for caffeine in IPA (3.3µg/cm^2/h). However, as steady state absorption was not achieved for caffeine absorption from the IPA vehicle (when applied as an infinite dose), it was difficult to make comparisons based on observed maximum absorption rates.

Absorption of benzoic acid through dermatomed human breast skin was much greater than caffeine when applied as a saturated, finite dose (concentration of 12mg/ml in IPA and IPM). Initial absorption was faster when applied in IPA; however, the total amount of benzoic acid absorbed from both vehicles was similar after 24 hours (approximately 115µg/cm^2). Absorption of benzoic acid was expected to be greater through the skin than for caffeine, due to the more lipophilic nature of benzoic acid and its interaction with both IPA and PG vehicles. IPA is amphipathic, and PG is a hydrophilic solvent, therefore, benzoic acid partitioned into the stratum corneum more readily than caffeine applied to the skin in the same two vehicles.

It was impossible to ascertain a true maximum absorption rate for either caffeine or benzoic acid applied in IPA as an infinite dose due to the volatility of the vehicle. Despite being applied as an infinite saturated dose (1ml/cm^2), the vehicle volume depleted rapidly from the skin surface, and so steady state absorption was never achieved. Absorption of both chemicals from PG however, did achieve and maintain a steady state as PG is much less volatile, and so steady state absorption was maintained over 24 hours.

Having defined the absorption profiles of caffeine and benzoic acid, dermal absorption studies were undertaken using the organophosphates chlorpyrifos, dichlorvos and phorate. Organophosphates are an accidental exposure threat to civilians and so it is important to generate absorption data for these chemicals. By comparison of their physicochemical properties with nerve agents it may be possible to extrapolate these dermal absorption results to nerve agents with which it was not possible to work in this project.

Application of dichlorvos to dermatomed human skin in 3 vehicles (IPA, IPM and PG) at the same absolute concentration resulted in differing cumulative absorption profiles. Absorption from the IPA vehicle was fastest over the first few hours, and resulted in the fastest observed absorption rate. This was likely to be due to rapid evaporation of the IPA vehicle from the skin surface leading to a transient increase in skin surface concentration of dichlorvos. The greatest absorption of dichlorvos from IPA occurred over the first 3 hours of exposure, suggesting that *in vivo*, an early wash-off (within the first hour) would be necessary to prevent significant dermal absorption. Despite

differences in the cumulative absorption profiles between vehicles, the overall amount of dichlorvos absorbed from each vehicle over a 24 hour period was not significantly different. However, the observed maximum absorption rate of dichlorvos from the IPM and PG vehicles was lower than from IPA, and so from a decontamination perspective, may present a wider window of opportunity to successfully remove the majority of the chemical in contact with the skin.

The same three vehicles were used to investigate the dermal absorption of chlorpyrifos. Application of chlorpyrifos to the skin surface in the PG vehicle resulted in a two-fold increase in absorption compared with chlorpyrifos in IPA, and a ten-fold increase in absorption compared with chlorpyrifos in IPM. The observed difference in absorption of chlorpyrifos is likely to be due to the different physicochemical properties of the solvent vehicles. Chlorpyrifos is a lipophilic chemical, and so it had a greater thermodynamic activity in the hydrophilic PG vehicle than in IPA or IPM. This resulted in a steeper thermodynamic gradient across the skin and led to greater absorption of chlorpyrifos through the skin. The least absorption of chlorpyrifos was observed from the IPM vehicle, as this was the most lipophilic of the solvent vehicles used. Despite greater absorption resulting from application of chlorpyrifos in PG and IPA compared with IPM, long lag times were also observed following use of these vehicles. This suggests that wash-off from the skin surface up to 6 hours after exposure to chlorpyrifos is likely to significantly reduce the amount reaching systemic circulation *in vivo*. Overall, dermal absorption of dichlorvos was greater than chlorpyrifos from all

application vehicles. Absorption of dichlorvos ranged from approximately 30-40% of the applied dose from the 3 vehicles, whereas absorption of chlorpyrifos ranged from approximately 5-20% when applied in the same vehicles to the skin surface. However, a greater proportion of the applied dose of chlorpyrifos was retained within the skin (skin digests and tape strips, approximately 25-30% of the dose) compared with dichlorvos (10-20% retained in the skin) when applied as a finite dose in the 3 different vehicles. It is possible that chlorpyrifos may have the potential to be further absorbed from within the skin by slowly penetrating through the stratum corneum and epidermis to the more hydrophilic regions of the skin where it can become systemically available. From a civilian exposure perspective, there may be more potential for removal of a larger proportion of the dose of chlorpyrifos from the skin surface than dichlorvos, as chlorpyrifos was slower to penetrate the skin and resulted in a greater proportion of the dose remaining unabsorbed on the skin surface when compared with dichlorvos applied in all vehicles (chapter 4). However, chlorpyrifos showed a greater propensity to be retained in the upper layers of the skin and so could lead to further systemic absorption in an *in vivo* scenario, it is also possible that decontamination of the skin surface may result in a ‘wash-in effect’, causing further absorption of chlorpyrifos that may be re-solubilised within the decontaminant. However, a previous study by Hattersley *et al*. 2008 investigating the skin reservoir of HD showed that it is possible to extract non-bound HD from within the stratum corneum by using acetonitrile.

A small study investigating the influence of vehicle on absorption of phorate through dermatomed pig abdomen skin showed that the proportion of the applied dose of phorate absorbed was increased when applied to the skin in IPA compared with application of neat phorate. No data were obtained for dermal distribution of either neat phorate of phorate diluted in IPA, however, based on the properties of phorate and the proportion of the applied dose recovered from the receptor fluid after 24 hours, it is likely that a significant proportion of the applied dose of phorate would have been retained within the skin, in particular in the stratum corneum due to the lipophilic nature of phorate. The enhanced absorption of phorate from the IPA vehicle was probably due to the vehicle properties, taking into account the volatility of IPA leading to a rapid increase in skin surface concentration of phorate, and also the fact that IPA is mildly lipophilic and so phorate would readily partition into the lipophilic stratum corneum from the IPA vehicle. Application of phorate in IPA also resulted in a reduced observed lag time compared with neat phorate, and so from a skin surface decontamination perspective, there would potentially be less time to remove the majority of the applied dose from the skin surface in the event of a lipophilic chemical being administered in a mildly lipophilic/hydrophilic vehicle. However, it is important to note that even though a larger percentage of the applied dose of phorate applied in IPA was absorbed compared with neat phorate; the actual amount reaching the receptor fluid was greater from the neat dose.

HD was investigated because exposure to this chemical could be a civilian threat and it was available to study with collaboration with Dstl. HD has been

extensively researched in dermal absorption studies (Chilcott *et al*. 2000, Chilcott *et al*. 2001, and Hattersley *et al*. 2008), and the primary route of exposure to HD is through the skin. IPA was chosen for finite exposure due to its volatility, meaning that application of a finite dose would more closely mimic *in vitro* what may happen as a result of exposure to low levels of HD in droplet form *in vivo*. It is likely that civilian exposure to chemicals in the atmosphere will be to small volumes, and so small dose volumes (10µl/cm^2) were applied to the skin surface. This is the largest volume that can be applied to unclothed skin without the chemical falling off the skin surface (OECD, 2004, Wilkinson *et al*. 2010). However, in the presence of clothing it may be possible to load greater volumes of chemicals which may be retained in the clothing above the skin surface.

Absorption of HD through full thickness human skin after 24 hours was similar when applied as neat HD or as a dilution in IPA when expressed as a percentage of the dose applied to the skin (approximately 25%). The observed flux rate for neat HD through full thickness human breast skin (129.1 ± 14.4µg/cm^2h) was in keeping with the literature (71-294µg/cm^2/h, Chilcott *et al* .2000). The concentration of HD used in IPA in this project was lower than the dose used in previous published studies and an order of magnitude lower than for neat HD. The observed lag time for HD in IPA was shorter than for neat HD, this was likely to be as a result of HD readily partitioning into the skin from the amphipathic IPA vehicle. From a skin decontamination perspective, it is likely that HD applied in a moderately lipophilic/hydrophilic solvent vehicle, such as IPA will penetrate more efficiently into the skin as a result of an

increase in thermodynamic activity of HD in the IPA vehicle, and result in a shorter window of opportunity to remove a significant amount of HD from the skin surface. However, this does not mean that a greater amount of chemical will reach systemic circulation in an *in vivo* scenario from a vehicle compared with a neat chemical. It is possible that even though a shorter window of opportunity for removal of a chemical from the skin surface may be observed from a dilute dose, the local and systemic toxic effects that may occur as a result of dermal exposure are likely to be worse from a neat chemical with low level absorption compared with a low dose with a higher level of absorption. Prediction of the degree of absorption of HD into the systemic circulation is further complicated by binding of HD to proteins and other molecules in the stratum corneum and viable skin, due to the high reactivity of HD with functional groups found in proteins and other biomolecules.

A large proportion of HD was measured within the skin after 24 hours when applied as neat HD and diluted in IPA. This was expected as sulphur mustard has been shown to form a reservoir within the skin from which it can elicit its local toxic effects (Hattersley *et al*. 2008).

The amount of HD remaining in full thickness skin *in vitro* is likely to be an overestimate of what would be expected to be retained in the skin *in vivo*, particularly with the constant migration of cells from the basal to epidermal membranes and desquamation of the stratum corneum. As suggested by Hattersley *et al* .2008, some of the dose retained in the skin becomes irreversibly bound to proteins within the stratum corneum, and can no longer

be extracted from the skin, although some of the retained dose can still become available for further penetration through the skin.

Comparisons were also made between full and split thickness pig abdomen skin, as pig skin has previously been suggested as a good model for human exposure to HD (Chilcott *et al*. 2001). HD was applied to full and split thickness pig skin as a neat solution, and also diluted in IPA to enable comparisons to be made with the data obtained from human skin exposure. As expected, absorption of HD (both neat and diluted) was greater through split thickness skin than full thickness skin (chapter 5). The data obtained from full thickness pig skin exposure to HD suggest that full thickness pig skin is a good model for exposure to full thickness human breast skin. The similarity in absorption in terms of percentage of applied dose between neat HD and HD diluted in IPA, suggests that the application vehicle had little impact on the proportion of HD absorbed through either full or split thickness pig skin. This is in keeping with the data obtained from exposure of HD to full thickness skin.

Due to time constraints during the work placement at Dstl, only HD in IPA was compared with absorption of neat HD through human skin. From the data obtained in this project, the absorption profile that most closely matched that of HD through human skin was that of benzoic acid. Similar results were obtained when comparing finite dose exposures of benzoic acid and HD in an IPA vehicle. Both benzoic acid and HD are lipophilic compounds (benzoic acid Log p, 1.87, HD Log p, 2.41) that were retained within the skin following 24 hour dermal absorption (benzoic acid, approximately 55% measured in

stratum corneum, HD, 60% in the skin digest). However, it is impossible to identify the exact location of HD within the skin, as no tape stripping was carried out to remove the stratum corneum in the HD studies, although it is likely that HD would be retained within the stratum corneum due to its lipophilicity and reactivity with proteins in the stratum corneum.

As a proportion of the dose applied to the skin surface, similar amounts of benzoic acid and HD applied in IPA were absorbed through the skin, and comparable kinetic parameters were observed (absorption rates; benzoic acid, 18.5µg/cm^2/h, HD, 11.6µg/cm^2/h, Kp; benzoic acid 17.2cm/h, HD, 10.4cm/h).

A smaller proportion of the applied dose of both dichlorvos and chlorpyrifos was measured within the skin after 24 hour exposure (approximately 5-35%) when applied in IPA, compared with HD (60%). This is likely to be due to the retention of HD within the skin as a result of a proportion of the applied dose being bound to proteins and other structures within the skin (Hattersley *et al*. 2008). Measurement of chemical within the skin was not seen to the same extent with dichlorvos or chlorpyrifos, despite chlorpyrifos being a more lipophilic compound than HD (chlorpyrifos Log p: 4.96, HD Log p: 2.41). This reflects the importance of HD binding to skin, an effect which cannot be predicted from measuring the dermal absorption of surrogate compounds with similar molecular size and lipophilicity. It may be that less toxic analogues of HD which also exhibit similar reactivity, such as chloroethyl ethyl sulphide (CEES) may be useful in predicting HD binding within the skin. However,

despite the lack of distribution data from the phorate study, it may be possible that phorate may have had an affinity for the stratum corneum and could potentially form a reservoir in the skin in a similar way to HD. Further work is needed to identify the absorption profile of phorate through human skin for comparison with HD absorption and distribution within the skin.

As dichlorvos and chlorpyrifos are organophosphate compounds with different physicochemical properties (table 28 below), it is possible that they may be suitable surrogate compounds for other organophosphate chemicals, (e.g. sarin). In previous studies, methyl salicylate has been shown to be a useful surrogate compound for HD absorption through pig skin in terms of absorption kinetics (Riviere *et al*. 2001), and so this may be a useful chemical to use as a surrogate for human exposure to HD. However, due to HD being a more reactive chemical in terms of skin exposure than methyl salicylate (Riviere et al. 2001, Chilcott *et al*. 2000), it is likely that methyl salicylate may not be as useful for modelling for the distribution of HD within the skin as it is for modelling for HD kinetic parameters.

Compound	Log P	Molecular Weight	Vapour Pressure (at 25˚C)
Caffeine	-0.07	194.19	15 (at 89˚C)
Benzoic Acid	1.87	122.12	7.00E-04
Chlorpyrifos	4.96	350.59	2.03E-05
Dichlorvos	1.47	220.98	0.0158
Phorate	3.56	260.38	6.38E-04
Sulphur Mustard	2.41	159.08	0.1059
Methyl Salicylate	2.55	152.15	3.43E-02
Sarin	0.3	140.1	2.1
VX	2.09	267.38	7.00E-04

Table 28. Table showing the physicochemical properties of chemicals used in this project and similar chemicals

It is difficult to draw true comparisons between the dermal absorption of chemicals due to the variation in the concentration applied, and also because of the differences in solubility of chemicals in the vehicles used. For valid comparisons, it is important that chemical concentrations within vehicles should be matched based on solubility. For instance, a lipophilic chemical in a hydrophilic vehicle will have a lower solubility than a hydrophilic chemical in a hydrophilic vehicle. If these chemicals were applied to the skin surface at the same concentration, the thermodynamic activity of the lipophilic chemical would be greater than that of the hydrophilic chemical, which is likely to result in greater absorption of the lipophilic chemical through the skin. However, if the chemicals were dissolved in the same vehicle as saturated solutions, then the thermodynamic gradient would be the same for the two chemicals across

the skin, and would allow for more accurate comparison of dermal absorption of two chemicals applied to the skin in the same vehicle.

It is possible that differences in thermodynamic activity between vehicles and chemicals used may have influenced dermal absorption due to the range of chemicals used, and the differences in physicochemical properties seen between chemicals (table 28). This is demonstrated by comparison of the absorption profiles of chlorpyrifos applied as a finite dose in IPA, IPM and PG in chapter 4, where absorption of chlorpyrifos was greatly enhanced when applied in PG compared with IPA or IPM. This is likely to be an effect of thermodynamic activity, although the increase in absorption cannot be solely attributed to thermodynamic activity, as PG has been shown previously to enhance dermal absorption (Duracher *et al*. 2009).

9.1.2: The influence of everyday clothing and skin decontamination on the dermal absorption of chemicals *in vitro*

Due to the likelihood that civilians who become exposed to chemicals will not be wearing personal protective equipment, but are likely to be wearing normal clothing, experiments were undertaken to investigate the protective qualities of everyday clothing against dermal chemical absorption. In general, occupational chemical handlers should wear protective clothing that has been specifically designed to limit skin exposure to chemicals. However, workers in some parts of the world do not have, or do not use personal protective equipment, and as a result will be prone to greater exposure to hazardous chemicals. Civilians exposed to an accidental release will be wearing clothing

that may offer variable protection related to its nature. Therefore it is important to quantify the level of protection that normal clothing may provide against dermal exposure. To do this, a thin cotton shirt was used to cover skin to undertake *in vitro* flow through and static diffusion cell studies. In parallel to this, skin surface decontamination with a 5% soap solution was also assessed as a supplement to removal of contaminated clothing.

Everyday cotton shirt material retained between 80 and 90% of the applied dose of chlorpyrifos (in IPA and PG) when removed from the skin after 4 hours. Absorption of chlorpyrifos from the IPA vehicle through clothed skin at 24 hours was reduced approximately 10-fold compared with 24-hour exposure of unclothed skin to chlorpyrifos, whereas absorption of chlorpyrifos from the PG vehicle through clothed skin was reduced by approximately 20-fold compared with 24-hour exposure to unclothed skin. The effectiveness of everyday clothing was even greater at reducing dermal absorption of dichlorvos from IPA, IPM and PG vehicles. Approximately 65% to 75% of the applied dose of dichlorvos for all vehicles was retained within the clothing after 30-minute exposure. Absorption at 24 hours was reduced from 38% after 24-hour exposure to dichlorvos in IPA, to 2.6% of the applied dose in the presence of clothing in contact with the skin for 30 minutes after exposure. Similar reductions were also observed following application of dichlorvos in IPM and PG to clothed skin.

Everyday clothing had less of a protective effect against absorption of HD compared with chlorpyrifos and dichlorvos. Exposure of unclothed, full

thickness human skin to neat HD resulted in approximately 25% of the applied dose being absorbed; however, when neat HD was applied to clothed skin, absorption at 24 hours was between 6% and 8.5% of the applied dose, despite removal of the contaminated clothing after 1 hour. This represents a 3-4-fold reduction in absorption compared with 24-hour exposure. Absorption of HD diluted in IPA through clothed full thickness human skin was reduced by approximately 2 fold compared with 24-hour exposure to unclothed skin. Despite the lower reduction in absorption of HD through clothed skin compared with chlorpyrifos and dichlorvos, the clothing contaminated with HD left in contact with the skin for 1 hour still retained between 60% and 70% of the applied dose.

A previous study investigating the protective qualities of cotton shirt *in vivo* has shown that cotton shirt material provides between 84.1% and 92.5% protection against dermal exposure to agricultural pesticides based on actual dermal exposure expressed as a percentage of actual exposure combined with potential dermal exposure, which is defined as the total amount in contact with the skin and clothing combined (Protano *et al*. 2009). Unpublished work carried out in the Newcastle laboratory has also shown the protective qualities of a variety of clothing types (polyester, denim and cotton) against absorption of butoxyethanol through minipig skin (Wilkinson *et al*. 2010). All clothing types in this study significantly reduced systemic absorption through minipig skin in vitro with removal of clothing at 0.5 hours after exposure, although polyester was found to retain markedly less of the applied dose compared with cotton shirt material.

The results obtained from the *in vitro* studies undertaken in this project support the *in vivo* findings by Pretano *et al*. 2009 and the preliminary results obtained in the Newcastle laboratory that everyday clothing provides a degree of protection against chemical absorption through skin, despite the primary function of everyday clothing not being for protective purposes. It is clear that everyday clothing can potentially provide a sufficient barrier to significantly reduce initial dermal exposure if removed within 4 hours of exposure. Early removal of contaminated clothing also reduces the possibility of the contaminant (which may be retained in the clothing) from becoming resuspended in rainwater or sweat if left in contact with the skin. It is important to note that the clothing studies undertaken used a 1mm air gap between the skin surface and the clothing. This was done to represent the situation *in vivo* and to enable removal of the clothing during absorption studies without perturbing the skin, which would have been unavoidable if the clothing were sealed under the donor chamber. It is probable that more tight-fitting clothing without an air gap may result in greater transfer of chemicals from contaminated clothing to the skin, though it should also be mentioned that application of the dose solution resulted in intimate contact of the clothing with the skin, despite the air gap.

The results obtained also suggest that removal of clothing followed by immediate decontamination removed more of the chemical from the skin than removal of clothing alone. The ability to remove chemicals from the skin surface is likely to depend on the ability of the chemical or vehicle to interact with the skin, for instance, if a corrosive chemical came into contact with the

skin, the same degree of protection from skin exposure will not be provided by everyday clothing, and any damage to the skin caused by chemical irritation may lead to a decrease in the effectiveness of skin surface decontamination regimes.

Despite there being no significant differences in absorption between removal of clothing with immediate decontamination, and removal of clothing with 24 hour decontamination for all chemicals studied, it would be beneficial from the perspective of civilian exposure to an accidental chemical release that both removal of clothing and skin surface decontamination should be carried out to remove as much of the chemical in contact with the skin as soon as possible after exposure. This may help to reduce any potential local or systemic toxic effects that may occur as a result of dermal exposure to chemicals, and would certainly be preferable in the case of vesicants such as HD, which can have delayed effects. From a practical perspective in the event of civilian chemical exposure this would be hoped to be less than four hours, but there will be inevitable delay in removal of chemicals from the skin after exposure. It is encouraging that the time of removal of the chemical from the skin surface following disrobing does not significantly impact on systemic absorption with clothed skin; this suggests that once clothing was removed, medical countermeasures could be administered before immediate decontamination without a significant increase in the risk of harm from dermal absorption. One concern however, is that the presence of clothing over the skin may have an occlusive effect for *in vivo* or *in vitro* exposure scenarios, and result in proportionately greater absorption of chemical permeating through clothing to

the skin surface. These results show that despite the 1mm air-gap between the clothing and the skin surface, a small proportion of the applied dose of each chemical used was still recovered from the skin surface despite early removal of clothing. This is due to the contaminated clothing temporarily adhering to the skin and resulting in transfer of the chemical to the skin surface. However, compared with unclothed skin, the amount of chemical recovered from the skin surface and the amount penetrated was significantly reduced with the presence of clothing. It is encouraging from a decontamination perspective that there was some of the applied dose remaining on the skin surface after removal of the clothing, suggesting that there is little promotion of absorption as a result of occlusion by clothing. Extrapolating this to an *in vivo* scenario, it is likely that the potential occlusive effects of clothing to enhance chemical penetration is limited, and is far outweighed by the protective capabilities given by the presence of clothing for the chemicals used in these studies.

9.1.3: Predictive modelling of chemical absorption

Due to the limitations in carrying out appropriate *in vitro* studies with skin for all potential exposure chemicals, it would be of use to be able to make an initial prediction of dermal absorption for a chemical based on its physicochemical properties and the nature of the skin contamination using a predictive model. The model described by Buist *et al*. 2010 was selected for this study as this is one of the few mathematical models which attempts to predict finite exposures from different vehicles. The Buist model does not predict absorption on the basis of physicochemical parameters, but on the

basis of input parameters determined from experimental procedures or from other models. However the Buist model did not produce good predictions for absorption of caffeine and benzoic acid applied in IPA or PG, or dichlorvos applied to the skin in IPA, IPM or PG compared with experimental data. In most cases, absorption was vastly overestimated at later time points although it reasonably well predicted the early phase of absorption after the lag phase, with the exception of benzoic acid in PG, where the experimental outcome was almost twice that of the predicted outcome. However, it is likely that the under-prediction was due to the long observed experimental lag time, as the model described by Buist *et al*. 2010 assumes no absorption of chemicals into the systemic circulation prior to the lag time.

Due to the complexities of dermal absorption of chemicals, and the interaction of chemicals with the vehicles in which they are applied, it is extremely difficult to produce a model that can accurately predict experimental, or 'real life' outcomes for a wide range of chemicals. The difficulty in predicting exposure outcomes is underlined by the variety of mathematical models that have been produced and which are not particularly accurate. Many of these models have been reviewed (Bouwman *et al*. 2008).

It is important to develop a reliable mathematical model of dermal absorption to reduce the numbers of *in vitro* or *in vivo* experimental data needed to define the risk of dermal exposure to a wide range of chemicals. However, at present, there are few mathematical models that can predict absorption of a variety of compounds from real life exposure scenarios and, as is always the

case it is necessary to validate the model predictions by undertaking experiments to assess dermal absorption of chemicals, as this study has illustrated.

9.2: Conclusion

These studies have shown that the vehicle in which a chemical is applied to the skin can have a significant impact on the dermal absorption and dermal kinetics of a chemical. Chemical interactions with the vehicle in which it is applied to the skin is an important factor affecting dermal absorption and must be taken into consideration when using *in vitro* data to predict *in vivo* exposure scenarios. These studies indicate that benzoic acid can potentially model for HD absorption under similar exposure scenarios; however, the organophosphate compounds used in this project are shown to be poor for predicting dermal absorption of HD. Dichlorvos and chlorpyrifos are hazardous compounds for dermal exposure in their own right, and so the generation of novel dermal exposure data on these compounds can be useful for extrapolating to specific *in vivo* exposure scenarios. It is possible to use in vitro absorption data to predict absorption of other organophosphate chemicals with similar physicochemical properties.

It can also be seen from these studies that everyday civilian clothing can provide significant protection against dermal absorption *in vitro*. This may be important from a civilian exposure perspective, as limiting the amount of chemical in contact with the skin could significantly reduce the local and systemic toxic effects caused by chemical exposure.

References

References

Abdel – Rasoul, G. M., Abou – Salem, M. E., Mechael, A. A., Hendy, O. M., Rohlman, D. S., and Ismael, A. A. (2008). Effects of occupational pesticide exposure on children applying pesticides. *Neurotoxicology* **29**; 833-838.

Akomeah, F., Nazir, T., Martin, G. P., and Brown, M. B. (2004) Effect of heat on the percutaneous absorption and skin retention of three model penetrants. *European Journal of Pharmaceutical Sciences* **21**; 337-345.

Akomeah, F. K., Martin, G. P., and Brown, M. B. (2007). Variability in human skin permeability *in vitro*: Comparing penetrants with different physicochemical properties. *Journal of Pharmaceutical Sciences* **96**; 824-834.

Archibald, B. A., Solomon, K. R., and Stephenson G. R. (1995). Estimation of pesticide exposure to greenhouse applicators using video imaging and other assessment techniques. *American Industrial Hygiene Association Journal* **56**; 226-235.

Aust, G. F., (2007). Determination and prediction of dermal penetration of pesticide actives from formulation mixtures. Defra research project. Newcastle University.

Bach, M. and Lippold, B. C. (1998). Percutaneous penetration enhancement and its quantification. *European Journal of Pharmaceutics and Biopharmaceutics* **46**; 1-13.

Balali-Mood, M., and Hefazi, M. (2005). The clinical toxicology of sulphur mustard. *Archives of Iranian medicine* **8**; 162-179.

Baldi, I., Lebailly, P., Jean, S., Rougetet, L., Dulaurent, S., and Marquet, P. (2006). Pesticide contamination of workers in vineyards in France. *Journal of Exposure Science and Environmental Epidemiology* **16**; 115-124.

Barry, B. W., (1988). Action of skin penetration enhancers- the lipid protein partitioning theory. *International Journal of Cosmetic Science* **10**; 281-293.

Barry, B. W. (2001). Novel mechanisms and devices to enable successful transdermal drug delivery. *European Journal of Pharmaceutical Sciences* **14**; 101-114

Barry, B. W., (2002). Drug delivery routes in skin: a novel approach. *Advanced Drug Delivery Reviews* **54**; S31-S40.

Bast, G. E., Taeschner, D., and Kampffmeyer, H. G. (1996). Permethrin absorption not detected in single-pass perfused rabbit ear, and absorption with oxidation of 3-phenoxybenzyl alcohol. *Archives of Toxicology* **71**; 179-186.

Benson, H. A. E., Sarveiya, V., Risk, S., and Roberts, M. S. (2005). Influence of anatomical site and topical formulation on skin penetration of sunscreens. *Therapeutics and Clinical Risk Management* **1**; 209-218.

Bide, R. W., Schofield, L., and Risk, D. J. (2005). Immediate post-dosing paralysis following severe soman and VX toxicosis in guinea pigs. *Journal of Applied Toxicology* **25**; 410-417.

Billich, A., Vyplel, H., Grassberger, H., Schmook, F. P., Steck, A., and Stuetz, A. (2005). Novel cyclosporin derivatives featuring enhanced skin penetration despite increased molecular weight. *Bioorganic and Medicinal Chemistry* **13**; 3157-3167.

Bjarnason, S., Mikler, J., Hill, I, Tenn, C., Garrett, M., Caddy, N., and Sawyer, T. W. (2008). Comparison of selected skin decontaminant products and regimens against VX in domestic swine. *Human and Experimental Toxicology* **27**; 253-261.

Bodde, H. E., van den Brink, I., Koerten, H. K., and Haan, F. H. N., (1991). Visualization of in vitro percutaneous penetration of mercuric chloride: transport through intercellular spaces versus cellular uptake through desmosomes. *Journal of Controlled Release* **15**; 227-236.

Boman, A. and Maibach, H. I., (2000). Percutaneous absorption of organic solvents. *International Journal of Occupational and Environmental Health* **6**; 93-95. Review

Booth, E. D., Jones, E., and Elliott, B. M., (2007). Review of the in vitro and in vivo genotoxicity of dichlorvos. *Regulatory Toxicology and Pharmacology* **49**; 316-326.

Bos, J. D., and Meinardi, M. M. (2000). The 500 Dalton rule for the skin penetration of chemical compounds and drugs. *Experimental Dermatology* **9**; 165-169.

Boutsiouki, P., Thompson, J. P., and Clough, G. F. (2001). Effects of local blood flow on the percutaneous absorption of the organophosphorous compound Malathion: a microdialysis study in man. *Archives of Toxicology* **75**; 321-328.

Bouwman, T., Cronin, M. T. D., Bessems, J. G. M., and van de Sandt, J. J. (2008). Improving the applicability of (Q) SARs for percutaneous penetration in regulatory risk assessment. *Human and Experimental Toxicology* **27**; 269-276.

Bronaugh, R. L., Stewart, R. F., and Congdon, E. R. (1982). Methods for in vitro percutaneous absorption studies. II. Animal models for human skin. *Toxicology and Applied Pharmacology* **62**; 481-488.

Bronaugh, R. L., and Stewart, R. F. (1985). Methods for percutaneous absorption studies. IV. The flow through diffusion cell. *Journal of Pharmaceutical Sciences* **74**; 64-67.

Bronaugh, R. L., and Franz, T. J. (1986). Vehicle effects on percutaneous absorption: in vivo and in vitro comparisons with human skin. *British Journal of Dermatology* **115**; 1-11.

Bronaugh, R. L. (2000). In vitro percutaneous absorption models. In *Toxicology for the Next Millennium.* (Isfort, R. J., and Lederberg, J. Eds). Annals of the New York Academy of Sciences.

Bronaugh, R. L., Hood, H. L., Kraeling, M. E. K., and Yourick, J. J. (2001). Determination of percutaneous absorption by in vitro techniques. *Journal of Toxicology: Cutaneous and Ocular Toxicology* **20**; 423-427.

Bronaugh, R. L. (2004). Methods for in vitro percutaneous absorption. *Dermatotoxicology 6th edition* (Zhai, H, and Maibach, H. I, Eds). 519-529.

Buist, H. E., van Burgsteden, J. A., Freidig, A. P., Maas, W. J. M., and van der Sandt, J. J. M. (2010). New *in vitro* dermal absorption database and the prediction of dermal absorption under finite conditions for risk assessment purposes. *Regulatory Toxicology and Pharmacology*. **57**; 200-209.

Cattani, M., Cena, K., Edwards, J., and Pisaniello, D. (2001). Potential dermal and inhalation exposure to chlorpyrifos in Australian pesticide workers. *Annals of Occupational Hygiene*.**45**; 299-308.

Charbonnier, V., Payne, M., and Maibach, H. I. (2004). Determination of subclinical changes of barrier function. *Dermatotoxicology 6th Edition* (Zhai, H., and Maibach, H. I. Eds). P 939-955. CRC Press, Boca Raton.

Cherrie, J. W., Semple, S., and Brouwer, D. (2004). Gloves and dermal exposure to chemicals: Proposals for evaluating workplace effectiveness. Annals of Occupational Hygiene **48**; 607-615.

Chilcott, R. P., Jenner, J., Carrick, W., Hotchkiss, S. A. M., and Rice, P. (2000). Human skin absorption of bis-2-(chloroethyl) sulphide (sulphur mustard) *in vitro*. *Journal of Applied Toxicology* **20**; 349-355.

Chilcott, R. P., Jenner, J., Hotchkiss, S. A. M., and Rice, P. (2001). *In vitro* skin absorption and decontamination of sulphur mustard: Comparison of human and pig-ear skin. *Journal of Applied Toxicology* **21**; 279-283.

Chilcott, R. P., Dalton, C. H., Emmanuel A. J., Allen, C. E., and Bradley, S. T. (2002a). Transepidermal water loss does not correlate with skin barrier function *in vitro*. *Journal of Investigative Dermatology* **118**; 871-875.

Chilcott, R. P., Jenner, J., Hotchkiss, S. A. M., and Rice, P. (2002b). Evaluation of barrier creams against sulphur mustard I. In vitro studies using human skin. *Skin Pharmacology and Applied Skin Physiology* **15**; 225- 235.

Chilcott, R. P., Barai, N., Beezer, A. E., Brain, S. I., Brown, M. B., Bunge, A. L., Burgess, S. E., Cross, S., Dalton, C. H., Dias, M., Farinha, A., Finnin, B. C., Gallagher, S. J., Green, D. M., Gunt, H., Gwyther, R. L., Heard, C. M., Jarvis, C. A., Kamiyama, J., Kasting, G. B., Ley, E. E., Lim, S. T., McNaughton, G. S., Morris, A., Nazemi, M. H., Pellett, M. A., Du Plessis, J., Quan, Y. S., Raghavan, S. L., Roberts, M., Romonchuk, W., Roper, C. S., Schenk, D., Simonsen, L., Simpson, A., Traversa, B. D., Trottet, L., Watkinson, A., Wilkinson, S. C., Williams, F. M., Yamamoto, A., and Hadgraft, J. (2005). Inter- and intralaboratory variation of *in vitro* diffusion cell measurements: An international multicenter study using quasi-standardized methods and materials. *Journal of Pharmaceutical Sciences* **94**; 632-638.

Chilcott, R. P., Dalton, C. H., Ashley, Z., Allen, C. E., Bradley, S. T., Maidment, M. P., Jenner, J., Brown, R. F. R., Gwyther, R. J., and Rice, P. (2007). Evaluation of barrier creams against sulphur mustard: (II) *in vivo* and *in vitro* studies using the domestic white pig. *Cutaneous and Ocular Toxicology* **26**; 235-247.

Chilcott, R. P., and Price, S., (2008). Principles and Practice of Skin Toxicology, Wiley & Sons Ltd.

Choi, K., Joo, H., Rose, R. L., and Hodgson, E. (2006). Metabolism of chlorpyrifos and chlorpyrifos oxon by human hepatocytes. *Journal of Biochemical and Molecular Toxicology* **20**; 279-291.

Cnubben, N. H. P., Elliot, G. R., Hakkert, B. C., Meuling, W. J. A., and van de Sandt, J. J. M. (2002). Comparative *in vitro-in vivo* percutaneous penetration of the fungicide *ortho*-phenylphenol. *Regulatory Toxicology and Pharmacology* **35**; 198-208.

Creely, K. S., and Cherrie, J. W., (2001). A novel method of assessing the effectiveness of protective gloves – results from a pilot study. *Annals of Occupational Hygiene* **45**; 137-143.

Dale, B. A., Resing, K. A., and Lonsdale-Eccles, J. D., (1985). Filaggrin: a keratin filament associated protein. *Annals of New York Academy of Sciences* **455**; 330-342.

Dalton, C. H., Hattersley, I. J., Rutter, S. J., and Chilcott, R. P. (2006). Absorption of the nerve agent VX (*0*-ethyl-*S*-[2(di-isopropylamino) ethyl] methyl phosphonothioate) through pig, human and guinea pig skin *in vitro*. *Toxicology in Vitro* **20**; 1532-1536.

Daly, J. W., and Fredholm, B. B. (1998). Caffeine – an atypical drug of dependence. *Drug and Alcohol Dependence* **51**; 199-206.

Dick, I. P., and Scott, R. C. (1992). Pig ear as an in vitro model for human skin permeability. *Journal of Pharmacy and Pharmacology* **44**; 640-645.

Dick, I. P., Blain, P. G., and Williams, F. M. (1996). Improved in vitro skin absorption of lipophilic compounds following addition of albumin to receptor fluid in the flow through system. In *Prediction of Percutaneous Penetration. Volume 4b* (Brain, K. R., James, V. R., and Walters, K. A. Eds.) pp 267-270. STS Publishing, Cardiff, UK.

Dick, I. P., Blain, P. G., and Williams, F. M. (1997a).The percutaneous absorption and distribution of lindane in man. I. in vivo studies. *Human Experimental Toxicology* **16**; 645-651.

Dick, I. P, Blain, P. G., and Williams, F. M. (1997b). The percutaneous absorption and distribution of lindane in man. II. In vitro studies. *Human Experimental Toxicology* **16**; 652-657.

Diembeck, W., Beck, H., Benech-Kieffer, F., Courtellemont, P., Dupuis, J., Lovell, W., Payne, M., Spengler, J., and Steiling, W. (1999). Test guidelines for assessment of dermal absorption and percutaneous penetration of cosmetic ingredients. *Food and Chemical Toxicology* **37**; 191-205.

Duncan, E. J. S., and Gudgin Dickson, E. F., (2003). A new whole-body vapour exposure chamber for protection performance research on chemical protective ensembles. *American Industrial Hygiene Association Journal* **64**; 212-221.

Duracher, L., Blasco, L., Hubaud, J-C, Vian, L., and Marti-Mestres, G. (2009) .The influence of alcohol, propylene glycol and 1, 2-pentanediol on the permeability of hydrophilic model drug through excised pig skin. *International Journal of Pharmaceutics* **374**; 39-45.

Ehntholt, D. J., Bodek, I., Valentine, J. R., Schwope, A. D., Royer, M. D., Nielsen, U., and Frank, A. P. (1989). The effects of solvent type and concentration on the permeation of pesticide formulations through chemical protective glove materials. In; Chemical Emergency Response (Perkins, J. L., and Stull, J. O., eds). Philadelphia, PA: American Society for Testing and Materials; 146-156.

Elias, P. M and Friend, D. S. (1975). The permeability barrier in mammalian epidermis. *Journal of Cell Biology* **65**; 180-191.

Elkeeb, R., Hui, X., Chan, H., Tian, L., and Maibach, H. I. (2010). Correlation of transepidermal water loss with skin barrier properties in vitro: comparison of three evaporimeters. *Skin Research and Technology* **16**; 9-15.

Elmahjoubi, E., Frum, Y., Eccleston, G. M., Wilkinson, S. C., and Meiden, V. (2009). Transepidermal water loss for probing full-thickness skin barrier function: correlation with tritiated water flux, sensitivity to punctures and diverse surfactant exposures. *Toxicology in Vitro* **23**; 1429-1435.

FAO/WHO. (2000). Pesticide residues in food-1999 evaluations. Part II – Toxicological. Geneva, World Health Organisation, Joint FAO/WHO meeting on pesticide residues.

Farahat, F. M., Fenske, R. A., Olson, J. R., Galvin, K., Bonner, M. R., Rohlman, D. S., Lein, P. J., and Anger, W. K. (2010). Chlorpyrifos exposures in Egyptian cotton field workers. *Neurotoxicology*. Doi: 10.1016/j.neuro.2010.02.005.

Fluhr, J. W., Feingold, K. R., and Elias, P. M. (2006). Transepidermal water loss reflects permeability status: validation in human and rodent in vivo and ex vivo models. *Experimental Dermatology* **15**; 483-492.

Flynn, G. L., (1990a). Physicochemical determinants of skin absorption. In *Principles of Route-to-Route Extrapolation for Risk Assessment* (Gerrity, T. R., and Henry, C. J., Eds.) Elsevier Science Publishing Co, Amsterdam.

Flynn, G. L, (1990b). Skin as a route of exposure to protein allergens. *Principles of route-to-route extrapolation for risk assessment.* (Gerrity, T. R, and Henry, C. J, Eds). Elsevier Science Publishing Co, Amsterdam.

Fox, S. I. (1996). *Human Physiology: Fifth Edition*. Wm C. Brown Publishers, Dubuque, IA.

Franz, T. J. (1975). Percutaneous absorption. On the relevance of in vitro data. *Journal of Investigative Dermatology* **64**; 190–195.

Franz, T. J., (1978). The finite dose technique as a valid in vitro model for the study of percutaneous absorption. *Current Problems in Dermatology* **7**; 58.

Gan, S. Q., McBride, O .W., Idler, W. W., Markova, N., and Steinert, P. M. (1990). Organization, structure, and polymorphisms of the human profilaggrin gene. *Biochemistry* **29**; 9432-9440.

Geer, L. A., Cardello, N., Dellarco, M. J., Leighton, T. J., Zendzian, R. P., Roberts, J. D., and Buckley. T. J. (2004). Comparative analysis of passive dosimetry and biomonitoring for assessing chlorpyrifos exposure in pesticide workers. *Annals of Occupational Hygiene* **48**; 683-695.

Godin, B., Touitou, E. (2007). Transdermal skin delivery: predictions for humans from in vivo, ex vivo and animal models. *Advanced Drug Delivery Reviews* **59**; 1152-1161.

Grams, Y. Y., and Bouwstra, J. A., (2002). Penetration and distribution of three lipophilic probes in vitro in human skin focusing on the hair follicle. *Journal of Controlled Release* **83**; 253-262.

Grandjean, P., (1990). Percutaneous absorption. In *Skin Penetration: Hazardous Chemicals at Work,* pp.3-34. Taylor & Francis, London.

Greaves, L. C., Wilkinson, S. C., and Williams, F. M., (2002). Factors affecting percutaneous absorption of caffeine in vitro. *Toxicology* **178**; 65-66.

Griffin, P., Mason, H., Heywood, K., and Cocker, J. (1999). Oral and dermal absorption of chlorpyrifos: a human volunteer study. *Occupational and Environmental Medicine* **56**; 10-13.

Griffin, P., Payne, M., Mason, H., Freedlander, E., Curran, A. D., and Cocker, J. (2000). The *in vitro* percutaneous penetration of chlorpyrifos. *Human and Experimental Toxicology* **19**; 104-107.

Gudgin Dickson, E. F., (2008). Estimates of percutaneous toxicity of sulfur mustard vapor suitable for use in protective equipment standards. *Journal of Toxicology and Environmental Health* **71**; 1382-1391.

Guy, R. H., Hadgraft, J., and Maibach, H. I., (1982). A pharmacokinetic model for percutaneous absorption. *International Journal of Pharmaceutics* **11**; 119-129.

Hamilton, M. G., Hill, I., Conley, J., Sawyer, T. W., Caneva, D. C., and Lundy, P. M. (2004). Clinical aspects of percutaneous poisoning by the chemical warfare agent VX: effects of application site and decontamination. *Military Medicine* **169**; 856-862.

Harrison, S. M., Barry, B. W., and Dugard, P. H. (1984). Effects of freezing on human skin permeability. *Journal of Pharmacy and Pharmacology* **36**; 261-262.

Hattersley, I. J., Jenner, J., Dalton, C., Chilcott, R. P., and Graham, J. S. (2008). The skin reservoir of sulphur mustard. *Toxicology in vitro* **22**; 1539-1546.

Hawkins, G. S., and Reifenrath, W. G. (1986). Influence of skin source, penetration cell fluid, and partition coefficient on in vitro skin penetration. *Journal of Pharmaceutical Sciences* **75**; 378-381.

Heylings, J. R., Diot, S., Esdaile, D. J., Fasano, W. J., Manning, T. O., and Owen, H. M. (2001). A prevalidation study on the in vitro skin irritation function test (SIFT) for prediction of acute skin irritation in vivo: results and evaluation of ECVAM phase III. *Toxicology in Vitro* **17**; 123-138.

Howes, D., Guy, R., Hadgraft, J., Heylings, J., Hoeck, U., Kemper, F., Maibach, H. I., Marty, J. P., Merk, H., Parra, J., Rekkas, D., Rondelli, I., Schaefer, H., Tauber, U., and Verbiese, N. (1996). Methods for assessing percutaneous absorption – The report and recommendations of ECV AM workshop 13. *ATLA-Alternatives to Laboratory Animals* **24**; 81-106.

Jacobi, U., Gautier, J., Sterry, W., and Lademann, J. (2005). Gender-related differences in the physiology of the stratum corneum. *Dermatology* **211**; 312-317.

Jacobi, U., Tassopoulos, T., Surber, C., and Lademann, J. (2006). Cutaneous distribution and localisation of dyes affected by vehicles all with different lipophilicity. *Archives of Dermatological Research* **297**; 303-310.

Jewell, C., Heylings, J., Clowes, H. M., and Williams, F. M. (2000). Percutaneous absorption and metabolism of dinitrochlorobenzene in vitro. *Archives of Toxicology* **74**; 356-365.

Jewell, C., Prusakiewicz, J. J., Ackermann, C., Payne, N. A., Fate, G., Voorman, R., and Williams, F. M., (2007). Hydrolysis of a series of parabens by skin microsomes and cytosol from human and minipigs and in whole skin in short-term culture. *Toxicology and Applied Pharmacology* **225**; 221-228.

Karr, C., Demers, P., Costa, L. G., Daniell, W. E., Barnhart, S., Miller, M., Gallagher, G., Horstman, S. W., Eaton D., and Rosenstock, L. (1992). Organophosphate pesticide exposure in a group of Washington state orchard applicators. *Environmental Research* **59**; 229-237.

Kitson, N., and Thewalt, J. L. (2000). Hypothesis: the epidermal permeability barrier is a porous medium. *Acta Dermato-Venereologica* **208**; 12-15.

Kretsos, K., Miller, M. A., Zamora-Estrada, G., and Kasting, G. B. (2008). Partitioning, diffusivity and clearance of skin permeants in mammalian dermis. *International Journal of Pharmaceutics* **346**; 64-79.

Lampe, M. A., Burlingame, A. L., Whitney, J., Williams, M. L., Brown, B. E., Roitman, E., and Elias, P. M. (1983). Human stratum corneum lipids: characterization and regional variations. *Journal of Lipid Research* **24**; 120-130.

Lee, F. W. (2004). Investigation of factors influencing the dermal absorption of lipophilic chemicals. PhD Thesis. University of Newcastle upon Tyne.

Levin, J., and Maibach, H. I. (2005). The correlation between transepidermal water loss and percutaneous absorption: An overview. *Journal of Controlled Release* **103**; 291-299.

Liu, K. H., and Kim, J. H. (2003). In vitro dermal penetration study of carbofuran, carbosulfan, and furathiocarb. *Archives of Toxicology* **77**; 255-260.

Luty, S., Latuszynska, J., Halliop, J., Tochman, A., Obuchowska, D., Przylepa, E., Korczak, E., and Bychawski, E. (1998). Toxicity of dermally absorbed dichlorvos in rats. *Annals of Agricultural and Environmental Medicine* **5**; 57-64.

Maibach, H. I., Feldmann, R. J., Hilby, T. H., and Servat, W. F. (1971). Regional variation in percutaneous absorption in man. *Archives of Environmental Health* **23**; 208-211.

Marchera, K., Tsakirakis, A., Charistou, A., Anastasiadou, P., and Glass, C. R. (2009). Dermal exposure of pesticide applicators as a measure of coverall performance under field conditions. *Annals of Occupational Hygiene* **53**; 573-584.

Martiin, E., Neeilssen-Subnel, M. T. A., de Haan, F. H. N., and Bodde, H. E. (1996). A critical comparison of methods to quantify stratum corneum removed by tape stripping. *Skin Pharmacology* **9**; 69-77.

Maynard, R. L., Meredith, T. J., Marrs, T. C., and Vale, J. A. (1991). Management of chemical warfare injuries (letter). *Lancet* **337**; 122.

Menon, G. K, (2002). New insights into skin structure: scratching the surface. *Advanced drug delivery reviews* **54**; 13-317.

Merk, H. F., Jugert, F. K., and Frankenberg, S. (1996). Biotransformations in the skin. In *Dermatotoxicology: 5th Edition* (Marzulli, F. N., and Maibach, H. I., Eds.), p61-73. Taylor & Francis, Bristol, PA.

Meuling, W. J. A., Ravensberg, L. C., Roza, L., and van Hemmen, J. J. (2005). Dermal absorption of chlorpyrifos in human volunteers. *International Archives of Occupational and Environmental Health* **78**; 44-50.

Miller, M. A., and Kasting, G. B. (2010). Toward a better understanding of pesticide dermal absorption: diffusion model analysis of parathion absorption in vitro and in vivo. *Journal of Toxicology and Environmental Health, Part A* **73**; 284-300.

Monteiro-Riviere, N. A., Bristol, D. G., Manning, T. O., Rogers, R. A., and Riviere, J. E., (1990). Interspecies and interregional analysis of the comparative histologic thickness and laser Doppler blood flow measurements at five cutaneous sites in nine species. *Journal of Investigative Dermatology* **95**; 582-586.

Monteiro-Riviere, N. A. (1996). Anatomical factors affecting barrier function. In *dermatotoxicology*: 5th edition (Marzulli, F. N., and Maibach, H. I., Eds.), p3-17. Taylor & Francis, Bristol, PA.

Montiero-Riviere, N. A. (2004). Anatomical factors affecting barrier function. *Dermatotoxicology 6th edition* (Zhai, H and Maibach, H. I, Eds) 43-70. CRC Press, Boca Raton.

Monti, D., Giannelli, R., Chetoni, P., and Burgalassi, S. (2001). Comparison of the effect of ultrasound and of chemical enhancers on transdermal permeation of caffeine and morphine through hairless mouse skin in vitro. *International Journal of Pharmaceutics* **229**; 131-137.

Moser, K., Kriwet, K., Naik, A., Kalia, Y. N., and Guy, R. H. (2001). Passive skin penetration enhancement and its quantification in vitro. *European Journal of Pharmaceutics and Biopharmaceutics* **52**; 103-112.

Moss, G. P., Dearden, J. C., Patel, H., and Cronin, M. T. D. (2002). Quantitative structure-permeability relationships (QSPRs) for percutaneous absorption. *Toxicology in Vitro* **16**; 299-317.

Mutch, E. and Williams, F. M. (2006). Diazinon, chlorpyrifos and parathion are metabolised by multiple cytochromes P450 in human liver. *Toxicology* **224**; 22-32.

Nangia, A, Patil, S., Berner, B., Boman, A., and Maibach, H. I. (1998). In vitro measurement of transepidermal water loss: a rapid alternative to tritiated water permeation for assessing skin barrier functions. *International Journal of Pharmaceutics* **170**; 33-40.

Nielsen, J. B., and Andersen, H. R. (2001). Dermal in vitro penetration of methiocarb, paclobutrazol, and pirimicarb: Effect of nonylphenolethoxylate and protective gloves. Environmental Health Perspectives **109**; 129-132.

Nielsen, J. B. (2005). Percutaneous penetration through slightly damaged skin. *Archives of Dermatological Research* **296**; 560-567.

Nielsen, J. B., Sorensen, J. A., and Nielsen, F. (2009). The usual suspects: Influence of physicochemical properties on lag time, skin deposition, and percutaneous penetration of nine model compounds. *Journal of Toxicology and Environmental Health*, *Part A* **72**; 315-323.

Norlen, L., Nicander, I., Lundh Rozell, B., Ollmar, S., and Forslind, B. (1999). Inter- and intra-individual differences in human stratum corneum lipid content related to physical parameters of skin barrier function in vivo. *The Journal of Investigative Dermatology* **112**; 72-77.

OECD, (2004). OECD guideline for the testing of chemicals. Skin absorption in vitro method. 428. P 1-8, Paris.

Oestmann, E., Lavrijsen, A., Hermans, J., and Ponec, M. (1993). Skin barrier function in healthy volunteers as assessed by transepidermal water loss and vascular response to hexyl nicotinate: Intra and inter-individual variability. *British Journal of Dermatology* **128**; 130-136.

Potts, R. O., and Guy, R. H. (1992). Predicting skin permeability. *Pharmaceutical Research* **9**; 663-669.

Protano, C., Guidotti, M., and Vitali, M. (2009). Performance of different work clothing types for reducing skin exposure to pesticides during open field treatment. *Bulletin of Environmental Contamination and Toxicology* **83**; 115-119.

Raheel, M., and Dai, G. X., (1997). Chemical resistance and structural integrity of protective glove materials. *Journal of Environmental Science and Health*. *Part A: Environmental Science and Engineering and Toxic and Hazardous Substance Control; A32*, 567-579.

Rawson, B. V., Cocker, J., Evans, P. G., Wheeler, J. P., and Akrill, P. M. (2005). Internal contamination of gloves: Routes and consequences. *Annals of Occupational Hygiene* **49**; 535-541.

Reifenrath, W. G., Chellquist, E. M., Shipwash, E. A., and Jederberg, W. W. (1984). Evaluation of animal models for predicting skin penetration in man. *Fundamental and Applied Toxicology* **4**; 224-230.

Reifenrath, W. G., Hawkins, G. S., and Kurtz, M. S. (1991). Percutaneous penetration and skin retention of topically applied compounds: an in vitro-in vivo study. *Journal of Pharmaceutical Sciences* **80**; 526-532.

Riviere, J. E., Smith, C. E., Budsaba, K., Brooks, J. D., Olajos, E. J., Salem, H., Montiero-Riviere, N. A. (2001). Use of methyl salicylate as a simulant to predict the percutaneous absorption of sulfur mustard. *Journal of Applied Toxicology* **21**; 91-99.

Saladi, R. N., Smith, E., and Persaud, A. N. (2005). Mustard: A potential agent for chemical warfare and terrorism. *Clinical and Experimental Dermatology* **31**; 1-5. Blackwell Publishing Ltd.

Sartorelli, P., Aprea, C., Bussani, R., Novelli, M. T., Orsi, D., and Sciarra, G. (1997). In vitro percutaneous penetration of methyl parathion from a commercial formulation through the human skin. *Occupational and Environmental Medicine* **54**; 524-525.

Sayer, N. M., Whiting, R., Green, A. C., Anderson, K., Jenner, J., and Lindsay, C. D., (2009). Direct binding of sulfur mustard and chloroethyl ethyl sulphide to human cell membrane-associated proteins; implications for sulfur mustard pathology. *Journal of Chromatography B,* Doi: 10.1016/j.jchromb.2009.11.030

Scheuplein, R. J. (1965). Mechanism of percutaneous adsorption. 1. Routes of penetration and the influence of solubility. *Journal of Investigative Dermatology* **45**; 334-346.

Scheuplein, R. J., and Blank, I. H. (1971). Permeability of the skin. *Physiological Reviews* **51**; 702-747.

Schreiber, S., Mahmoud, A., Vuia, A., Rubbelke, M. K., Schmidt, E., Schaller, M., Kandarova, H., Haberland, A., Schafer, U. F., Bock, U., Korting, H. C., Liebsch, M., and Schafer-Korning, M. (2005). Reconstructed epidermis versus human and animal skin in absorption studies. *Toxicology in Vitro* **19**; 813-822.

Schwope, A. D., Goydan, R., Ehntholt, D., Frank, U., and Nielsen, A. (1992). Permeation resistance of glove materials to agricultural pesticides. *American Industrial Hygiene Association Journal* **53**; 352-361.

Scott, R. C., Dugard, P. H., Ramsey, J. D., and Rhodes, C. (1987). In vitro absorption of some o-phthalate diesters through human and rat skin. *Environmental Health Perspectives* **74**; 223-227.

Shakarjian, M. P., Heck, D. E., Gray, J. P., Sinko, P. J., Gordon, M. K., Casillas, R. P., Heindel, N. D., Gerecke, D. R., Laskin, D. L., and Laskin, J. D. , (2010). Mechanisms mediating the vesicant actions of sulfur mustard after cutaneous exposure. *Toxicological Sciences* **114**; 5-19.

Simon, G. A., and Maibach, H. I. (2000). The pig as an experimental animal model of percutaneous permeation in man: qualitative and quantitative observations – an overview. *Skin Pharmacology and Applied Skin Physiology* **13**; 229-234.

Singh, B., and Dogra, T. D., (2009). Rapid method for the determination of some organophosphorous insecticides in a small amount of serum in emergency and occupational toxicological cases. *Indian Journal of Occupational and Environmental Medicine* **13**; 84-87.

Smith, H. W., Clowes, G. H. A., and Marshall Jr, E. K. (1919). On dichloroethylsulfide (mustard gas) IV. The mechanism of absorption by the skin. *Journal of Pharmacological and Experimental Therapy* **13**; 1-30.

Southwell, D., Barry, B. W., and Woodford, R. (1984). Variations in permeability of human skin within and between specimens. *International Journal of Pharmaceutics* **18**; 299-309.

Surber, C., Wilhelm, K. P., and Maibach, H. I. (1991). In vitro skin pharmacokinetics of acitrecin: percutaneous absorption studies in intact and modified skin from three different species using different receptor fluids. *Journal of Pharmacy and Pharmacology* **43**; 836-840.

Tang, J., Cao, Y., Rose, R. L., Brimfield, A. A., Dai, D., Goldstein, J. A., and Hodgson, E. (2001). Metabolism of chlorpyrifos by human cytochrome P450 isoforms and human, mouse and rat liver microsomes. *Drug metabolism and disposition* **29**; 1201-1204.

Taysse, L, Daulon, S., Delamanche, S., Bellier, B., and Breton, B. (2007). Skin decontamination of mustards and organophosphates: comparative efficiency of RSDL and Fuller's Earth in domestic swine. *Human and Experimental Toxicology* **26**; 135-141.

Tomalik-Scharte, D., Lazar, A., Meins, J., Bastian, B., Ihrig, M., Wachall, B., Jetter, A., Tantcheva-Poor, I., Mahrle, G., and Fuhr, U. (2005). Dermal absorption of permethrin following topical administration. *European Journal of Clinical Pharmacology* **61**; 399-404.

Traynor, M. J., Wilkinson, S. C., and Williams, F. M., (2008). Metabolism of butoxyethanol in excised human skin in vitro. *Toxicology Letters* **177**; 151-155.

Tsai, J. C., Shen, L. C., Sheu, H. M., and Lu, C. C. (2003). Tape stripping and sodium dodecyl sulfate treatment increase the molecular cutoff of polyethylene glycol penetration across murine skin. *Archives of Dermatological Research* **295**; 169-174.

Tungul, A., Bonin, A. M., He, S., and Baker, R. S. U. (1991). Micronuclei induction by dichlorvos in the mouse skin. *Mutagenesis* **6**; 405-408.

USEPA (1992). Dermal exposure assessment: principles and applications. Interim Report, pp 1-388. Office of Health and Environmental Assessment, Washington DC. EPA/600/8 -91/011B.

Vallet, V., Cruz, C., Josse, D., Bazire, A., Lallement, G., and Boudry, I. (2007). *In vitro* percutaneous penetration of organophosphorous compounds using full-thickness and split-thickness pig and human skin. *Toxicology in Vitro* **21**; 1182-1190.

van der Merwe, D., Brooks, J. D., Gehring, R., Baynes, R. E., Monteiro-Riviere, N. A., and Riviere, J. E. (2006). A physiologically based pharmacokinetic model of organophosphate dermal absorption. *Toxicological Sciences* **89**; 188-204.

van der Molen, R. G., Spies, F., van't Noordende, J. M., Boelsma, E., Mommaas, A. M., and Koerten, H. K. (1997). Tape stripping of human stratum corneum yields cell layers that originate from various depths because of furrows in the skin. *Archives of Dermatological Research* **289**; 514-518.

van de Sandt, J. J. M., van Burgsteden, J. A., Cage, S., Charmichael, P. L., Dick, I., Kenyon, S., Korinth, G., Larese, F., Limmaset, J. C., Maas, W. J. M., Montomoli, L., Nielsen, J. B., Payan, J. P., Robinson, E., Sartorelli, P., Schaller, K. H., Wilkinson, S. C., and Williams, F. M. (2004). In vitro predictions of skin absorption of caffeine, testosterone, and benzoic acid: A multi-centre comparison study. *Regulatory Toxicology and Pharmacology* **39**; 271-281.

Vecchia, B. E., and Bunge, A. L. (2002). Skin absorption databases and predictive equations. In *Transdermal Drug Delivery: 2nd Edition* (Hadgraft, J., and Guy, R. H., Eds.)

Wakefield, J. C. (2006). Influence of skin irritation on dermal absorption. PhD thesis, University of Newcastle upon Tyne.

Wertz, P. W., and Downing, D. T., (1989). Stratum corneum: biological and biochemical considerations. In *Transdermal Drug Delivery* (Hadgraft, J., and Guy, R. H., Eds), pp 1-22. Marcel Dekker Inc, New York and Basel.

Wertz, P. W. (2004). Percutaneous absorption: role of lipids. *Dermatotoxicology 6th edition* (Zhai, H and Maibach, H. I, Eds) 71-81. CRC Press, Boca Raton.

Wester, R. C., Quan, D., and Maibach, H. I. (1996). *In Vitro* Percutaneous Absorption of Model Compounds Glyphosate and Malathion from Cotton Fabric into and through Human Skin. *Food and Chemical Toxicology* **34**; 731-735.

Wester, R. M., Tanojo, H., Maibach, H. I., and Wester R. C. (2000). Predicted chemical warfare agent VX toxicity to uniformed soldier using parathion in vitro human skin exposure and absorption. *Toxicology and Applied Pharmacology* **168**; 149-152.

Wilkinson, S. C., and Williams, F. M. (2002). Effects of experimental conditions on absorption of glycol ethers through human skin in vitro. *International Archives of Occupational and Environmental Health* **75**; 519-527.

Wilkinson, S. C., Maas, W. J., Nielsen, J. B., Greaves, L. C., van de Sandt, J. J. M., and Williams, F. M. (2006). Interactions of skin thickness and physicochemical properties of test compounds in percutaneous penetration studies. *International Archives of Occupational and Environmental Health* **79**; 405-413.

Wilkinson S. C., Moore, C. A., Aust, G. A., Blain, P. G., and Williams, F. M. Final report on influence of protection and decontamination on percutaneous absorption/penetration of selected chemical and bioactive agents. Home Office Milestone Report 2010.

Williams, A. C., and Barry, B. W. (2004). Penetration enhancers. *Advanced Drug Delivery Reviews* **56**; 603-618.

Williams, F. M. (2006). In vitro studies – how good are they at replacing in vivo studies for measurement of skin absorption. *Environmental Toxicology and Pharmacology* **21**; 199-203.

Williams, F. M., (2008). Potential for metabolism locally in the skin of dermally absorbed compounds. *Human and Experimental Toxicology* **27**; 277-280.

Williams, M. L., and Elias P. M., (1993). From basket to barrier: unifying concepts for the pathogenesis of disorders of cornification. *Archives of Dermatology* **129**; 626-628.

Yoshida, M., Mori, K., Watanabe, T., Hasegawa, T., and Sugibayash, K. (2000). Effects of application of voltage and cathode and anode positions at electroporation on the in vitro permeation of benzoic acid through hairless rat skin. *Chemical and Pharmaceutical Bulletin (Tokyo)* **48**; 1807-1809.

Website of the European Commission, Joint Research Centre, institute for health and consumer protection http://ecb.jrc.it/reach/reach-legislation/